



universität
wien

DIPLOMARBEIT / DIPLOMA THESIS

Titel der Diplomarbeit / Title of the Diploma Thesis

„Biophysical characterization of metal- and polycation
based carriers for nucleic acid delivery“

verfasst von / submitted by

Daniel Paunov

angestrebter akademischer Grad / in partial fulfilment of the requirements for the degree of
Magister der Pharmazie (Mag.pharm.)

Wien, 2021 / Vienna, 2021

Studienkennzahl lt. Studienblatt /
degree programme code as it appears on
the student record sheet:

UA 449

Studienrichtung lt. Studienblatt /
degree programme as it appears on
the student record sheet:

Diplomstudium Pharmazie

Betreut von / Supervisor:

Univ.-Prof. Dipl.-Ing. Dr. Manfred Ogris

Mitbetreut von / Co-Supervisor:

Dr. Haider Sami

Acknowledgment / Danksagung

To start with I would like to thank all who have accompanied and supported me during my studies and during the writing of this thesis.

It is my greatest concern to first thank Prof. Ogris for giving me the opportunity to do my diploma thesis at MMCT and to be part of a familiar and friendly environment which made my work a pleasure.

Furthermore, I would like to express my gratitude to Dr. Sami Haider for always supporting me with valuable advice. Additionally, I would like to thank him for his patience and kindness he has shown me day after day.

I would also like to express my gratitude to the whole MMCT-team, who has helped to create a great working atmosphere.

Finally, I would like to thank my family and friends, who have shown me the greatest support every day. Especially to my mother Zaneta Paunova and my father Konstantin Paunov I would like to express the greatest appreciation and gratitude for always believing in me. I would also like to thank my sister Silvia Paunova with the greatest appreciation for always being a role model and always being there for me no matter what.

Table of contents

1 Abstract	7
2 Zusammenfassung	8
3 List of abbreviations	9
4 Introduction	11
4.1 Nucleic acid therapy	11
4.1.1 Antisense Oligonucleotides.....	11
4.1.2 Splice Switching Oligonucleotides.....	12
4.1.3 Plasmid DNA.....	13
4.2 Challenges of nucleic acid therapy	14
4.2.1 Delivery methods for nucleic acids	14
4.2.1.1 Viral vectors.....	14
4.2.1.2 Non-viral vectors	15
4.3 Metal and polycationic carriers	15
4.3.1 Polyplexes.....	15
4.3.2 Quantoplexes	17
4.3.3 Auropolyplexes.....	18
4.3.3.1 Gold nanoparticles	18
4.3.3.2 Surface plasmon resonance	19
4.3.3.3 Gold-thiol bond	20
4.4 Biophysical characterization methods.....	21
4.4.1 UV-VIS spectrophotometry	21
4.4.2 Gel electrophoresis	23
5 Aim of the thesis	25
6 Materials	26
6.1 Chemicals, Reagents	26
6.2 Nucleic Acids	26
6.3 Devices	27
6.4 Materials	27
7 Methods	28
7.1 Overview of projects.....	28
7.2 Effect of serum on <i>in vivo</i> SSO polyplexes.....	29

7.2.1	Workflow	29
7.2.2	Gel Preparation	29
7.2.3	Sample preparation.....	30
7.2.4	Electrophoresis.....	30
7.2.5	Gel imaging.....	30
7.3	Quantoplexes.....	31
7.3.1	Effect of serum on quantoplexes	31
7.3.1.1	Workflow	31
7.3.1.2	Gel Preparation of gel without ethidium bromide.....	31
7.3.1.3	Gel Preparation of gel with ethidium bromide	32
7.3.1.4	Sample preparation	32
7.3.1.5	Electrophoresis	33
7.3.1.6	Gel imaging.....	33
7.3.2	Quantum dots complexation with LPEI.....	34
7.3.2.1	Comparison of old and new quantum dots.....	34
7.3.2.1.1	Workflow	34
7.3.2.1.2	Gel preparation.....	34
7.3.2.1.3	Sample preparation	35
7.3.2.1.4	Polyplexing of quantum dots and LPEI	37
7.3.2.1.5	Electrophoresis	39
7.3.2.1.6	Gel imaging	39
7.3.2.2	Precise estimation of LPEI needed for QD (new batch) complexation	39
7.3.2.2.1	Workflow	39
7.3.2.2.2	Gel preparation.....	40
7.3.2.2.3	Sample preparation	40
7.3.2.2.4	Polyplexing of quantum dots and LPEI	42
7.3.2.2.5	Electrophoresis	44
7.3.2.2.6	Gel imaging	44
7.3.3	Testing stability of only quantum dots (new batch)	44
7.3.3.1	Workflow	44
7.3.3.2	Gel preparation	45
7.3.3.3	Sample preparation.....	45
7.3.3.4	Electrophoresis.....	46
7.3.3.5	Gel imaging.....	46

7.4 Auropolyplexes: Re-Optimization of LPEI-SH coating on gold nanoparticle	47
7.4.1 Workflow.....	47
7.4.2 Working with gold nanoparticles	47
7.4.3 Adjusting the pH of gold nanoparticles solution	48
7.4.4 Coating of gold nanoparticles with LPEI-SH.....	48
7.4.5 Characterization of LPEI-SH coating via UV-VIS spectrometry	49
8 Results and Discussion.....	50
8.1 Effect of serum on <i>in vivo</i> SSO polyplexes.....	50
8.2 Quantoplexes.....	54
8.2.1 Effect of serum on quantoplexes.....	54
8.2.2 Quantum dot complexation with LPEI	56
8.2.2.1 Comparison of old and new quantum dot batches	56
8.2.2.2 Precise estimation of LPEI needed for QD(new batch) complexation.....	57
8.2.3 Testing stability of only quantum dots (new batch)	60
8.3 Auropolyplexes: Re-Optimization of LPEI-SH coating of gold nanoparticles	64
8.3.1 Experiments with a stir-time of 24 hours	65
8.3.1.1 AuNP coating with LEPEI-SH of 1kDa	65
8.3.1.2 AuNP coating with LEPI-SH of 5kDa	75
8.3.2 Experiments with a stir-time of 72 hours	83
8.3.2.1 AuNP coating with LEPI-SH of 1kDa	83
8.3.2.2 AuNP coating with LEPI-SH of 5kDa	87
9 Conclusion and Outlook.....	90
10 References.....	93

1 Abstract

Polyplexes, Quantoplexes and Auropolyplexes belong to the group of non-viral vectors for nucleic acid delivery. They are formed by complexation of nucleic acids with polycations in absence or presence of metals like quantum dots and gold and represent a promising tool for the delivery of nucleic acid therapeutics. This thesis includes three main projects with each of these vectors being a separate project, and the focus is set on analyzing and modifying these vectors.

Polyplexes were formed by complexing nucleic acids like splice switching oligonucleotides with polyethyleneimine (PEI), which were mainly used for *in vivo* experiments for splice correction applications in other projects. Their behavior in serum was analyzed by gel electrophoresis to analyze the protection of nucleic acids against degradation by the polycations used, like cross-linked linear PEI.

Quantoplexes based on cadmium telluride quantum dots, PEI and plasmid DNA, were incubated in serum and similarly analyzed by gel electrophoresis. Furthermore, the complexation of quantum dots and PEI was optimized to improve the stability of quantoplexes.

Auropolyplexes were generated by complexation of gold nanoparticles coated with polyethyleneimine with nucleic acids. An explicit attempt was made to optimize the initial step of gold nanoparticle coating with PEI. In order to make this step reproducible, various parameters were tested and analyzed. UV-VIS spectrophotometry and surface plasmon resonance (SPR) was used to determine whether coating was successful or not.

2 Zusammenfassung

Polyplexe, Quantoplexe und Auropolyplexes gehören zu der Gruppe der nicht-viralen Vektoren für die Verabreichung von Nukleinsäure. Sie werden durch die Komplexierung von Nukleinsäuren mit Polykationen, in Abwesenheit oder Anwesenheit von Metallen wie Quantenpunkte oder Gold, gebildet und sind ein vielversprechendes Mittel für die Verabreichung von Nukleinsäure Therapeutika. Diese Arbeit beinhaltet 3 Hauptprojekte, wobei jeder dieser Vektoren ein eigenes Projekt darstellt und der Schwerpunkt auf der Analyse und Modifizierung dieser Vektoren gerichtet ist.

Polyplexe, welche hauptsächlich für *In vivo* Experimente zur Spleiß Korrektur in anderen Projekten verwendet wurden, wurden durch Komplexierung von Nukleinsäuren, wie Spleiß schaltende Oligonukleotiden, mit Polyethylenimin (PEI) hergestellt. Ihr Verhalten im Serum wurde mittels Gel Elektrophorese untersucht, um analysieren zu können ob die Nukleinsäuren durch die Polykationen, wie vernetztes lineares PEI, vor dem Abbau geschützt wurden.

Quantoplexe, bestehend aus Cadmiumtelluride-Quantenpunkte, PEI und Plasmid DNA, wurden in Serum inkubiert und ebenfalls durch Gel Elektrophorese analysiert. Außerdem wurde die Komplexierung der Quantenpunkte mit PEI optimiert, um die Stabilität der Quantoplexe zu verbessern.

Auropolyplexe wurden durch Komplexierung von mit Polyethylenimin beschichtete Goldnanopartikel mit Nukleinsäuren hergestellt. Es wurde explizit versucht den initialen Schritt des Umhüllens von Goldnanopartikel mit PEI zu optimieren. Um diesen Schritt reproduzierbar zu machen, wurden diverse Parameter untersucht und analysiert. UV-VIS Spektrophotometrie und die Oberflächen Plasmon Resonanz (SPR) wurden verwendet, um aussagen zu können, ob eine Umhüllung erfolgreich war oder nicht.

3 List of abbreviations

ASO	Antisense oligonucleotide
ATP	Adenosine triphosphate
Au	Gold
AuNP(s)	Gold nanoparticle(s)
BPEI	Branched Polyethyleneimine
Cd	Cadmium
CdTe	Cadmium Telluride
Conc	Concentration
Ctrl	Control
DLS	Dynamic light scattering
EtBr	Ethidium Bromide
Exp	Experiment
FCS	Fetal calf serum
HBG	HEPES buffered glucose solution
kDa	Kilo Dalton
LPEI	Linear Polyethyleneimine
Luc	Luciferase
MMCT	Center for Macromolecular Cancer Therapy
mRNA	Messenger RNA
NC	Negative Control
NTA	Nanoparticle Tracking Analysis
N/P ratio	Nitrogen to Phosphate ratio
pDNA	Plasmid DNA
PEG	Polyethylene glycol
PEI	Polyethyleneimine
Px	Polyplexes
QD	Quantum Dots
Qpx	Quantoplexes

RNase	Ribonuclease
RPM	Rounds per minute
SAM	Self-assembled- monolayer
Sec	Second
SH	Sulfhydryl
SPR	Surface plasmon resonance
SSO	Splice switching oligonucleotides
TEM	Transmission electron microscope
UV-VIS	UV-Visible
1M NaOH	1 Molar Sodium hydroxide

4 Introduction

4.1 Nucleic acid therapy

In the past decades nucleic acid-based therapeutics have aroused the interest of many researchers as a new type of biologics. Being able to deliver nucleic acids enables the development of new therapeutics for the treatment of a wide range of diseases, which have been difficult to treat with the therapies available so far, one of those diseases being cancer.¹ Surgery, radiotherapy, and chemotherapeutics are usually the first line therapy for solid cancers. Cure is often not achieved due to dose limitation through toxicity and the occurrence of resistance mechanisms. Through nucleic acid therapy the possibility is offered to create a specific therapy for a particular form of cancer, considering genetic abnormalities in cancer cells (in comparison to healthy tissue).²

Nucleic acid therapy is described as nucleic acids processed as drugs, which are used in the approach to cure diseases on a genetic level.³ As known, different gene mutations are responsible for the development of cancer. The combination of a complex network of signaling pathways and the ability to avoid apoptosis by cancer cells presents a big challenge in the treatment of cancer. Nucleic acids including antisense oligonucleotides, plasmid DNA and other nucleic acids revealed a promising potential in the therapy of cancer.⁴ Specificity, functional diversity and low toxicity is what distinguishes this kind of therapy.⁵ Cells are used as bioreactors where target proteins are synthesized. Therefore, nucleic acids have to be carried into the cytosol or even into the nucleus, which leads to challenges when it comes to choosing the right delivery method.⁶ Fast degradation in blood, low cellular uptake and inadequate endosomal escape are some of the obstacles faced.³ This thesis concentrates on non-viral vectors such as polyplexes, quantoplexes and gold nanoparticles, all formulations which aid in delivering nucleic acids into cells.

4.1.1 Antisense Oligonucleotides

Antisense Oligonucleotides (ASOs) are short, single stranded nucleic acid with 8-50 base pairs in length that are able to bind a targeted mRNA by Watson-Crick pairing.⁵ Basically two groups of ASOs can be defined, namely those inducing degradation of mRNA by RNase H and those

blocking the mRNA sterically and hence preventing the procedure of splicing or the translation process.⁷ The splicing process can be blocked, redirected, or promoted. Therefore, as a therapy option, ASOs can be used to change or correct RNA expression. Additionally, ASOs do not affect the genome directly.⁸

4.1.2 Splice Switching Oligonucleotides (SSO)

Splicing leads to the formation of multiple protein isoforms out of one pre-mRNA, which is important for the variety of the proteome. Though being a key process for normal development, abnormalities in splicing can be the cause for a wide range of diseases. That is why drugs, that are able to influence the splicing process, are needed. To achieve this goal, SSOs have been developed.⁹

SSOs are Antisense Oligonucleotides, that consist of 15-30 nucleotides. They are synthesized to bind pre-mRNA, block it sterically and therefore to inhibit the binding of splicing factors. The main function of SSOs is to achieve changes in the splicing process. Beside the inhibition of splicing, this could either result in exon skipping by binding to a splicing enhancer sequence or to exon inclusion by pairing with a splicing silencer sequence within the pre-mRNA.¹⁰ (See figure 1)

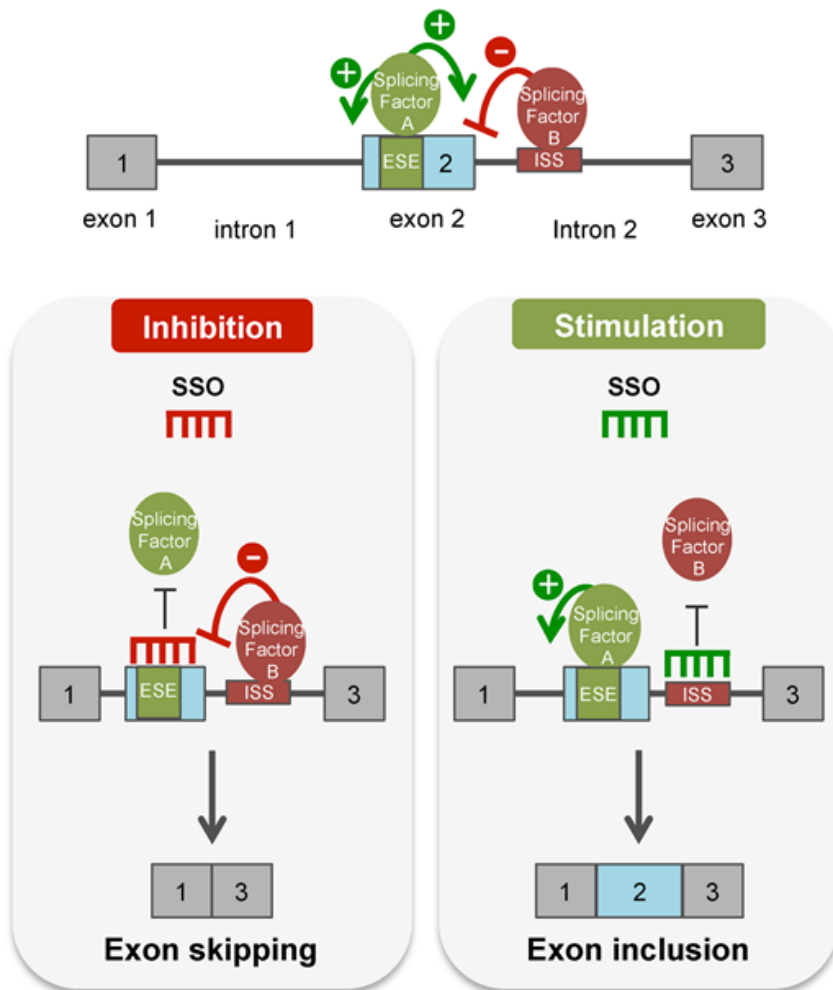


Figure 1: Modulation of splicing by SSOs, from reference⁷

4.1.3 Plasmid DNA

Naked plasmid DNA is the simplest non-viral vector with advantages like low toxicity, easy to design and cost effectively produced. On the other hand, naked pDNA shows a low transfection rate.¹¹ The challenge in the delivery of pDNA and genes in general is to find a way to deliver them to the tumor or target tissue without premature decomposition in the blood. Furthermore, they must be taken up by the target cells and in the case of pDNA, also enter the nucleus. Due to their easy degradation by nucleases some ways have been developed to condense plasmid DNA and prevent degradation. Neutral liposomes, cationic lipids, polycationic carries such as PEI, and hydrophobic polymers such as PEG have been used to prevent degradation in blood, to improve the uptake and transfection rate.^{11,12}

4.2 Challenges of nucleic acid therapy

Gene based therapeutics are aimed for the treatment of many diseases as well as the production of vaccines. Many obstacles need to be overcome when it comes to the development of such therapeutics. The cellular barriers, enzymatic degradation as well as a fast clearance are just a few of them. In order to achieve a sufficient transfer rate of nucleic acids, viral and non-viral vectors come into use. These vectors are necessary, since the administration of unmodified genetic material leads to its fast degradation by various enzymes, affecting the bioavailability of nucleic acids. Furthermore, nucleic acids are poorly taken up into cells due to their hydrophilic properties and high molecular weight.¹³

Another challenge, especially in the case of delivering pDNA in slow-or non-dividing cells, is the nuclear uptake. The uptake depends on two processes, namely on the transport to the nuclear membrane and penetration through the membrane. Larger molecules are not able to penetrate through the nuclear membrane but nucleic acids smaller than 40kDa with a particle size up to 25nm can enter the nucleus passively.¹³

A further hurdle in the application of nucleic acids faced is the release of inflammatory cytokines. By administration of exogenous DNA or RNA the innate immune system is activated, which can cause local and systemic inflammations. Complexation with cationic lipids or polymers often lead to an increased response of the immune system.¹³

4.2.1 Delivery methods for nucleic acids

Many methods have been explored to improve intracellular bioavailability of nucleic acids, including the modification of the chemical structures of nucleic acids and the integration of nucleic acids into viral and non-viral vectors.¹³

4.2.1.1 Viral vectors

There are different ways to deliver nucleic acids, the main groups being viral-vectors and non-viral vectors, such as nanoparticles.¹¹

A viral vector, as already stated in the name, is a specific type of virus used as a vehicle to transport genes into target cells or tissue. They are meant to be the most efficient way for *in*

vivo gene delivery. Adenoviruses, lenti-and retroviruses, vaccinia viruses, adeno associated viruses, and baculoviruses, are the most frequently used viral vectors. The virus used is selected on the basis of immunogenicity, transgene capacity, expression rate, cell tropism and the duration of gene expression.¹¹

A distinction in viral vectors can be made between integrating vectors, where the viral genome is integrated into the host genome, and non-integrating vectors, which do not possess this ability.¹¹

Although viruses have proven to be an efficient method for gene delivery, they have shown disadvantages such as their immunogenicity and inflammatory potential, as well as a fast clearance from the bloodstream, which has led to the search of alternatives, such as synthetic delivery vectors.¹¹

4.2.1.2 Non-viral vectors

Although, viral vectors are a very efficient tool for gene delivery, their numerous drawbacks have led to a large increase in research on non-viral vectors. A major advantage of non-viral vectors is the variety of design options available. They can be easily modified to reach specific targets, such as a particular tissue or target cells, with a high probability of success.

Moreover, by determining the size of the nanoparticles, biodistribution, cellular uptake as well as intracellular transport can be improved too. As with all gene delivery systems, the efficacy of non-viral vectors depends on how well barriers such as cellular uptake, the release from the endosomes, nuclear uptake and subsequent gene expression are overcome.¹¹ This thesis concentrates on metal and polycationic based non-viral vectors.

4.3 Metal and polycationic carriers

4.3.1 Polyplexes

Polyplexes are nanoparticles that are formed due to electrostatic interactions between positive charged polymers like polyethyleneimine (PEI) and negatively charged nucleic acids. PEIs are considered to be the golden standard when it comes to polycationic delivery vectors. One of the reasons is their high cationic charge density (23 μ mol protonable amines per 1mg

of PEI). Polyplexes are incorporated into cells by adsorptive endocytosis. This occurs through binding of the positively charged polyplex surface with negatively charged proteoglycans on the cell surface. Due to the proton sponge effect polyplexes are released from the endosomes. Protons enter the endosomes through an ATP-driven pump and lead to the uptake of chloride ions, which in turn leads to the uptake of water, causing the endosomes to finally burst due to the resulting osmotic imbalance.² (See figure 2)

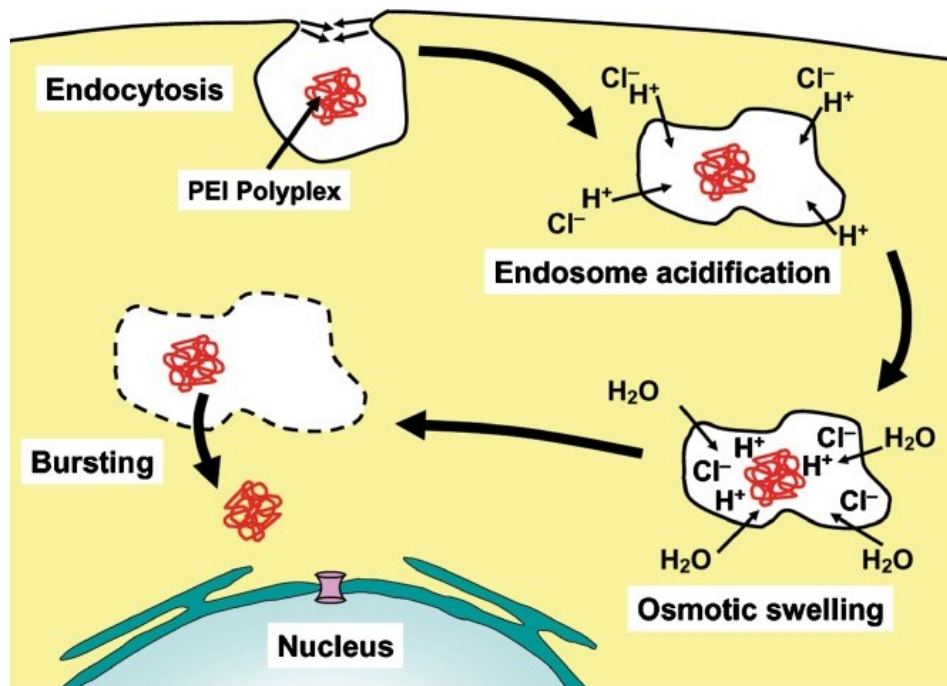


Figure 2: Illustration of the proton sponge effect, from reference.¹⁴

The two existing PEI types that are used in polyplexes are branched polyethyleneimine (BPEI) and linear polyethyleneimine (LPEI) (see figure 3). Whereby LPEI shows a higher transfection rate *in vitro* and *in vivo*.²

PEI can be synthesized in a wide range of molecular weights, with 5-25kDa being the most appropriate for nucleic acid delivery. A higher molecular weight, results in higher toxicity, which most likely is caused by aggregation of PEIs on the external cell membrane, causing necrosis. On the other hand, going lower than 5kDa has shown a low transfection rate. Furthermore, the molecular weight of PEI influences the polyplex size. Higher molecular weight leads to a smaller size. This phenomenon was observed up to a size of 25kDa. No

further reduction took place above 25kDa. Whereas a too low (2kDa) weight shows weakness to form small polyplexes at all. These weight dependencies are valid for both BPEI and LPEI.¹⁵ Besides molecular weight, and PEI type, the solvents properties as well as the N/P ratio play a big role for complexation and further for transfection.¹⁶ The N/P ratio describes the amine to phosphate ratio and hence the amount of PEI and nucleic acid used to form polyplexes.

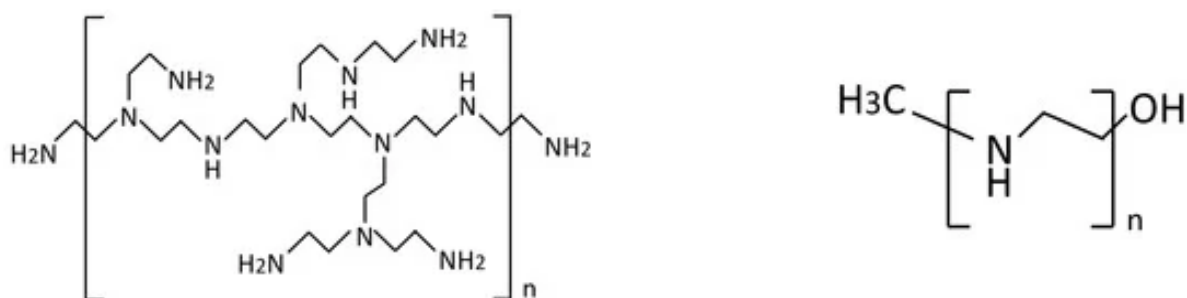


Figure 3: Branched polyethylenimine (left), and linear polyethylenimine (right), from reference.¹⁷

4.3.2 Quantoplexes

Quantoplexes are created by attaching negative charged quantum dots to PEI and plasmid DNA (pDNA). For example, this was done by mixing pDNA and cadmium telluride (CdTe) quantum dots in buffer and adding PEI afterwards. Due to electrostatic interactions virus-sized nanoparticles are formed.¹⁸

However, quantoplexes do not necessarily need DNA carriers. In general, quantoplexes can be formed by negative charged quantum dots binding noncovalently or covalently to self-assembling drug carries, like liposomes, micelles, and others, which allows their tracking in living tissue.^{18,19}

Quantum dots have several advantages compared to conventional organic dyes. In addition to an improved photostability, they show a narrow and tunable emission spectrum.

Another possibility is to produce polyethylene glycol (PEG) shielded quantoplexes, where PEI is replaced by PEG-PEI.¹⁸(See Figure 4)

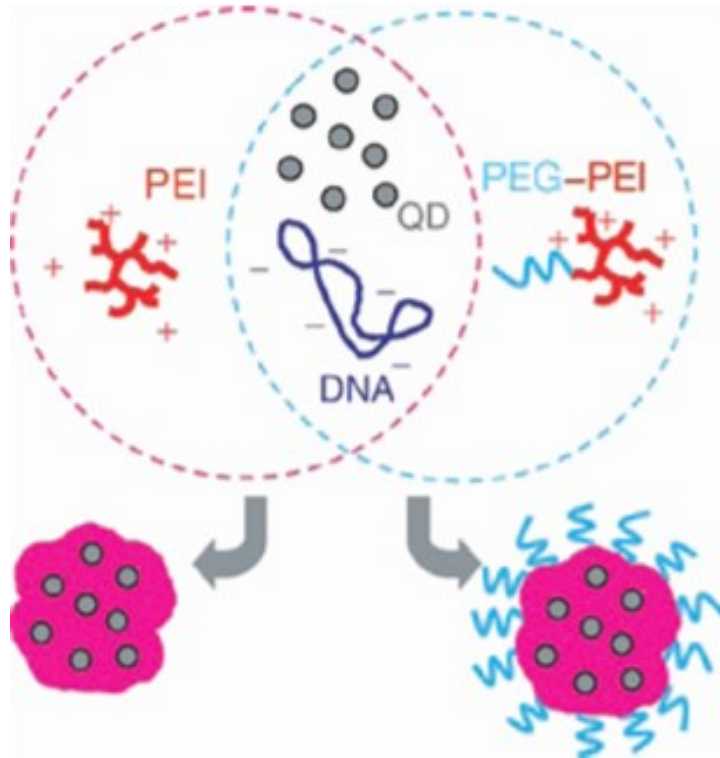


Figure 4: Procedure of quantoplex formation, adapted from reference.¹⁸ CdTe quantum dots are mixed with pDNA. Afterwards PEI is added and quantoplexes are formed. By adding PEG-PEI instead of PEI, PEG-shielded quantoplexes are formed.¹⁸

The idea of shielding comes from PEGylated polyplexes that show reduced blood interactions like aggregation of erythrocytes and plasma protein binding, as well as circulation in the bloodstream. Whereas non shielded BPEI polyplexes have not shown circulation. In fact, it has been shown that PEG-shielded quantoplexes do circulate for a short time (several minutes) compared to non-shielded quantoplexes.¹⁸

4.3.3 Auropolyplexes

4.3.3.1 Gold nanoparticles

As early as 150 years ago, Michael Faraday, who perhaps was the first to notice, found out that colloidal gold solutions have different properties than bulk gold.²⁰

Gold nanoparticles (AuNPs) have been considered as promising vectors for drug and nucleic acid delivery as well as diagnosis of a variety of cancer types. Stability, a high surface area to volume ratio, surface plasmon resonance, surface chemistry and multi-functionalization and the relatively simple synthesis are some of the properties that make gold nanoparticles such attractive tools. Furthermore, AuNPs are non-toxic, non-immunogenicity.^{21,22} Gold nanoparticles can be synthesized in a wide range of sizes. The existence of a negative charge on their surface simplifies modifications.²¹ Ligands with functional groups like thiols, phosphines, and amines, who all have a high affinity for the gold surface can easily be attached to AuNPs. This knowledge can be used to combine gold nanoparticles with oligonucleotides, proteins, and antibodies.²⁰

Gold nanoparticles can be synthesized in many ways. Normally starting with $\text{HAu}^{\text{III}}\text{Cl}_4$, following the reduction of Au^{III} to Au^0 in water by using citrate. This method was first introduced by Turkevich et al. in 1951 and is still used because it enables the replacement of the citrate ligands by ligands of scientific interest.²³ The citrate can be replaced by thiolated ligands by the establishment of a gold-thiol bond.²⁰ Peptides, polymers, oligonucleotides among others can be easily anchored to gold nanoparticles by taking advantage of this bond.²³ The resulting size of the gold nanoparticles (using the method by Turkevich) is about 20 nm. In 1973 a modification of this method was introduced by Frens, which made it possible to create AuNPs in sizes from 16-147 nm by variation of the citrate-to-gold ratio.²⁴

4.3.3.2 Surface plasmon resonance

One of the properties that made gold nanoparticles so interesting for nanoscience is the surface plasmon resonance (SPR).²⁵

Spherical gold nanoparticles develop different colors in water, depending on their size, and show a size-dependent absorption peak between 500-550nm. Aggregation for example leads to a red-shift of SPR frequency and to a color change of the solution from red to blue. The absorption band results from the fact that incident light with a certain resonance excites the electrons of the gold nanoparticles to oscillate collectively. This phenomenon is absent in nanoparticles < 2nm as well as bulk material.²⁶ Factors that affect the electron charge density on the surface of the nanoparticles impact the SPR band intensity and wavelength.²⁷

It depends on size, shape, solvent, surface ligand, core charge, temperature as well as the proximity between nanoparticles.²⁶

The Mie theory describes the SPR as electromagnetic frequency (light) that leads to the oscillation of free electrons on the surface of spherical nanoparticles (if the light's wavelength is larger than the nanoparticles size).²³

The electron density oscillates in resonance with the frequency of the passing light. After the light passes the AuNP solution, an energy loss occurs due to absorption and scattering processes. Absorption and scattering spectroscopy enable to monitor any changes in size or shape by investigating the condition of the resonance. Due to high light absorption induced by the SPR it can be measured by using UV-VIS spectroscopy. Changes in the surface geometry, such as size, shape and structure, among others, lead to changes in the electron density. That again results in changes of the frequency the electrons oscillate with, whereby absorption and scattering also alter. This specific frequency, where the amplitude of the oscillation achieves its maximum is called the surface plasmon resonance.^{27,28}

4.3.3.3 Gold-thiol bond

Stabilizing AuNPs can be done in many ways but using thiols has proven to be the strongest method to do so.²³ Soft bases like thiol groups have a high affinity for gold and therefore are used to modify the gold surface. Alkanethiols, with additional head groups such as carboxylic acids for example, interact with the gold surface, leading to a stable self-assembled monolayer (SAM) around the gold nanoparticle.²⁹

A rupture force between 1.4 +/- 0.3 nN was detected by Glaub et al. for a single gold-sulfur bond.³⁰ This unique and very strong bond, between gold and thiols, which is usually induced by the SH (sulfhydryl) group in thiols, is in the focus of a large number of studies. It has a strength that is comparable to the strength of the gold-gold bond.³¹

Initially the bond between the -SH-group and the gold surface is formed and subsequently the S-H bond is separated, leading to a thiyl radical, which finally results in a covalent bond between gold and sulfur.³⁰

Besides stabilization the bond between gold and thiols can be exploited to achieve a series of bioconjugations.²³

It was observed that gold nanoparticles, which are protected by thiols could be stable for years without aggregating. Although they precipitate after some time, they redissolve easily.³²

In this thesis AuNPs were functionalized with thiolated LPEI (LPEI-SH) to form cationic nanoparticles.³³ (See figure 5)

This was done to optimize the initial step in the production of auropolyplexes.

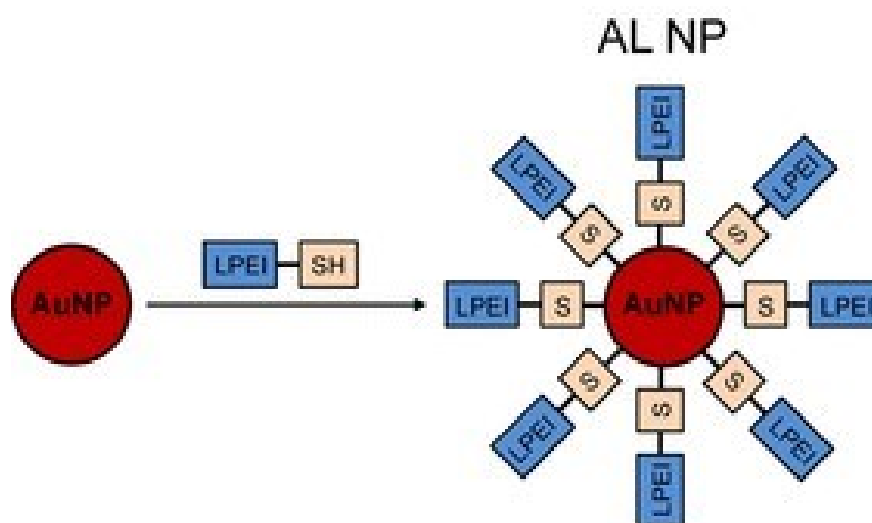


Figure 5: Coating of AuNP with LPEI-SH, from reference³³

4.4 Biophysical characterization methods

4.4.1 UV-VIS spectrophotometry

The most frequently used method to gain data regarding size and size distribution of AuNPs is the transmission electron microscopy (TEM). But when a fast and real-time measurement of gold nanoparticle size, and data about aggregation and concentration is needed, TEM is not the method to go with. In addition, the preparation of the samples is time-consuming which can lead to changes in the nanoparticles size and shape.³⁴

As described before the interest in AuNPs comes from several properties that distinguishes them, mostly their SPR. ³⁴ Using UV-VIS spectroscopy an absorbance band in the visible region

caused by the SPR of AuNPs is measurable.³⁵ Changes in size, shape and aggregation of gold nanoparticles cause changes in the SPR which results in changes of the extinction spectrum received.³⁴ (See figure 6)

UV-VIS instruments are found in almost every laboratory and enable measurements of all the above mentioned parameters. Furthermore, the procedure does not affect the samples and the implementation is done in a short time.³⁴

However, TEM, and Dynamic light scattering (DLS) instruments allow to achieve the best accuracy when it comes to size measurements of AuNPs, but due to high costs these devices are often not available and hence UV-VIS spectroscopy represents a good alternative.³⁶

Modifications of the gold nanoparticle surface, such as the binding of ligands can also be monitored by UV-VIS and are shown as a red shift of a few nanometers in the SPR spectrum.³⁵

Within this thesis, the obtained UV-VIS data was used to estimate whether the coating of the AuNPs was successful or not. Also, a suspected aggregation of the samples would be displayed in the received spectrum if present.

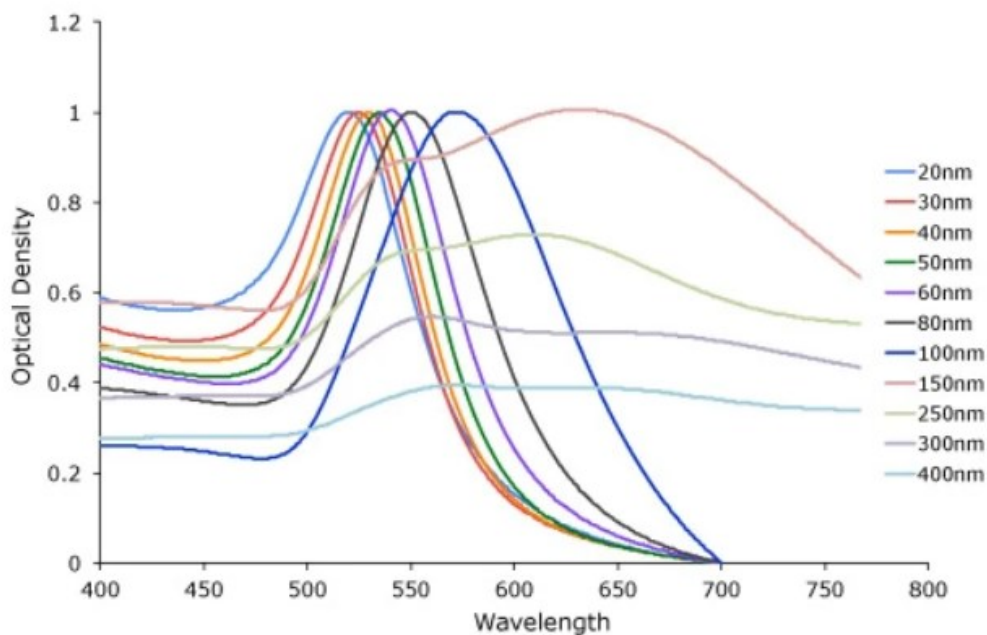


Figure 6: Differences in wavelength of gold nanoparticles due to changes of size and therefore SPR, from reference³⁵

4.4.2 Gel electrophoresis

Gel retardation is a widely used tool for the study of protein-nucleic acid interactions.³⁷ Moreover it is used to analyze the interaction between nucleic acids and any kind of material nucleic acids are bind to.

Agarose gel electrophoresis is commonly used to separate nucleic acids according to their size, by using an electric field, which allows negatively charged molecules to migrate to the positive electrode. Depending on their weight, the molecules migrate at different speeds, whereby the speed increases with lower molecular weight.³⁸

Agarose is composed of agarobiose subunits and is isolated from seaweed. While it gelates it forms a network of non-covalently associated agarose polymers, generating pores, which act as a sieve for the different molecules passing the gel. The pores size is determined by the concentration of agarose. As the concentration increases, the pore size decreases. Other factors that influence the migration rate of the molecules besides the agarose concentration are the molecule size and structure of the agarose, the voltage applied, the presence of ethidium bromide, the type of agarose as well as the buffer used.³⁹

If an appropriate dye has been applied the nucleic acids can be visualized with appropriate devices by exposing the gel with UV light³⁹

By including "ladders" in the gel, which are basically samples containing (nucleic acid) molecules of a known size, the sizes of the unknown molecules can be estimated by comparing the migration distances.⁴⁰

Agarose gel electrophoresis is very popular due to some benefits, such as easy handling and the possibility to store the resulting gel in a refrigerator. Moreover, the possibility to recover samples, by extracting them from the gel, as well as the fact that nucleic acids are not chemically changed during the process.³⁸

Most of the time this method is used for qualitative purposes, even though under certain conditions gel electrophoresis can provide quantitative data as well.⁴¹

The dye that is usually used for visualizing nucleic acids is ethidium bromide.³² In its free form it already shows background fluorescence but after binding to nucleic acids ethidium bromides fluorescence intensity increases significantly.⁴²

Ethidium bromide binds nucleic acids by intercalating between base pairs. The binding leads to changes in weight, charge, confirmation, and flexibility of the molecules.⁴³

When exposed to UV light, the maximum fluorescence emission of ethidium bromide between 500-590nm.³⁸

Due to the potential threats to human health, there are safer dyes available nowadays, although they still are not able to replace ethidium bromide because of several drawbacks.⁴²

5 Aim of the thesis

This thesis focuses on three different main projects, with the goal to test and/or optimize different non-viral vectors for nucleic acid delivery. The non-viral vectors dealt with in this work are polyplexes, quantoplexes and auropolyplexes.

The first project's aim was to test the effect of serum on SSO polyplexes that were used in *in vivo* experiments. Attention was paid to whether SSOs are protected by the polyplexes or whether SSOs get released and degraded by the serum or bound to components of the serum.

In the second project the focus was set on quantoplexes, with the aim to achieve a stable quantoplex formulation. For this, three different subprojects with three different goals have been carried out.

- The first goal was to find out if serum affects the quantoplexes or not and investigate if quantoplexes get degraded or bound to components of the serum.
- The second goal was to find the right amount of LPEI needed for the optimum quantoplexation with quantum dots.
- The third goal was to test the stability of the quantum dots alone to find out if the basis for the whole project is sound.

The third project's aim was to optimize the coating of gold nanoparticles with LPEI-SH, which is the initial step in the production of auropolyplexes. Surface plasmon resonance (SPR) from gold nanoparticles was employed as a quick screening tool to study this coating step as a function of different parameters like pH, duration of stirring, and molecular weight of thiolated polymer. UV-VIS spectroscopy was done to document the SPR peak and absorption profile to see if the LPEI-SH coating outcome was successful or aggregation.

6 Materials

6.1 Chemicals, Reagents

- Agarose
- Aqua Regia
- AuNP solution
- Ethidium bromide (Sigma-Aldrich)
- MilliQ-Water (Sartorius)
- HBG buffer (20mM HEPES, 5% Glucose, pH = 7.4, sterile filtrated)
- Linear polyethyleneimine (LPEI 10kDa; made by AT/FI) in H₂O
- LPEI-SH 1kDa / 5kDa (20 mg/ml in MilliQ; made by SD)
- Purple ladder (FastRuler Middle Range DNA Ladder™ by Thermo Scientific)
- Mercaptopropionic acid capped CdTe Quantum Dots were a kind gift from Prof. Rogach
- Serum (FCS): Bovine serum albumin (Sigma-Aldrich)
- 1M NaOH
- 20x SB Buffer (Sodium borate buffer, 4.8% boric acid, 0.8% NaOH, adjusted to pH = 8.0-8.2)

6.2 Nucleic Acids

- Antisense oligonucleotides (Luc SSO, NC SSO; GSK Medicines Research Centre, Stevenage, UK) synthesized by Glynn Williams and Jonathan Northall as part of their contribution to the EU funded IMI project COMPACT.
- pDNA pCpG-hCMV-EF1a-LucSH

6.3 Devices

- Arium® pro VF (Sartorius)
- ChemiDoc MP Imaging System (Bio-Rad)
- Power supplies (PowerPac™; Bio-Rad)
- GeneQuant™ 1300 Spektrophotometer (Biochrom™)
- Magnetic stirrer (Heidolph Instruments)
- Microwave
- Mini Centrifuge (Thermo Scientific™)
- NanoVue Plus Spektrophotometer (Biochrom™)
- ThermoMixer® (Eppendorf)
- Vortex Mixer (Velp Scientific)

6.4 Materials

- Centrifuge Tube 15 ml (CT-15) (Starlab)
- Centrifuge Tube 50 ml (CT-50) (Starlab)
- Eppendorf Research® plus pipettes
- Eppendorf® tubes (Nerbe Plus GmbH)
- Pipette tips (Nerbe plus GmbH)
- Syringe
- Syringe filters, cellulose acetate, 0.22 µm (VWR)
- UV-cuvette [semi]-micro (Brand GmbH)

7 Methods

7.1 Overview of projects

Effect of serum on in vivo SSO polyplexes

- a) Naked SSOs compared to Polyplexed SSOs
- b) Behaviour in HBG compared to behaviour in Serum
- c) 30 minute incubation compared to 4 hour incubation

Quantoplexes

- a) Effect of serum on Quantoplexes
- b) Complexation of Quantum Dots and LEPI to re-optimize the amount of Quantum Dots needed for Quantoplexation
- c) Testing of only Quantum Dots to check their stability

Auropolyplexes: Re-optimization of LPEI-SH coating of gold nanoparticles

- a) Coating with LPEISH 1kDa compared to coating with LPEISH 5kDa
- b) Gold nanoparticle solution with pH 5-6, pH 7-8, pH 8-9
- c) C1 (25µl of LPEISH) vs. C2 (50µl of LPEISH) vs. C3 (100µl of LPEISH)

Figure 7: Overview of the projects, subprojects, and parameters in this thesis

7.2 Effect of serum on *in vivo* SSO polyplexes

7.2.1 Workflow

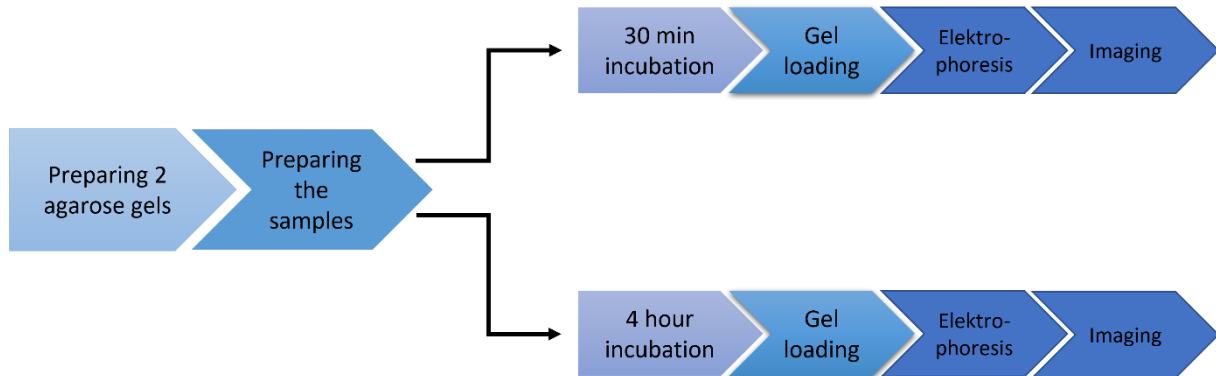


Figure 8: Workflow of SSO polyplex project

7.2.2 Gel Preparation

Firstly, nitrile gloves and protection glasses needed to be put on due to working with ethidium bromide. To ensure security two gloves on each hand were used. The equipment was cleaned and dried before starting to prepare the gel, to make sure it is free from anything that could affect the electrophoresis. The installation was prepared by placing the gel cast correctly into the cast holder by ensuring it sits exactly horizontally. Depending on the desired number of wells an appropriate comb was added to the gel cast.

To get a 1.5 % agarose gel, 1.8g agarose was mixed with 120ml of 1xSB buffer. Agarose was dissolved by microwaving the mixture for about 1 minute for about 3-4 times until the liquid was clear. The solution was cool downed for approx. 30-60 sec. Afterwards 4.2 μ l ethidium bromide were gently added and homogenized by gently shaking the flask.

The solution was gently poured into the gel cast that was previously prepared and air bubbles were gently removed. After gelation the comb was removed, and the gel cast was transferred into the electrophoresis-chamber. 1x SB buffer was poured into the chamber up to the mark so the gel was fully covered by buffer. Two gels were prepared since two different incubation times were tested with two groups of samples. Now the samples could be prepared.

7.2.3 Sample preparation

Table 1 gives an overview of how the samples were prepared before they were loaded on the gel. The samples were prepared in doubles. The first group of samples were incubated for 30 minutes at 37°C and 300RPM. The doubles were incubated for 4 hours at 37°C and 300RPM. For incubation, an Eppendorf thermomixer was used. After the according incubation each sample was mixed with 4µl of 60% glycerol by up and down pipetting. A total of 24µl of each sample were loaded on a previously prepared agarose gel. In addition, a purple DNA ladder was also loaded onto the gel.

Table 1: Sample preparation for the SSO polyplex project

	Amount Sample	Amount HBG	Amount Serum	Final amount of SSO	Volume
Serum	-	10µl	10µl	-	20µl
Naked SSO in HBG	10µl	10µl	-	400ng	20µl
Naked SSO in Serum	10µl	-	10µl	400ng	20µl
Px 1 (HBG)	10µl	10µl	-	400ng	20µl
Px 1 (Serum)	10µl	-	10µl	400ng	20µl
Px 2 (HBG)	10µl	10µl	-	400ng	20µl
Px 2 (Serum)	10µl	-	10µl	400ng	20µl

7.2.4 Electrophoresis

After the samples, as well as the DNA ladder were pipetted into the wells, the lid of the electrophoresis unit was attached to the chamber and the device was connected to a power supply. Each gel was run for 40 minutes at 80 Volt.

7.2.5 Gel imaging

After the electrophoresis, the gel was imaged by using the ChemiDoc MP imager. To make sure the whole gel was captured the gel was placed correctly (centrally) on the transilluminator. Ethidium bromide was selected as chemiluminescent substance and the desired image size was set. The first image was taken with auto-detection, which led to a

perfectly exposed image. To see how the intensity of the signal changes the exposure time was changed manually for additional images.

7.3 Quantoplexes

7.3.1 Effect of serum on quantoplexes

7.3.1.1 Workflow

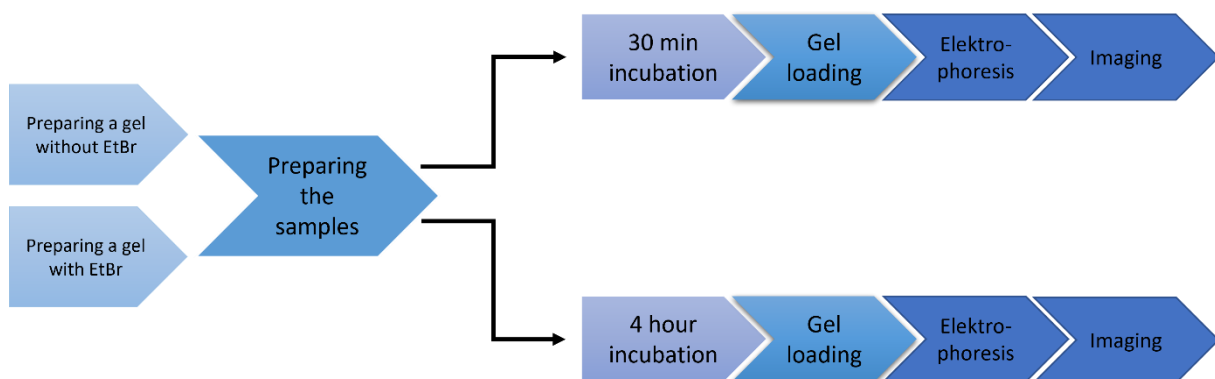


Figure 9: Workflow of the quantoplex project: Effect of serum on quantoplexes

7.3.1.2 Gel Preparation of gel without ethidium bromide

To ensure security two gloves on each hand were used. All parts that were used for the gel preparation had to be cleaned properly and left in water and soap over night to make sure all ethidium bromide from previously done experiments was removed and to make sure it is free from anything that could affect the electrophoresis. The installation was prepared by placing the gel cast correctly into the cast holder by ensuring it sits exactly horizontally. Depending on the desired number of wells an appropriate comb was added to the gel cast. A 0.75 % agarose gel was prepared by mixing 0.9g agarose with 120ml of 1xSB buffer. Agarose was dissolved by microwaving the mixture for about 1 minute for about 3-4 times until the liquid was clear. The solution was cool downed for approx. 30-60 sec. The solution was gently poured into the gel cast that was previously prepared and air bubbles were gently removed. After gelation the comb was removed, and the gel cast was transferred into the electrophoresis-chamber. 1x SB

buffer was poured into the chamber up to the mark so the gel was fully covered by buffer. Now the samples could be prepared.

7.3.1.3 Gel Preparation of gel with ethidium bromide

Firstly, nitrile gloves and protection glasses needed to be put on due to working with ethidium bromide. To ensure security two gloves on each hand were used. The equipment was cleaned and dried before starting to prepare the gel, to make sure it is free from anything that could affect the electrophoresis. The installation was prepared by placing the gel cast correctly into the cast holder by ensuring it sits exactly horizontally. Depending on the desired number of wells an appropriate comb was added to the gel cast. A 0.75 % agarose gel was prepared by mixing 0.9g agarose with 120ml of 1xSB buffer. Agarose was dissolved by microwaving the mixture for about 1 minute for about 3-4 times until the liquid was clear. The solution was cool downed for approx. 30-60 sec. Afterwards 4.2µl ethidium bromide were gently added and homogenized by gently shaking the flask. The solution was gently poured into the gel cast that was previously prepared and air bubbles were gently removed. After gelation the comb was removed, and the gel cast was transferred into the electrophoresis-chamber. 1x SB buffer was poured into the chamber up to the mark so the gel was fully covered by buffer. Two gels were prepared since two different incubation times were tested with two groups of samples. Now the samples could be prepared.

7.3.1.4 Sample preparation

Table 2 gives an overview of how the samples were prepared before loading them on the gel. The Samples were prepared in doubles, to be able to load each sample on each gel. All samples were incubated for 30 minutes at 37°C and 300 RPM. For incubation, an Eppendorf thermomixer was used. Afterwards each serum sample was mixed with 4µl of 60% glycerol, and all other samples were mixed with 8µl of 60% glycerol, by up and down pipetting. One serum sample was loaded on each gel and 24µl of each other sample was loaded on each gel.

Table 2: Sample preparation for the quantoplex project

	Amount Sample	Amount HBG	Amount Serum	Volume
Serum	-	10µl	10µl	20µl
Serum	10µl	10µl	-	20µl
pDNA	20µl	20µl	-	40µl
pDNA	20µl	-	20µl	40µl
Quantum dots	20µl	20µl	-	40µl
Quantum dots	20µl	-	20µl	40µl
Quantoplexes	20µl	20µl	-	40µl
Quantoplexes	20µl	-	20µl	40µl

7.3.1.5 Electrophoresis

After the samples were pipetted into the wells, the lid of the electrophoresis unit was attached to the chamber and the device was connected to a power supply. Each gel was run for 40 minutes at 80 Volt.

7.3.1.6 Gel imaging

After the electrophoresis the gel was imaged by using the ChemiDoc MP imager. To make sure the whole gel was captured the gel was placed correctly (centrally) on the transilluminator. Ethidium bromide was selected as chemiluminescent substance (also when imaging the gel where no ethidium bromide was used) and the desired image size was set. The first image was taken with auto-detection, which led to a perfectly exposed image. To see how the intensity of the signal changes the exposure time was changed manually for additional images.

7.3.2 Quantum dots complexation with LPEI

7.3.2.1 Comparison of old and new quantum dots

7.3.2.1.1 Workflow

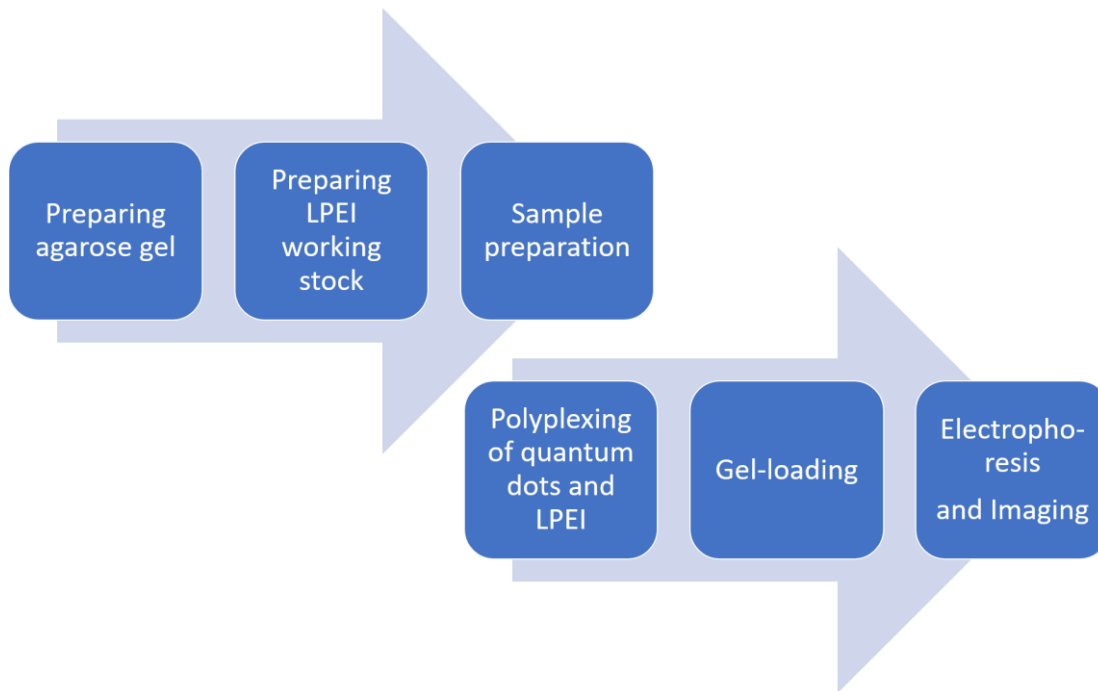


Figure 10: Workflow of the quantoplex project: Comparison of old and new quantum dots

7.3.2.1.2 Gel preparation

Firstly, nitril gloves needed to be put on and all parts that were used for the gel preparation had to be cleaned properly and left in water and soap over night to make sure all ethidium bromide from previously done experiments was removed and to make sure it is free from anything that could affect the electrophoresis. The installation was prepared by placing the gel cast correctly into the cast holder by ensuring it sits exactly horizontally. Depending on the desired number of wells an appropriate comb was added to the gel cast. A 0.75 % agarose gel was prepared by mixing 0.9g agarose with 120ml of 1xSB buffer. Agarose was dissolved by microwaving the mixture for about 1 minute for about 3-4 times until the liquid was clear. The solution was cool downed for approx. 30-60 sec. The solution was gently poured into the gel cast that was previously prepared and air bubbles were gently removed. After gelation the

comb was removed, and the gel cast was transferred into the electrophoresis-chamber. 1x SB buffer was poured into the chamber up to the mark so the gel was fully covered by buffer. Now the samples could be prepared.

7.3.2.1.3 Sample preparation

LPEI working stock and dilutions preparation

From a LPEI mother stock a LPEI working stock with a concentration of 128ng/μl (128μg/ml) was prepared by diluting the right amount of the mother stock in HBG buffer. The working stock was used to prepare further LPEI dilutions (see table 3). While making all the dilutions the stocks were mixed after each step by vortexing and spin down. The following table shows how the dilutions were prepared and what concentration each dilution had.

Table 3: LPEI dilutions preparation by using a previously prepared working stock.

Conc (ng/μl)	Volume taken from working stock (μl)	HBG(μl)	Final volume after mixing (μl)	
64	40	40	80	
	Volume to be taken from preceding dilution (μl)			LPEI stock tube name
32	40	40	80	L1
16	40	40	80	L2
8	40	40	80	L3
4	40	40	80	L4
2	40	40	80	L5

Two groups of tubes were prepared. Apart from a control that was added in the first group (table 4), the two groups are identical. Within each group the tubes differ in the amount of LPEI. Table 4 and 5 show how each group was prepared.

Table 4: LPEI tubes preparation for the polyplexing process with the old quantum dots stock.

Tube name	Stock taken from (Concentration of the stock)	Volume taken (μl)	HBG(μl)	LPEI amount in the taken volume (ng)
L-A1	L5 (2ng/ μl)	10	-	20
L-B1	L4 (4ng/ μl)	10	-	40
L-C1	L3 (8ng/ μl)	7.5	2.5	60
L-D1	L3 (8ng/ μl)	10	-	80
L-E1	L2 (16ng/ μl)	6.25	3.75	100
L-F1 (control)	L2 (16ng/ μl)	6.25	3.75	100

Table 5: LPEI tubes preparation for the polyplexing process with the new QD stock

Tube name	Stock taken from (Concentration of the stock)	Volume taken (μl)	HBG(μl)	LPEI amount in the taken volume (ng)
L-A2	L5 (2ng/ μl)	10	-	20
L-B2	L4 (4ng/ μl)	10	-	40
L-C2	L3 (8ng/ μl)	7.5	2.5	60
L-D2	L3 (8ng/ μl)	10	-	80
L-E2	L2 (16ng/ μl)	6.25	3.75	100

Quantum dots stock and tubes preparation for polyplexation with LPEI

From the quantum dots mother stocks (QD-stock C) that were provided by Dr. Haider Sami, working stocks were prepared in the following way:

Preparation of working Stock QD1-Stock D from QD1-StockC (old quantum dots):

- Take 36.4 μl HBG in an Eppi
- Add 33.6 μl of QD1-Stock C
- \rightarrow Vortex

Preparation of working Stock QD2-Stock D from QD2-StockC (new quantum dots):

- Take 36.4 μl HBG in an Eppi
- Add 33.6 μl of QD2-Stock C
- \rightarrow Vortex

Afterwards from each QD-Stock D a group of quantum dots tubes were prepared as shown in table 6 and 7.

Table 6: Preparation of a group of tubes with quantum dots from the old stock (QD1-StockC) for the polyplexing process with LPEI.

Tube name	Stock taken from	Volume taken (in μl)
Q-A1	QD1-stock-D	10
Q-B1	QD1-stock-D	10
Q-C1	QD1-stock-D	10
Q-D1	QD1-stock-D	10
Q-E1	QD1-stock-D	10
Q-F1 (control)	QD1-stock-D	10

Table 7: Preparation of a group of tubes with quantum dots from the new stock (QD2-StockC) for the polyplexing process with LPEI.

Tube name	Stock taken from	Volume taken (in μl)
Q-A2	QD2-stock-D	10
Q-B2	QD2-stock-D	10
Q-C2	QD2-stock-D	10
Q-D2	QD2-stock-D	10
Q-E2	QD2-stock-D	10
Q-F2 (control)	QD2-stock-D	10

7.3.2.1.4 Polyplexing of quantum dots and LPEI

After every LPEI and quantum dots tube was prepared polyplexing was done by using the flash pipetting method. For that, a 20 μl Eppendorf pipette was adjusted to 15-18 μl . To make sure that the pipette would not get damaged while flash pipetting, pipette tips with filter were used. For each polyplexing process 10 μl of a desired LPEI dilution have been mixed with 10 μl of quantum dots. To avoid air in the tip 10 μl of LPEI were carefully taken up with the previously adjusted pipette. The LPEI was mixed with the quantum dots by fast up and down pipetting (=flash pipetting). When all quantoplexes were done, 4 μl of 60% glycerol was added into each tube of quantoplexes. From those 24 μl , that were in each tube, 20 μl were loaded into a separate well on the previously prepared agarose gel (see table 8).

Table 8: Overview of how the final samples were prepared.

N	LPEI tube name	Volume of LPEI it has (μ l)	QD tube name	volume of QD it has (μ l)	HBG added (μ l)	Glycerol (μ l)	Loaded onto gel (μ l)	Well no
	L-F1	10	-	-	10	4	20	1
	-	-	-	-	-	-	-	2
	-	-	Q-F1 (ctrl)	10	10	4	20	3
	L-A1	10	Q-A1	10	-	4	20	4
	L-B1	10	Q-B1	10	-	4	20	5
	L-C1	10	Q-C1	10	-	4	20	6
	L-D1	10	Q-D1	10	-	4	20	7
	L-E1	10	Q-E1	10	-	4	20	8
	-	-	-	-	-	-	-	9
	-	-	Q-F2 (ctrl)	10	10	-	-	10
	L-A2	10	Q-A2	10	-	4	20	11
	L-B2	10	Q-B2	10	-	4	20	12
	L-C2	10	Q-C2	10	-	4	20	13
	L-D2	10	Q-D2	10	-	4	20	14
	L-E2	10	Q-E2	10	-	4	20	15

7.3.2.1.5 Electrophoresis

After the samples were pipetted into the wells, the lid of the electrophoresis unit was attached to the chamber and the device was connected to a power supply. Each gel was run for 45 minutes at 80 Volt.

7.3.2.1.6 Gel imaging

After the electrophoresis the gel was imaged by using the ChemiDoc MP imager. To make sure the whole gel was captured the gel was placed correctly (centrally) on the transilluminator. Ethidium bromide was selected as chemiluminescent substance (though no ethidium bromide was used) and the desired image size was set. The first image was taken with auto-detection, which led to a perfectly exposed image. To see how the intensity of the signal changes the exposure time was changed manually for additional images.

7.3.2.2 Precise estimation of LPEI needed for QD (new batch) complexation

7.3.2.2.1 Workflow

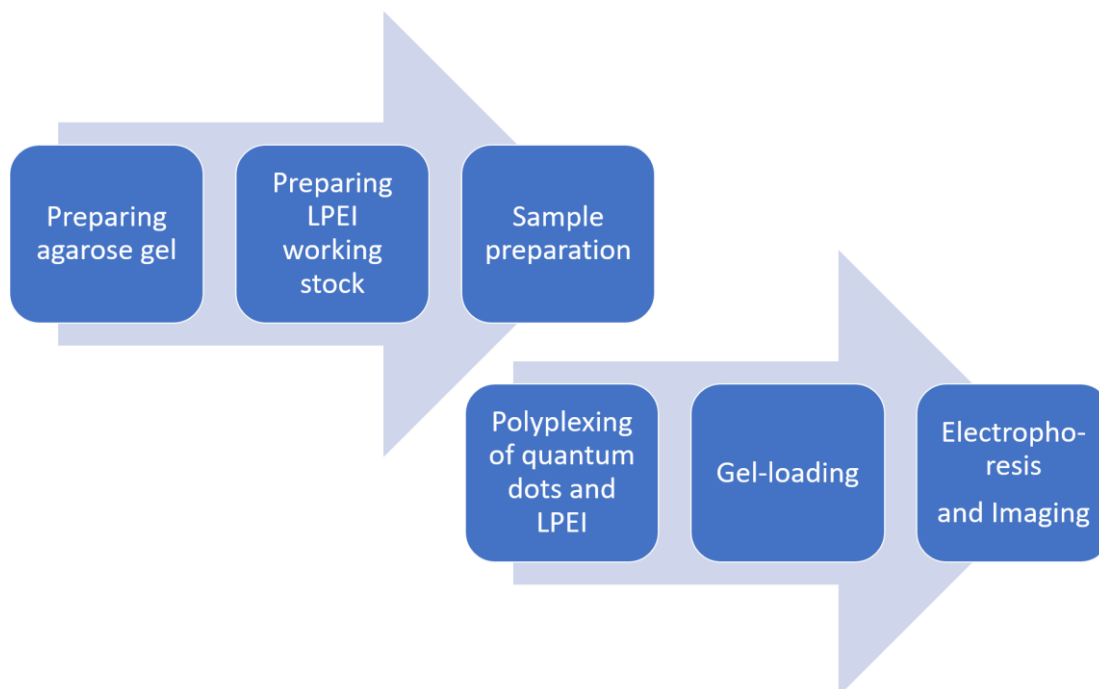


Figure 11: Workflow of the quantoplex project: Precise estimation of LPEI needed for complexation with new QD

7.3.2.2.2 Gel preparation

Firstly, nitril gloves needed to be put on and all parts that were used for the gel preparation had to be cleaned properly and left in water and soap over night to make sure all ethidium bromide from previously done experiments was removed and to make sure it is free from anything that could affect the electrophoresis. The installation was prepared by placing the gel cast correctly into the cast holder by ensuring it sits exactly horizontally. Depending on the desired number of wells an appropriate comb was added to the gel cast. A 0.75 % agarose gel was prepared by mixing 0.9g agarose with 120ml of 1xSB buffer. Agarose was dissolved by microwaving the mixture for about 1 minute for about 3-4 times until the liquid was clear. The solution was cool downed for approx. 30-60 sec.

The solution was gently poured into the gel cast that was previously prepared and air bubbles were gently removed. After gelation the comb was removed, and the gel cast was transferred into the electrophoresis-chamber. 1x SB buffer was poured into the chamber up to the mark so the gel was fully covered by buffer.

Now the samples could be prepared.

7.3.2.2.3 Sample preparation

LPEI working stock and dilutions preparation

From a LPEI mother stock a working stock with a concentration of 128ng/μl (128μg/ml) was prepared by diluting the right amount of the mother stock in HBG buffer. The working stock was used to prepare further LPEI dilutions (see table 9). While making all the dilutions the stocks were mixed after each step by vortexing and spin down. The following table shows how the dilutions were prepared and what concentration each dilution had.

Table 9: LPEI dilutions preparation by using a previously prepared working stock

Conc (ng/ μ l)	Volume taken from working stock (μ l)	HBG(μ l)	Final volume after mixing (μ l)	
64	60	60	120	
	Volume to be taken from preceding dilution (μ l)			LPEI stock tube name
32	60	60	120	L1
16	60	60	120	L2

LPEI tubes preparation for polyplexation with new quantum dots

A group of tubes were prepared by using the LPEI dilutions and HBG buffer. The tubes differ in the amount of LPEI (see table 10)

Table 10: LPEI tubes preparation for the polyplexing process with the new QD stock

Tube name	Stock taken from (Concentration of the stock)	Volume taken (μ l)	HBG(μ l)	LPEI amount in the taken volume (ng)
L-A1	L2 (16ng/ μ l)	4.06	5.94	65
L-B1	L2 (16ng/ μ l)	4.38	5.62	70
L-C1	L2 (16ng/ μ l)	4.7	5.3	75
L-D1	L2 (16ng/ μ l)	5	5	80
L-E1	L2 (16ng/ μ l)	5.3	4.7	85
L-F1	L2 (16ng/ μ l)	5.62	4.38	90
L-G1	L2 (16ng/ μ l)	5.94	4.06	95
L-H1	L2 (16ng/ μ l)	6.26	3.74	100
L-I1	L2 (16ng/ μ l)	6.56	3.44	105
L-J1	L2 (16ng/ μ l)	6.88	3.22	110
I-K1(control)	L2 (16ng/ μ l)	6.88	3.22	110

Quantum dots stock and tubes preparation for polyplexation with LPEI

From the quantum dots mother stocks (QD-stock C) that were provided by Dr. Haider Sami, working stocks were prepared in the following way:

Dr. Haider Sami gave me the QD mother stock with a concentration of 2.21 μ g/ml Cd:

Preparation of working Stock QD2-Stock D from QD2-StockC:

- Take 62.4 μ l HBG in an Eppi
- Add 57.6 μ l of QD2-Stock C

- → Vortex

From the working stock QD2-Stock D tubes were prepared for the polyplexing process with LPEI (see table 11)

Table 11: Preparation of a group of tubes with quantum dots from the new stock (QD2-StockC) for the polyplexing process with LPEI.

Tube name	Stock taken from	Volume taken
Q-A2	QD2-stock-D	10
Q-B2	QD2-stock-D	10
Q-C2	QD2-stock-D	10
Q-D2	QD2-stock-D	10
Q-E2	QD2-stock-D	10
Q-F2	QD2-stock-D	10
Q-G2	QD2-stock-D	10
Q-H2	QD2-stock-D	10
Q-I2	QD2-stock-D	10
Q-J2	QD2-stock-D	10
Q-K2 (control)	QD2-stock-D	10

7.3.2.2.4 Polyplexing of quantum dots and LPEI

After every LPEI and quantum dots tube was prepared polyplexing was done by using the flash pipetting method. For that a 20µl Eppendorf pipette was adjusted to 15-18µl. To make sure that the pipette would not get damaged while flash pipetting, pipette tips with filter were used. For each polyplexing process 10µl of a desired LPEI dilution have been mixed with 10µl of quantum dots. To avoid air in the tip 10µl of LPEI were carefully taken up with the previously adjusted pipette. The LPEI was mixed with the quantum dots by fast up and down pipetting (=flash pipetting). The quantum dots control and the LPEI control were each mixed with 10µl HBG buffer in the same way. When all quantoplexes were done, 4µl of 60% glycerol was added into each tube of quantoplexes. From those 24µl, that were in each tube, 20µl were loaded into a separate well on the previously prepared agarose gel (see table 12)

Table 12: Overview of how the final samples were prepared.

N	LPEI tube name	volume of LPEI it has (ul)	QD tube name	volume of QD it has (ul)	HBG added (ul)	Glycerol (ul)	Loaded onto gel	Well no
	L-K1 (ctrl)	10	-	-	10	4	20	1
	-	-	-	-	-	-	-	2
	-	-	Q-K1 (ctrl)	10	10	4	20	3
	L-A1	10	Q-A1	10	-	4	20	4
	L-B1	10	Q-B1	10	-	4	20	5
	L-C1	10	Q-C1	10	-	4	20	6
	L-D1	10	Q-D1	10	-	4	20	7
	L-E1	10	Q-E1	10	-	4	20	8
	L-F1	10	Q-F1	10	-	4	-	9
	L-G1	10	Q-G1	10	-	4	-	10
	L-H1	10	Q-H1	10	-	4	20	11
	L-I1	10	Q-I1	10	-	4	20	12
	L-J1	10	Q-J1	10	-	4	20	13

7.3.2.2.5 Electrophoresis

After the samples were pipetted into the wells, the lid of the electrophoresis unit was attached to the chamber and the device was connected to a power supply. Each gel was run for 45 minutes at 80 Volt.

7.3.2.2.6 Gel imaging

After the electrophoresis the gel was imaged by using the ChemiDoc MP imager. To make sure the whole gel was captured the gel was placed correctly (centrally) on the transilluminator. Ethidium bromide was selected as chemiluminescent substance (though no ethidium bromide was used) and the desired image size was set. The first image was taken with auto-detection, which led to a perfectly exposed image. To see how the intensity of the signal changes the exposure time was changed manually for additional images.

7.3.3 Testing stability of only quantum dots (new batch)

7.3.3.1 Workflow

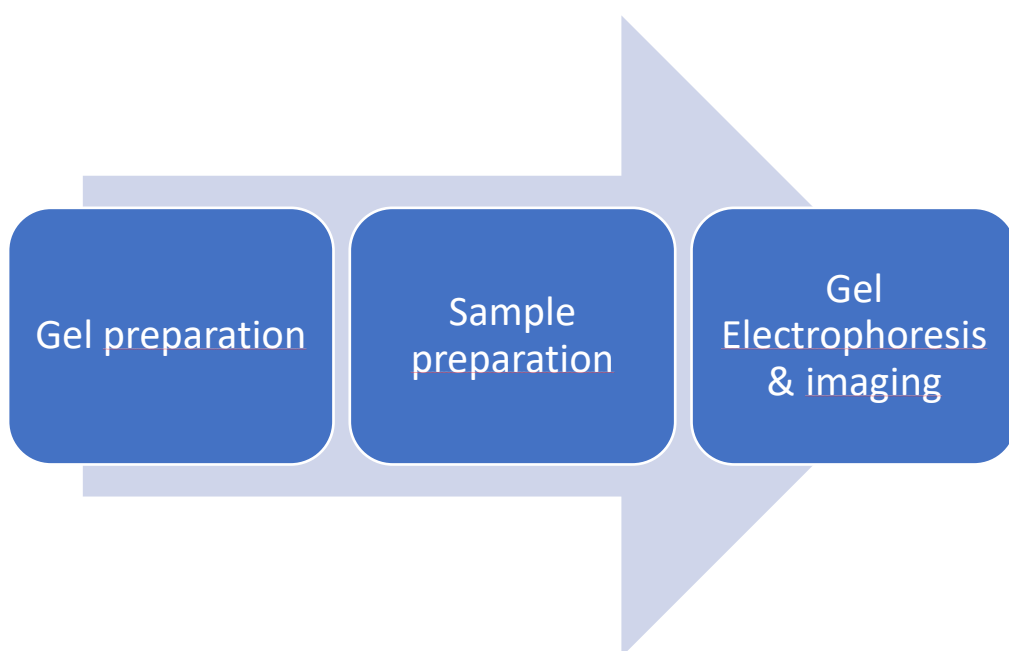


Figure 12: Workflow of the quantoplex experiment: Testing of only quantum dots from the new batch to check their stability.

7.3.3.2 Gel preparation

Firstly, nitril gloves needed to be put on and all parts that were used for the gel preparation had to be cleaned properly and left in water and soap over night to make sure all ethidium bromide from previously done experiments was removed and to make sure it is free from anything that could affect the electrophoresis. The installation was prepared by placing the gel cast correctly into the cast holder by ensuring it sits exactly horizontally. Depending on the desired number of wells an appropriate comb was added to the gel cast. A 0.75 % agarose gel was prepared by mixing 0.9g agarose with 120ml of 1xSB buffer. Agarose was dissolved by microwaving the mixture for about 1 minute for about 3-4 times until the liquid was clear. The solution was cool downed for approx. 30-60 sec.

The solution was gently poured into the gel cast that was previously prepared and air bubbles were gently removed. After gelation the comb was removed, and the gel cast was transferred into the electrophoresis-chamber. 1x SB buffer was poured into the chamber up to the mark so the gel was fully covered by buffer.

7.3.3.3 Sample preparation

Dr. Haider Sami provided the QD2 mother stock, from which a 1:20 dilution needed to be made to get the QD2 Stock C.

Preparation of working stock QD2-Stock D1 from QD2-Stock C:

- Take 18.6 μ l HBG in an Eppi
- Add 16.4 μ l of QD2-Stock C
- → Vortex

From QD2-Stock D1 samples were prepared according to table 13.

Table 13: Sample preparation with QD2-Stock D1.

Sample name	Amount Quantum dots (from stock D1)	Amount HBG	Amount glycerol	Total loaded per well
C1	2.5 μ l	17.5 μ l	4 μ l	20 μ l
C2	5 μ l	15 μ l	4 μ l	20 μ l
C3	10 μ l	10 μ l	4 μ l	20 μ l

Preparation of working QD2-Stock D2 from QD2-Stock C: → to double the concentration of quantum dots in further wells:

- Take 2.8µl HBG in an Eppi
- Add 67.2µl of QD2-Stock C
- → Vortex

From QD2-Stock D2 samples were prepared according to table 14.

Table 14: Sample preparation with QD2-Stock D2.

Sample name	Amount Quantum dots (from stock D2)	Amount HBG	Amount glycerol	Total loaded per well
C4	10µl	10µl	4µl	20µl
C5	20µl	-	4µl	20µl

7.3.3.4 Electrophoresis

After the samples were pipetted into the wells, the lid of the electrophoresis unit was attached to the chamber and the device was connected to a power supply. Each gel was run for 45 minutes at 80 Volt.

7.3.3.5 Gel imaging

After the electrophoresis the gel was imaged by using the ChemiDoc MP imager. To make sure the whole gel was captured the gel was placed correctly (centrally) on the transilluminator. Ethidium bromide was selected as chemiluminescent substance (though no ethidium bromide was used) and the desired image size was set. The first image was taken with auto-detection, which led to a perfectly exposed image. To see how the intensity of the signal changes the exposure time was changed manually for additional images.

7.4 Auropolyplexes: Re-Optimization of LPEI-SH coating on gold nanoparticle

7.4.1 Workflow

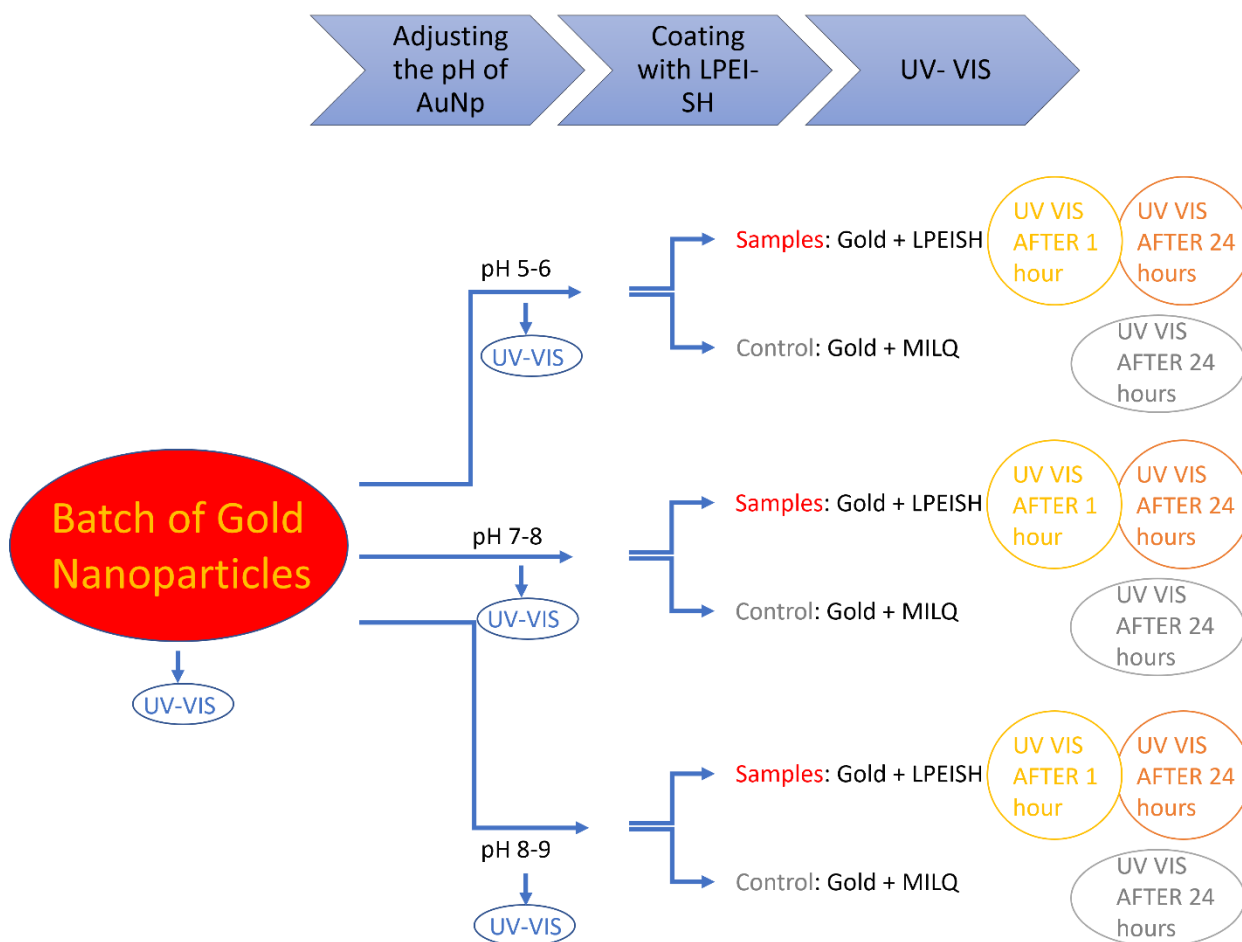


Figure 13: Workflow of the AuNP coating experiments

7.4.2 Working with gold nanoparticles

Before starting to work with gold nanoparticles the working space was cleaned with ethanol to make sure no dust or any other kind of impurity could affect the nanoparticles used. Fresh gloves were put on and cleaned with ethanol. Before using the gold batches the cap of the used batch was also cleaned by spraying a bit of ethanol on a piece of kitchen role and wiping off possible dust and impurities. When eppis were taken out of the plastic bag, they were stored in, the gloves were again cleaned with ethanol and the plastic bag was also wiped off with ethanol and a piece of kitchen role. To take out the eppis in the right way the amount of

eppis needed was pushed in the front of the bag, so when they were taken out only those that were needed would have been touched. Glassware that was used has been prerinsed with MilQ a few times. Magnetic stir bars were cleaned by using aqua regia if they were used before. New magnetic stir bars were just prerinsed with MilQ before usage. Before touching the gold nanoparticles with pipette tips, they were also prerinsed at least 3 times with MilQ. In general pipette tips were always prerinsed at least 3 times before using them. While coating or setting the pH of gold nanoparticles the work was done under a chemical hood.

7.4.3 Adjusting the pH of gold nanoparticles solution

Firstly, the SPR peak of the gold batch that was used was measured by UV-VIS. To adjust the pH a 1M NaOH was prepared by dissolving 2g NaOH in 10ml MilQ and filling it up to 50ml in total. To be sure that no impurities were present the 1M NaOH was filtrated through a 0.22 μm cellulose acetate filter. 5ml of gold nanoparticles were pipetted into a prerinsed snap cap vial. A fitting and clean magnetic stir bar was added. Under vigorous stirring the pH was adjusted by slowly adding 1M NaOH in 1-2 μl portions to the gold nanoparticles. The pH was controlled after every portion was added by using a pH paper. After adjusting the desired pH, the SPR peak was measured again by UV-VIS.

7.4.4 Coating of gold nanoparticles with LPEI-SH

Before the coating was started the SPR peak of the adjusted gold nanoparticle solution was measured by using a UV-VIS spectrophotometer. For the coating process four 2ml eppis were carefully taken out of the plastic bag they were stored in, in the way it is described in section "7.4.2 working with gold nanoparticles". 400 μl of AuNP with a specific pH was added into each eppi, as well as a fitting and clean mag bar. Under vigorous stirring the right amount (C1, C2, C3) of the desired LPEI-SH (1kDa or 5kDa) was slowly added drop by drop into 3 of the eppis. Into eppi number 4, which in every experiment served as a control, 100 μl of MilQ were added in the same way LPEI-SH was added to the other samples (drop by drop). (See table 15) Depending on the experiment the stirring time was either 24 hours or 72 hours. One hour after the coating process the SPR peak of each sample was measured, as well as at the end of the experiment (after 24h or 72h).

Table 15: Overview of the different quantities used for C1, C2, C3 and the control. Concentrations of the mother stocks of LPEISH 1kDa and 5kDa were the same.

Sample name	LPEISH Mother Stock (c= 20µg/µl) added	Amount LPEISH added (in µg)	Amount AuNP solution added	Amount Milq added
C1	25µl	500µg	400µl	-
C2	50µl	1000µg	400µl	-
C3	100µl	2000µg	400µl	-
Control	-	-	400µl	100µl

7.4.5 Characterization of LPEI-SH coating via UV-VIS spectrophotometry

To check changes in particle size and therefore to differ between coated, not coated or aggregated samples, gold nanoparticles were characterized by UV-VIS spectrophotometry. The UV-VIS measurement was done before adjusting the pH, after adjusting the pH (before coating), 1 hour after coating and at the end of every experiment (after 24 hours or 72 hours). The SPR peak and the shape of the resulting curve of the coated samples were compared to the ones of the non-coated gold nanoparticles.

The UV-VIS device (GeneQuant 1300) was adjusted to a wavelength from 400nm to 700nm because the expected peak of gold nanoparticles lies around 530nm-545nm (depending on if coated or not coated). MiliQ was set as a reference. After that every sample was measured. Each measurement was done with 70µl of sample and at least two spectra were taken from each sample.

8 Results and Discussion

8.1 Effect of serum on *in vivo* SSO Polyplexes

The effect of Serum on SSO degradation was tested. Naked SSOs were compared to SSO polyplexes. 4 experiments were done in which the samples were incubated for 30 minutes, and 3 experiments were done in which the samples were incubated for 4 hours. Agarose gel electrophoresis images showing effect of serum on naked and CLPEI-polyplexed SSOs, in comparison with HBG. 400ng SSOs were loaded per well. Each agarose gel (1.5%) was run for 40 minutes at 80 Volt.

In Figure 14 four independent experiments are shown with similar parameters but with some exceptions: in experiments 1 the polyplex samples were applied as duplicates; in experiment 1 and 2 NC and Luc ASOs were used ; in experiment 3 and 4 only NC ASOs were used; exposure time while imaging was 2.5 sec for exp. 1, 3 sec for exp. 2, 3 sec for exp. 3 and 3.5 sec for exp. 4.

All experiments, in which the samples were incubated for 30 minutes (figure 14) had the same outcome. When naked SSOs are in HBG buffer a clear single band of SSOs is visible indicating no degradation. On the other hand, when naked SSOs are exposed to serum they are either bound to components of the serum or get degraded as visible in the image.

When SSOs were loaded in polyplexes, the SSOs were not degraded or binding to the serum components as is visible in the Px1 and Px2 samples (experiment 1; figure 14). The polyplexes are not affected by Serum or HBG and remain in the well. There is no release of SSOs from the polyplexes, but as seen in some experiments the polyplexes seem to open up slightly because of serum, which leads to a partial staining of SSOs with ethidium bromide. This might explain the visibility of polyplexes in some wells (experiment 1, 2 and 4; Figure 14). But the overall results were the same as just discussed.

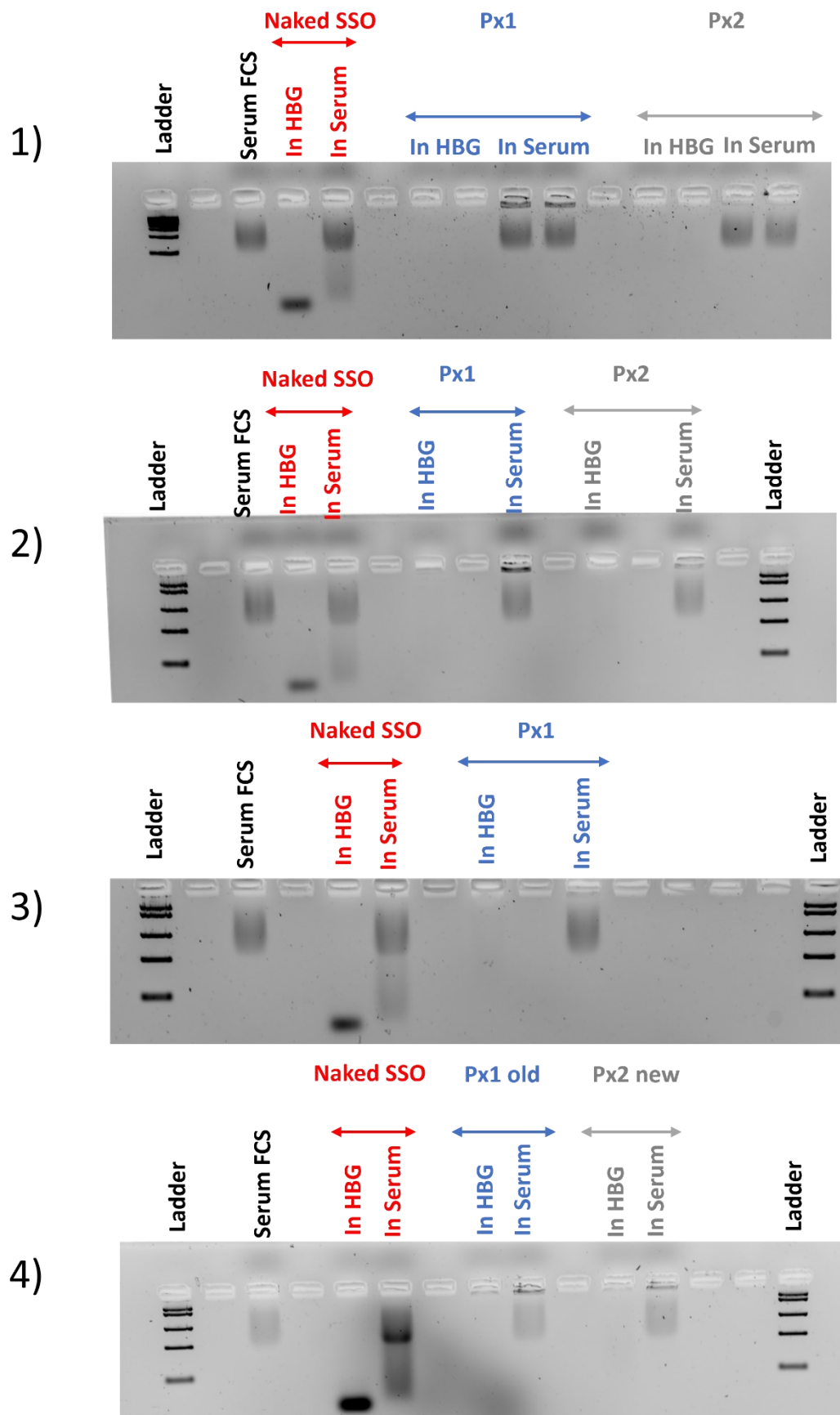


Figure 14: 1-4: gel electrophoresis of naked SSOs and SSO polyplexes after 30 minutes of incubation in the indicated medium (HBG or serum). Px1 refers to polyplexes that were made

with NC ASOs and Px2 refers to polyplexes that were made using Luc ASOs. In experiment 4, Px1 old refers to polyplexes that were made with the old batch of NC ASOs, and Px2 new refers to polyplexes that were made with a new batch of NC ASOs. A fast ruler middle range DNA ladder by Thermo Scientific was used. Serum (FCS) used was Bovine serum albumin.

The same results have been received for the experiments in which the samples were incubated for 4 hours, compared to the 30 minutes incubation experiments, as seen in figure 15. Three independent experiments are shown with similar parameters except that in experiments 1 NC and Luc ASOs were used and in experiment 2 and 3 only NC ASOs were used. Exposure time while imaging was 3 sec for exp. 1, 3 sec for exp. 2, 3.5 sec for exp. 3.

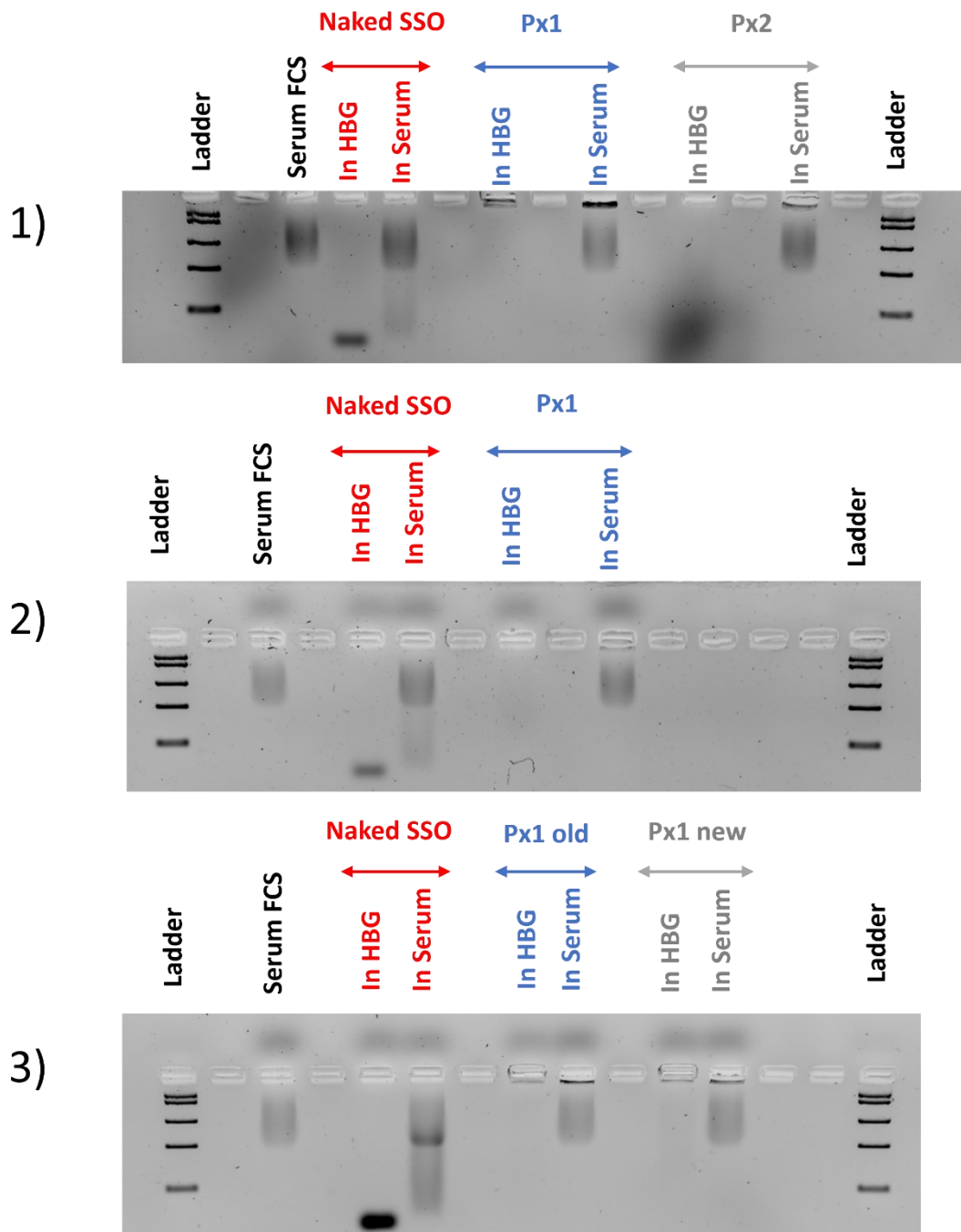


Figure 15: 3 experiments of gel electrophoresis, in which naked SSOs and SSO polyplexes were incubated for 4 hours. Px1 refers to polyplexes that were made with NC ASOs and Px2 refers to polyplexes that were made using Luc ASOs. In experiment 3, Px1 old refers to polyplexes that were made with the old batch of NC ASOs, and Px2 new refers to polyplexes that were made with a new batch of NC ASOs. A fast ruler middle range DNA ladder by Thermo Scientific was used. Serum (FCS) used was Bovine serum albumin.

8.2 Quantoplexes

This project was divided into 3 subprojects. First the effect of Serum on the quantoplexes was tested. Secondly it was tried to optimize the complexation between quantum dots and LPEI. After a few irregularities occurred, the quantum dots that were used for the quantoplexes became the focus of testing, and their stability was checked.

8.2.1 Effect of Serum on Quantoplexes

Two experiments were done within this Subproject. In each experiments the samples were applied on a gel without ethidium bromide, to analyze the quantum dots, and on a gel with ethidium bromide, to analyze the DNA. In advance the samples were incubated for 30 minutes. Each agarose gel (0.75%) was run for 40 minutes at 80 Volt.

As seen in the first experiment (see figure 16), no quantoplex degradation by the serum is visible in both gels, hence it can be assumed that quantum dots and DNA are well protected by the quantoplexes in serum and HBG buffer. Exposure time of gel without EtBr was 30 sec, and of gel with EtBr 2.2 sec.

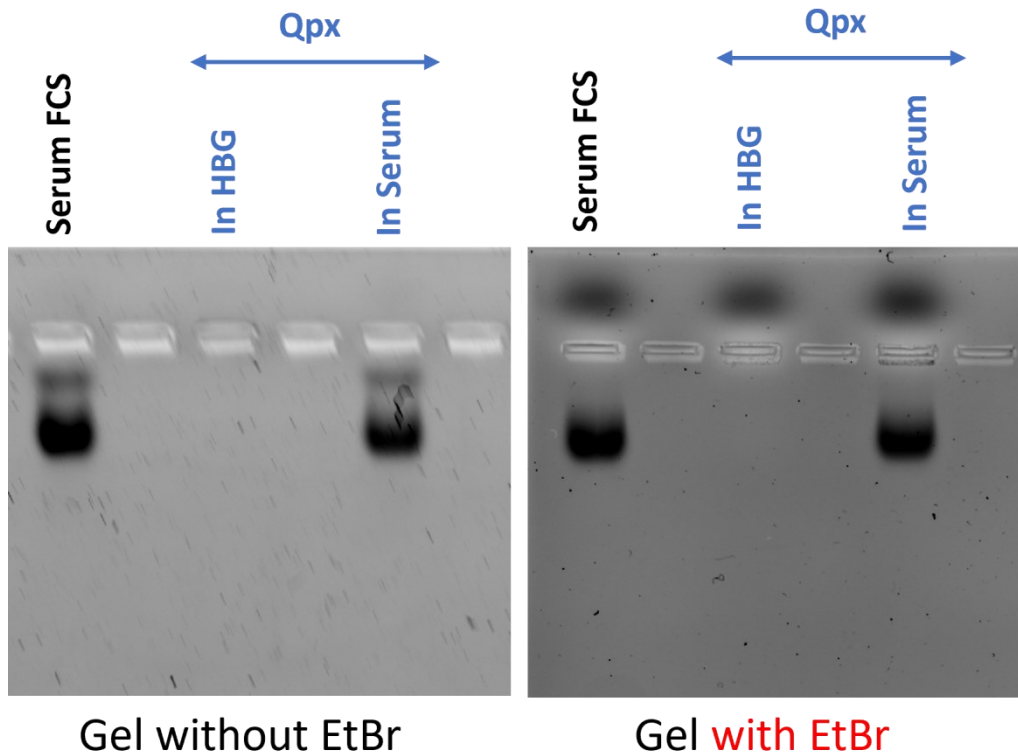


Figure 16: Agarose gel electrophoresis images showing the effect of serum on quantoplexes (Qpx), in comparison with HBG. Serum (FCS) used was bovine serum albumin.

In the second experiment additional control samples were integrated into the gels. Besides the quantoplexes, pDNA in serum and HBG, as well as quantum dots in serum and HBG were added to the gels.

The naked pDNA gets degraded in serum in comparison to the pDNA in HBG (see figure 17 in the gel with EtBr). Whereas the pDNA, as well as the quantum dots within the quantoplexes are not affected by degradation through HBG or serum (Figure 17, seen in both gels).

When QDs are in HBG buffer a band with a strong signal is visible in the gel without EtBr (Figure 17, gel without EtBr) in comparison to the gel with EtBr. This comes due to differences in the exposure time while imaging each gel. While the gel without EtBr had an exposure time of 23 sec, the gel with EtBr had an exposure time of 0.9 sec.

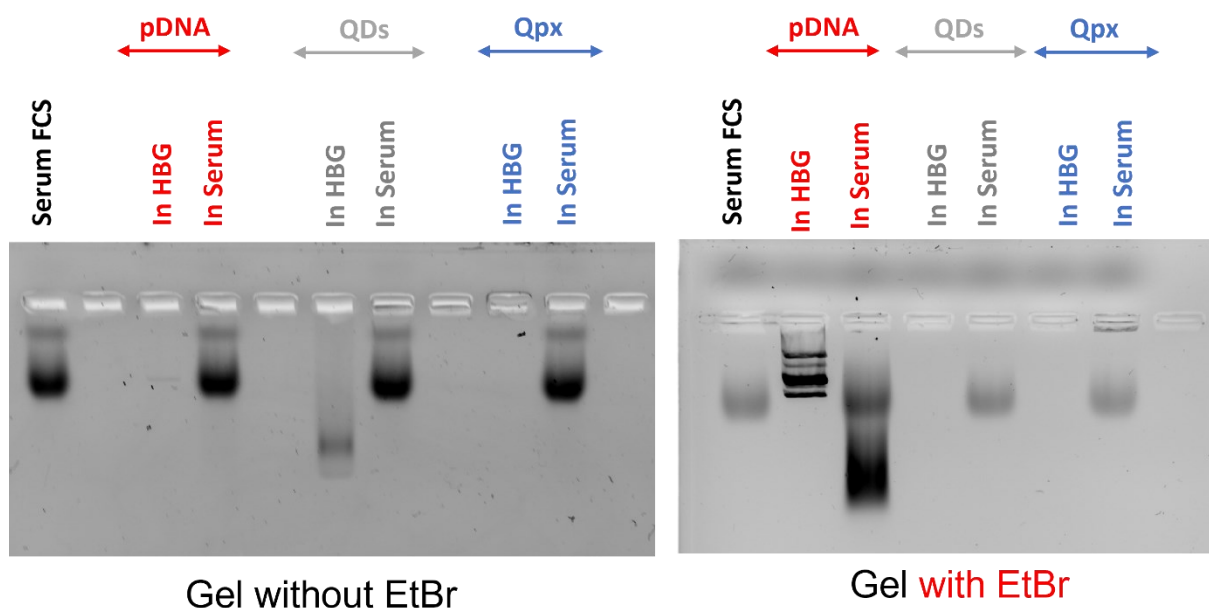


Figure 17: Agarose gel electrophoresis images showing the effect of serum on naked pDNA, naked QDs and Qpx, in comparison with HBG. Serum (FCS) used was bovine serum albumin.

8.2.2 Quantum dot complexation with LPEI

8.2.2.1 Comparison of old and new quantum dot batches

In the first phase of this subproject the new quantum dots were compared to the old batch of quantum dots, in terms of their ability to complex with LPEI. At a certain amount, LPEI completely complexes with the quantum dots and prevents the negatively charged quantum dots from migrating to the positively charged electrode. The positive charge of LPEI takes over and the complex remains in the well and does not migrate.

Each agarose gel (0.75%) was run for 45 minutes at 80 Volt. 3 experiments were done, all with similar results (see figure 18). The new quantum dots show a complexation with LPEI starting at 80ng (Figure 18; D2) of LPEI in each experiment. Because of the light band at 60ng LPEI (Figure 18; C2), it was assumed that a complexation of the new quantum dots is also possible with an amount of LPEI between 60ng and 80ng. The old quantum dots on the other hand show a complexation starting at 100ng (Figure 18; E1) of LPEI, although a complexation starting at 80ng of LPEI has been shown in a previous thesis.

Exposure time while imaging was 30 sec for exp. 1, 20 sec for exp. 2 and 20 sec for exp. 3.

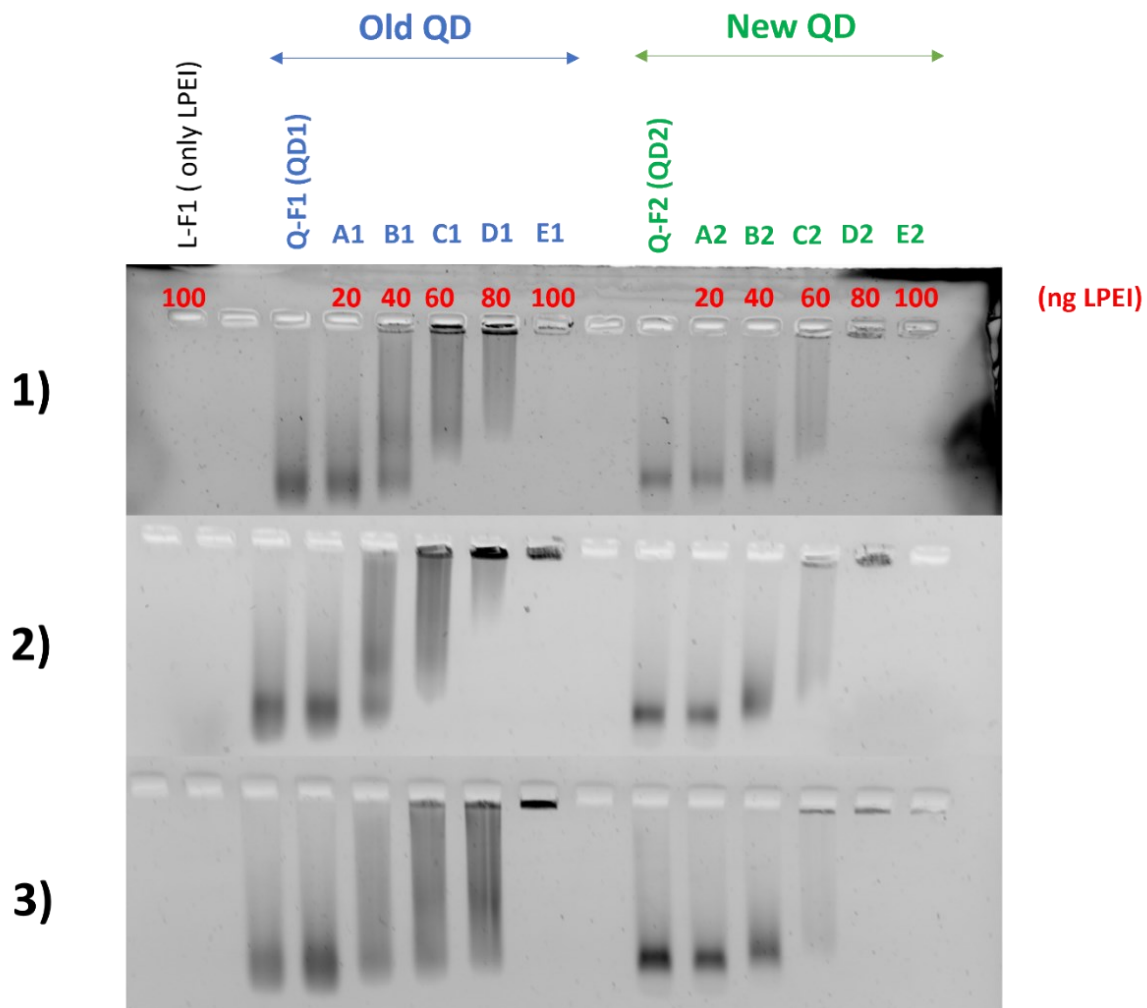


Figure 18: Comparison of new and old quantum dot batches regarding their complexation behavior with LPEI by using gel electrophoresis. Different amounts of LPEI as mentioned in red were mixed with the same amount of QDs as per the details in the methods section. Only-LPEI and only-QD controls are L-F1, Q-F1 and Q-F2.

8.2.2.2 Precise estimation of LPEI needed for QD(new batch) complexation

The second phase of this subproject, aimed to find a precise estimation of LPEI needed for the complexation with the new batch of quantum dots.

Since it was observed in the first phase that the complexation was fully done with 80ng of LPEI (Figure 18; D2), but the band at 60ng (Figure 18; C2) foreshadowed that there might be a complexation with a lower amount than 80ng, the experiments were started with an amount of 65ng LPEI. The amount of LPEI was increased in steps of 5ng. Each agarose gel (0.75%) was run for 45 minutes at 80 Volt. Exposure time of each gel was 30 sec.

In the first experiment, complexation started at a level of 90ng LPEI (Figure 19; Exp. 1; L-F1), which does not resemble the data from the experiments in the previous subproject.

However, the second experiment exactly mirrors the data from the previous experiments. Complete complexation, as assumed started at 70ng (Figure 19; Exp. 2; L-B1) and even at 65ng (Figure 19; Exp. 2; L-A1) of LPEI partial complexation took place. The difference in the data of these two experiments can be explained by the result of experiment 3. As the red arrow indicates, an unusual degradation of the quantum dots occurred in this experiment resulting in additional bands (Figure 19; Exp. 3).

Overall, the new batch of quantum dots behaved irreproducible and showed 3 different bands, which indicates degradation.

This irreproducibility of the new quantum dots led to subproject 3, where the stability of the new quantum dots was tested

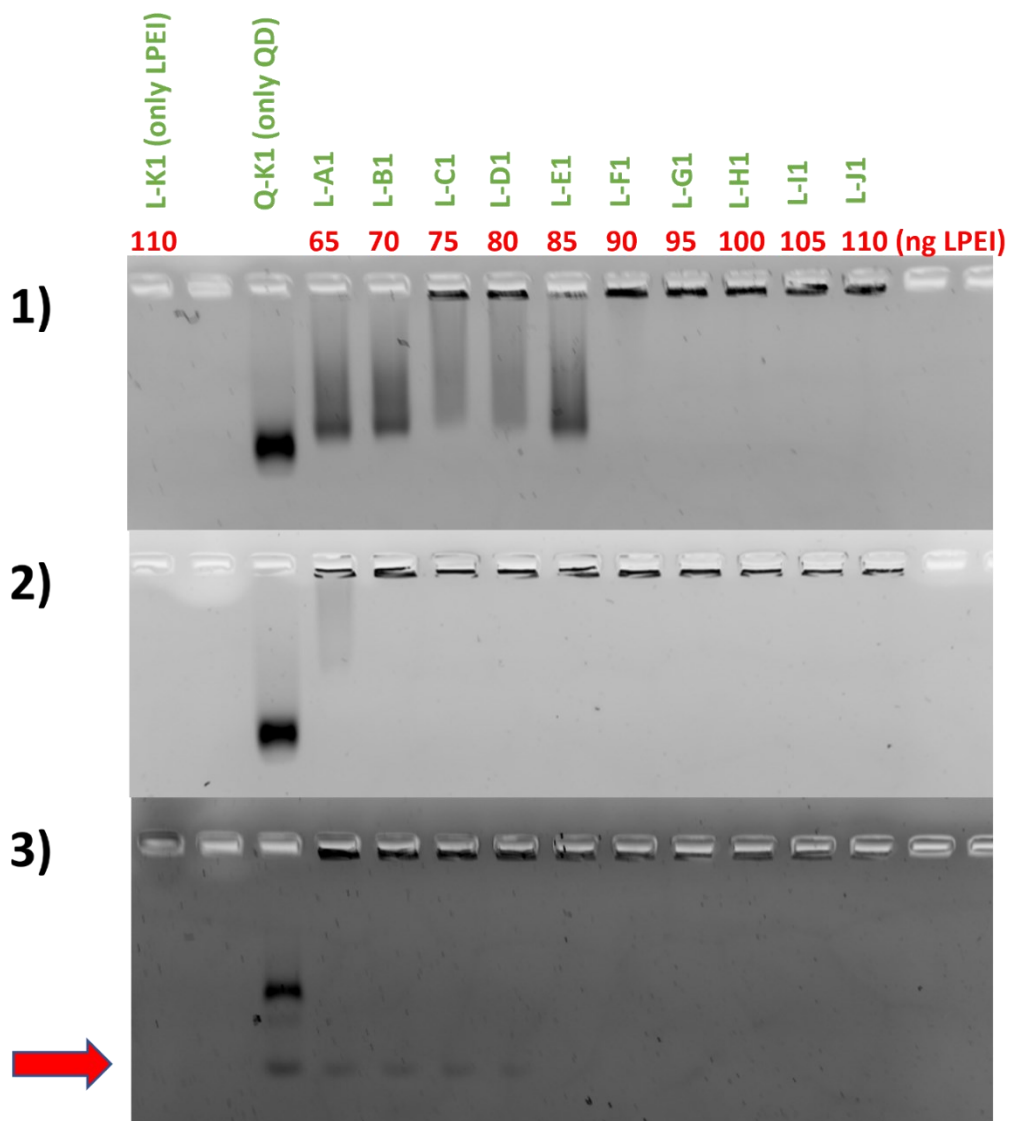


Figure 19: Complexation of the new batch of quantum dots with different amount of LPEI, using gel electrophoresis. Different amounts of LPEI as mentioned in red were mixed with the same amount of QDs as per the details in the method section. Only-LPEI and only-QD controls are L-K1 and Q-K1.

8.2.3 Testing stability of only quantum dots (new batch)

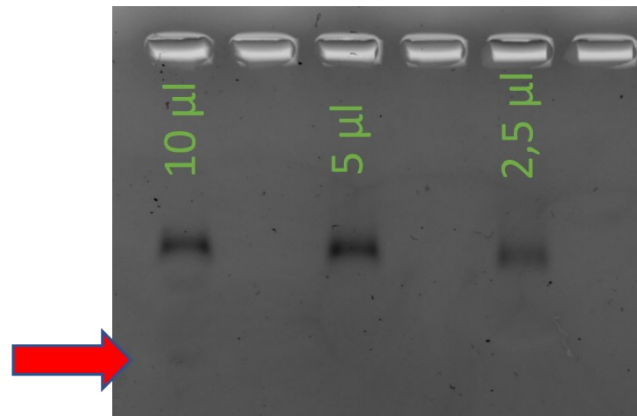
Due to the irregularities that occurred within the quantoplex results, it was planned to perform gel electrophoresis of only quantum dots to visualize if they appear as one single band (indicating purity/stability) or as multiple bands (indicating impurity/degradation).

In each experiment increasing amounts of QDs from the new batch were applied to an agarose gel to see if degradation occurred. Each agarose gel (0.75 %) was run for 45 minutes at 80 Volt.

In the first experiment 2 gels were made with different types of agarose, to exclude that the degradation is related to the agarose type used (see figure 20). 3 different amounts of quantum dots were applied on each gel, as per the details in the method section, with the highest concentration being on the far left.

As pointed out by the red arrow in figure 20, in case of the highest applied amount an additional band is slightly visible in both gels, which led to the suspicion of impurity presence or degradation and the conclusion that the agarose type is not responsible for this observation. Exposure time of each gel was 40 sec. (See Figure 20)

Agarose as in Experiment before



Different type of agarose

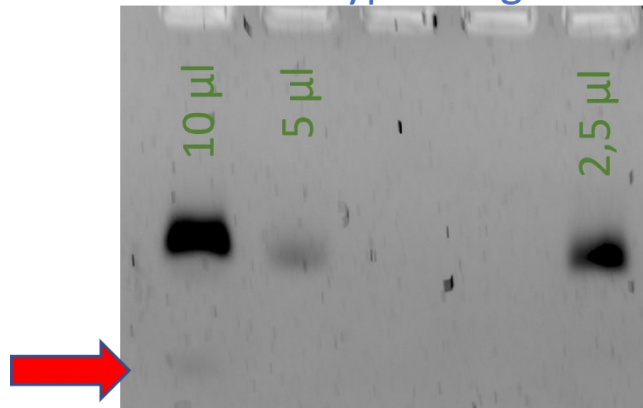


Figure 20: Agarose gel electrophoresis of different amounts of QDs (new batch) loaded on gels made from agarose from different manufacturers. Red arrows indicate presence of additional band.

In the second experiment, two additional higher amounts of quantum dots were applied on the gel as per the details in the method section, with the highest concentration being on the far right this time (see figure 21). The same agarose was used as in the subprojects before. The additional bands indicating impurity presence or degradation can be seen very clearly as pointed out by the red arrows in figure 21. Exposure Time of the gel was 40 sec.

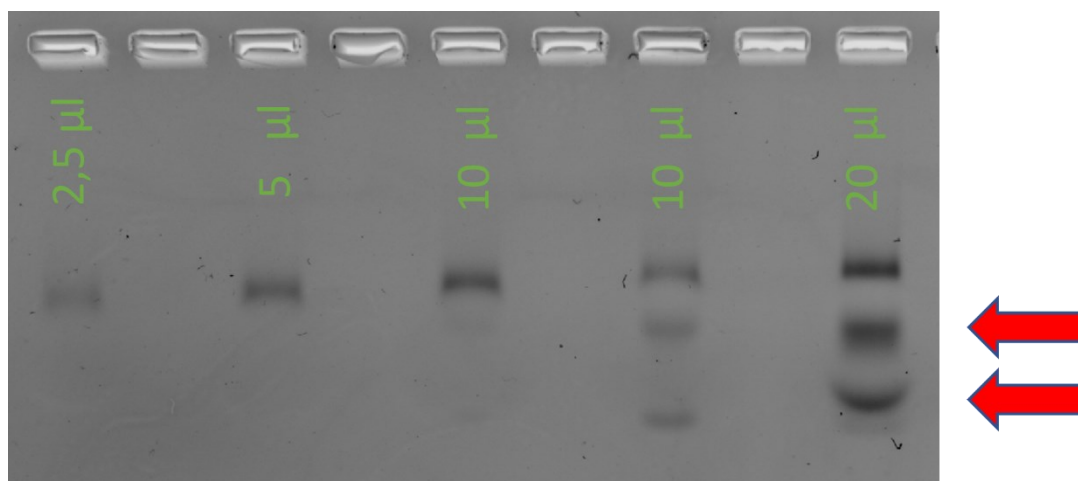


Figure 21: Agarose gel electrophoresis of different amounts of QDs (new batch) in gel made from the same agarose as used in subprojects before. Red arrows indicate the presence of additional bands.

To have the assurance that there was a difference between the new batch of quantum dots and the old batch, in experiment 3 these two batches were compared to each other, as seen in figure 22. Again, five different amounts of QDs were applied on the gels, as per the details in the method section, with the highest concentration being on the far right. The same agarose was used as in the subprojects before.

As in the second experiment the new quantum dots show additional bands indicating impurity presence or degradation (Figure 22; red arrows; upper gel), whereas the old quantum dots show a band that becomes more intense (Figure 22; bottom gel). It was also observed that the fluorescence intensity of the new batch of quantum dots was lower than the old batch. Exposure time of the upper gel (new QD) was 30 sec, and of the gel below (old QD) 20 sec. These differences between the batches could come from the fact that the batches were made by different people and due to possible production differences.

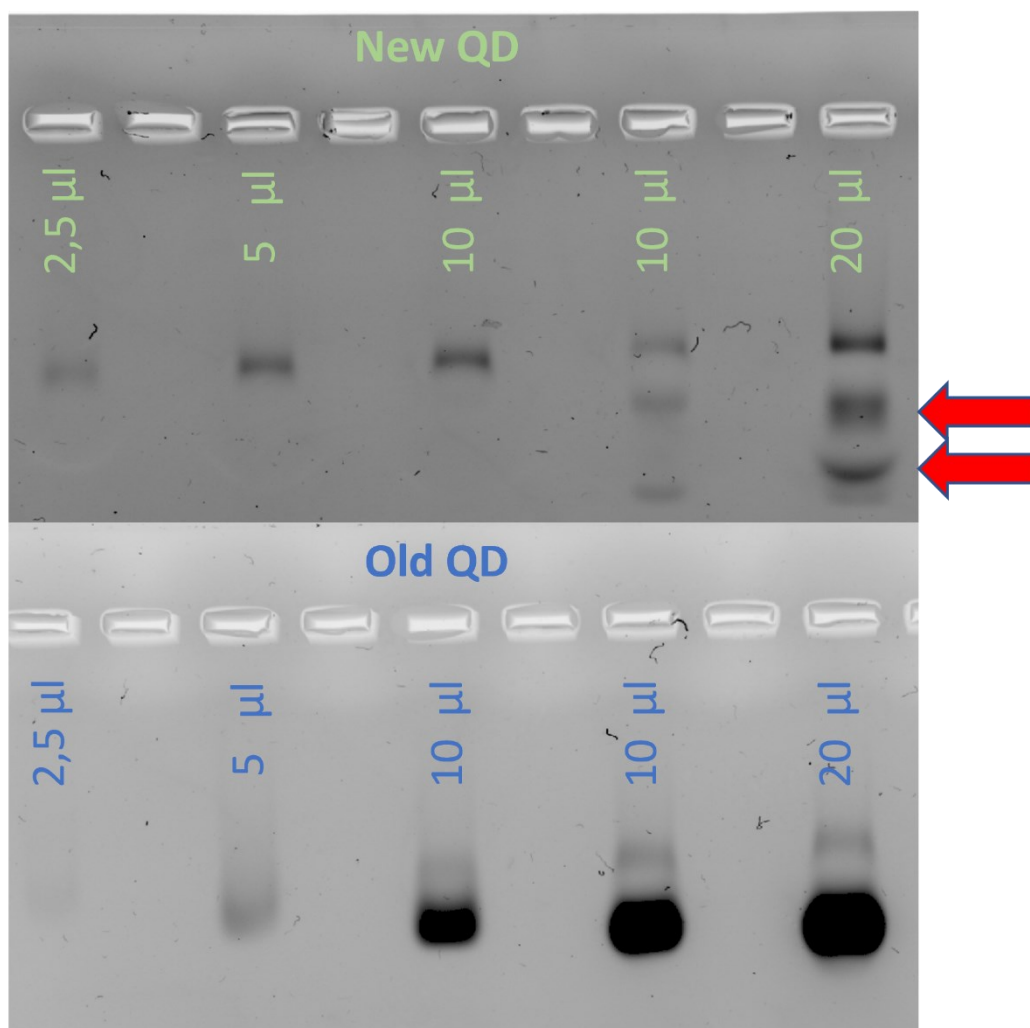


Figure 22: Agarose gel electrophoresis of different amounts of QDs (new batch on upper gel; old batch on bottom gel) in gels made from the same agarose as used in subprojects before. Red arrows indicate presence of additional band.

8.3 Auopolyplexes: Re-Optimization of LPEI-SH coating of gold nanoparticles

In this Project gold nanoparticles were coated with different types of LPEI-SH. To optimize this initial production step of auopolyplexes, different parameters were tested.

To determine if coating took place UV-VIS spectroscopy was used. SPR from gold nanoparticles was used as a fast-screening method to study this coating step as a function of LPEI-SH molecular weight, pH, and duration of stirring. SPR peak and UV-absorption profile was plotted to see if the LPEI-SH coating was successful (no-aggregation), or if it led to total aggregation or partial tendency to aggregate. SPR shift of few nanometers or no shift but without huge absorbance drop indicates successful coating. However, very huge SPR shifts or drastic drop in UV-VIS absorbance indicates aggregation and a lack of successful coating. With this context, UV-VIS absorbance and SPR peak was plotted 1 hour, 24 hours or 72 hours (depending on the experiment) after the coating process and was compared to the SPR of a control sample (treated with water instead of LPEI-SH). Also, the SPR of the nanoparticles before coating was documented for comparison as shown in a representative example in figure 23. Thereby attention was paid to changes in the SPR peak as well as changes regarding the curves such as the overall width, and intensity. A significant SPR shift was achieved if a difference of at least 2 nm occurred between measurements. On the other hand, no changes were expected in the control sample. However, some control samples got aggregated because of insufficient aqua-regia cleaning of the magnetic bar used in the coating experiment. Such experiments are identified in the plotted data by underlining the SPR peak in the table of the respective figure and were disregarded as failed experiments.

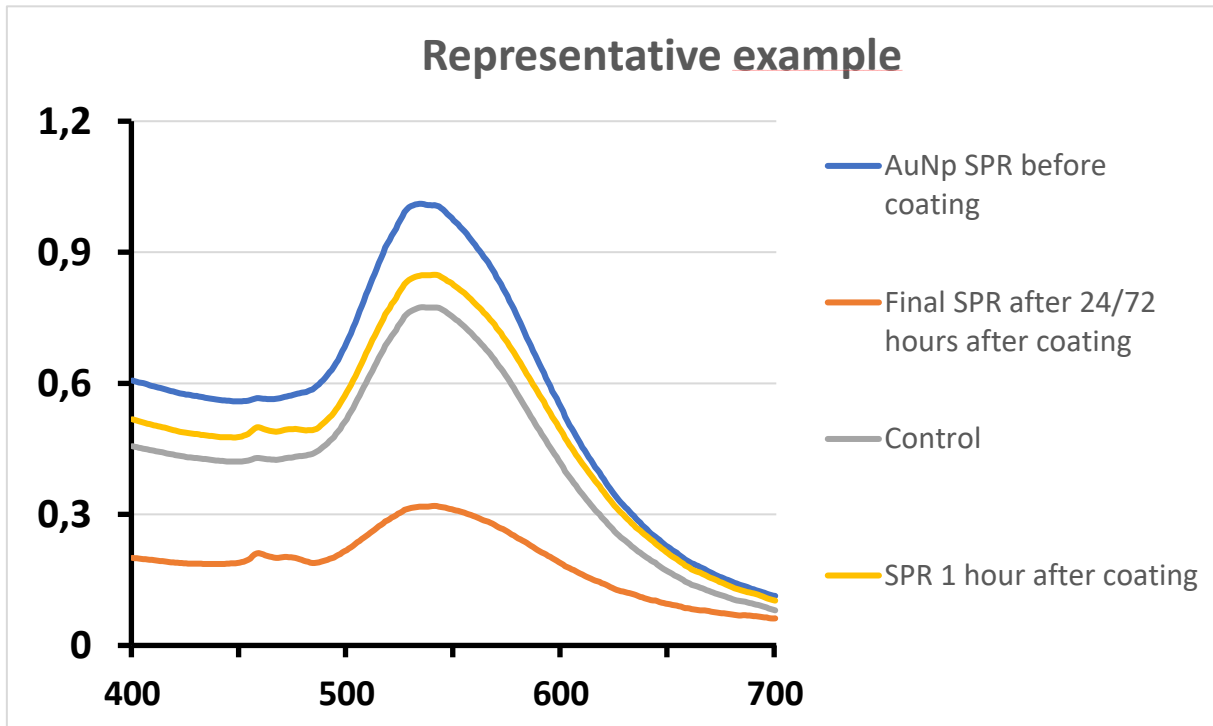


Figure 23: Representative example of UV-VIS absorption profile of gold nanoparticles showing the explanation of different parameters and the colors used to depict them. The same pattern of colors has been used in all such graphs for auropolyplex project results in the thesis.

8.3.1 Experiments with a stir-time of 24 hours

8.3.1.1 AuNP coating with LEPEI-SH of 1kDa

C1 (25µl of LPEISH-1kDa)

The samples were coated with 25µl of LPEISH-1kDa. 3 different pH were tested, and the samples were stirred for 24 hours.

AuNP with a pH of 5-6

The control of experiment 1 and 3 showed a SPR shift, which makes these experiments invalid, as it can be assumed that the aqua regia cleaning of the mag bars was incomplete. Although experiment 2 showed an indication of coating due to a 2nm shift of the SPR, no conclusion can be made for these parameters because 2 out of 3 experiments are invalid. (See figure 24).

C1/ LPEISH-1kDa/ pH 5-6/ 24h

pH	Exp.:	SPR before coating	SPR 1hour after coating	Final SPR 24h after coating	Shift in nm
5-6	1	534	536	542	/
	Ctrl	534	536	541	
	2	534	536	536	2
	Ctrl	534	535	535	
	3	535	535	535	/
	Ctrl	535	535	542	

(A)

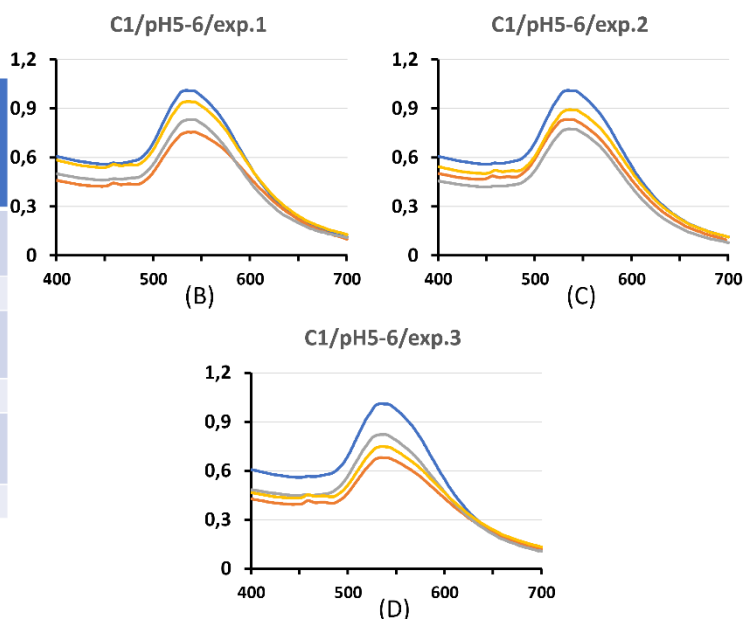


Figure 24: UV-VIS spectroscopy of 3 experiments showing SPR peaks (A) and absorption profiles (B-D) where AuNPs with a pH of 5-6 were coated with either 25 μ l (C1) of LPEI-SH-1kDa or water (ctrl). LPEI-SH coated and control AuNPs were continuously stirred and subjected to UV-Vis spectroscopy before coating, after 1h and 24h of coating. Blue curve: AuNP before coating, yellow curve: AuNP after 1h of coating, orange curve: AuNP after 24h of coating, grey curve: control AuNPs.

AuNP with a pH of 7-8

The control of experiment 2 showed a SPR shift, which makes this experiment invalid (see figure 25), as it can be assumed that the aqua regia cleaning of the mag bars was incomplete. Experiment 1 and 3 showed signs of coating, as it came to a SPR shift (7nm and 8nm), but with a tendency for aggregation with time, as the curve of the final SPR after 24 hours is approaching the x-axis (figure 25; B, D; orange curve).

C1/ LPEISH-1kDa/ pH 7-8/ 24h

pH	Exp.:	SPR before coating	SPR 1hour after coating	Final SPR 24h after coating	Shift in nm
7-8	1	535	542	542	7
	Ctrl	535	536	535	
	2	535	540	541	/
	Ctrl	535	543	541	
	3	535	541	543	8
	Ctrl	535	535	535	

(A)

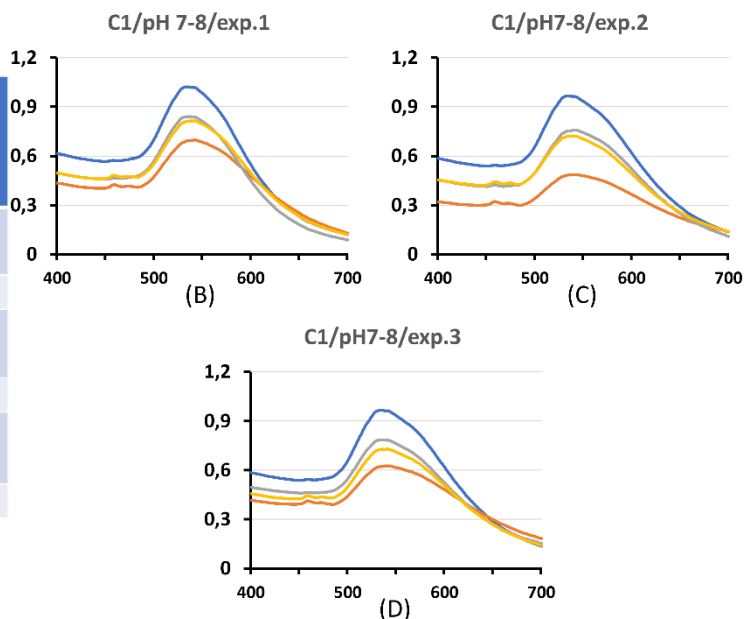


Figure 25: UV-VIS spectroscopy of 3 experiments showing SPR peaks (A) and absorption profiles (B-D) where AuNPs with a pH of 7-8 were coated with either 25 μ l (C1) of LPEI-SH-1kDa or water (ctrl). LPEI-SH coated and control AuNPs were continuously stirred and subjected to UV-Vis spectroscopy before coating, after 1h and 24h of coating. Blue curve: AuNP before coating, yellow curve: AuNP after 1h of coating, orange curve: AuNP after 24h of coating, grey curve: control AuNPs.

AuNP with a pH of 8-9

The SPR shift in experiment 1 and 2 leads to the assumption that coating was successful, but with a tendency for aggregation in experiment 1, as the curve received 24 hours after coating approaches the x-axis (figure 26; B; orange curve). Experiment 3 is invalid due to a SPR shift of the control sample, as it can be assumed that the aqua regia cleaning of the mag bars was incomplete. (See figure 26)

C1/ LPEISH-1kDa/ pH 8-9/ 24h

pH	Exp.:	SPR before coating	SPR 1hour after coating	Final SPR 24h after coating	Shift in nm
8-9	1	536	537	542	7
	Ctrl	536	536	535	
	2	535	541	543	8
	Ctrl	535	535	535	
	3	535	541	539	/
	Ctrl	535	541	543	

(A)

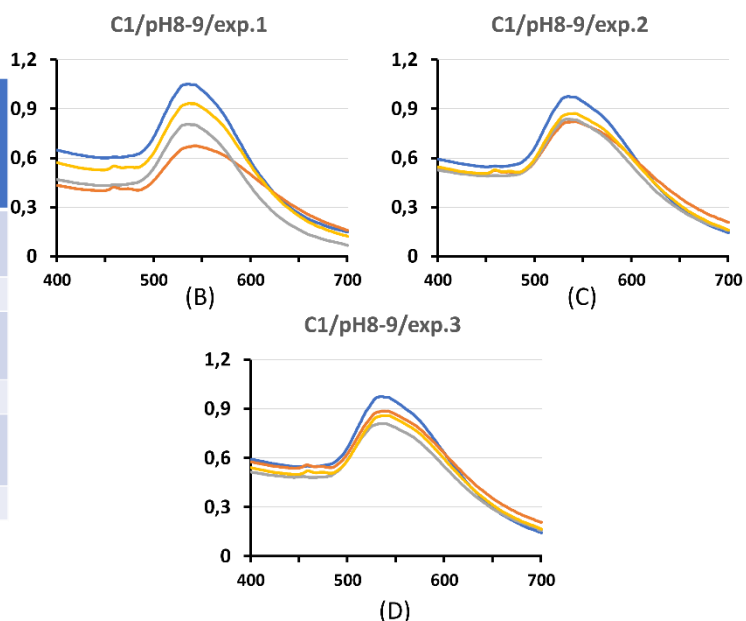


Figure 26: UV-VIS spectroscopy of 3 experiments showing SPR peaks (A) and absorption profiles (B-D) where AuNPs with a pH of 8-9 were coated with either 25 μ l (C1) of LPEI-SH-1kDa or water (ctrl). LPEI-SH coated and control AuNPs were continuously stirred and subjected to UV-Vis spectroscopy before coating, after 1h and 24h of coating. Blue curve: AuNP before coating, yellow curve: AuNP after 1h of coating, orange curve: AuNP after 24h of coating, grey curve: control AuNPs.

C2 (50 μ l of LPEISH-1kDa)

The samples were coated with 50 μ l of LPEISH-1kDa. 3 different pH were tested, and the samples were stirred for 24 hours.

AuNP with a pH of 5-6

Even though experiment 1 showed a SPR shift, by the fact that the control shifted as well, this experiment is not valid, as it can be assumed that the aqua regia cleaning of the mag bars was incomplete. Experiment 2 and 3 are not valid due to aggregation of the final samples. Additionally, the control of experiment 3 also showed a SPR shift. For this experiment it can also be assumed that the aqua regia cleaning of the mag bars was incomplete. (See figure 27)

C2/ LPEISH-1kDa/ pH 5-6/ 24h

pH	Exp.:	SPR before coating	SPR 1hour after coating	Final SPR 24h after coating	Shift in nm
5-6	1	534	536	543	/
	Ctrl	534	536	541	
	2	534	543	Agg	/
	Ctrl	534	535	535	
	3	535	540	Agg	/
	Ctrl	535	535	541	

(A)

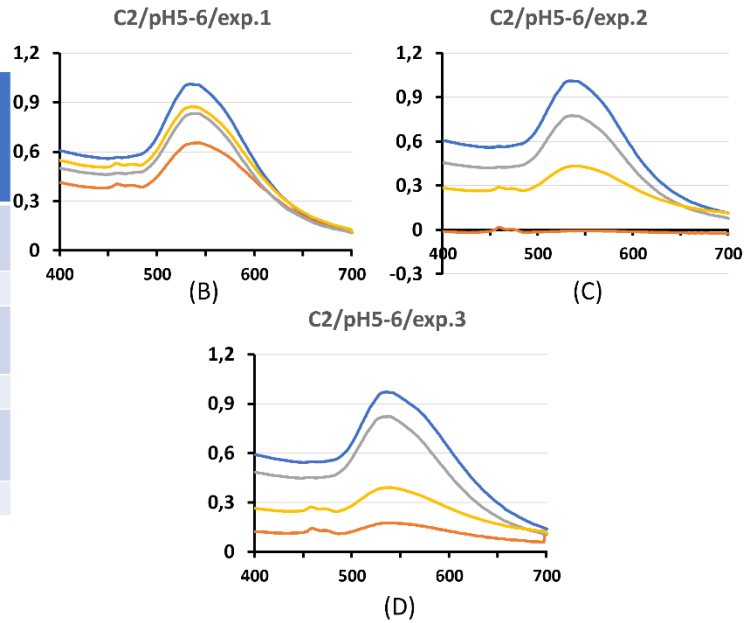


Figure 27: UV-VIS spectroscopy of 3 experiments showing SPR peaks (A) and absorption profiles (B-D) where AuNPs with a pH of 5-6 were coated with either 50µl (C2) of LPEI-SH-1kDa or water (ctrl). LPEI-SH coated and control AuNPs were continuously stirred and subjected to UV-Vis spectroscopy before coating, after 1h and 24h of coating. Blue curve: AuNP before coating, yellow curve: AuNP after 1h of coating, orange curve: AuNP after 24h of coating, grey curve: control AuNPs.

AuNP with a pH of 7-8

All experiments showed aggregation after 24 hours at the latest. Whereby the sample of experiment 2 already aggregated after 1 hour and the control additionally showed a SPR shift (it can be assumed that the aqua regia cleaning of the mag bars was incomplete), which is why no measurement was taken after 24 hours for this experiment. (See figure 28)

Therefore, it can be said that coating with these parameters was not successful.

C2/ LPEISH-1kDa/ pH 7-8/ 24h

pH	Exp.:	SPR before coating	SPR 1hour after coating	Final SPR 24h after coating	Shift in nm
7-8	1	535	543	Agg	/
	Ctrl	535	536	535	
	2	535	Agg	Agg	/
	Ctrl	535	542	541	
	3	535	542	Agg	/
	Ctrl	535	535	535	

(A)

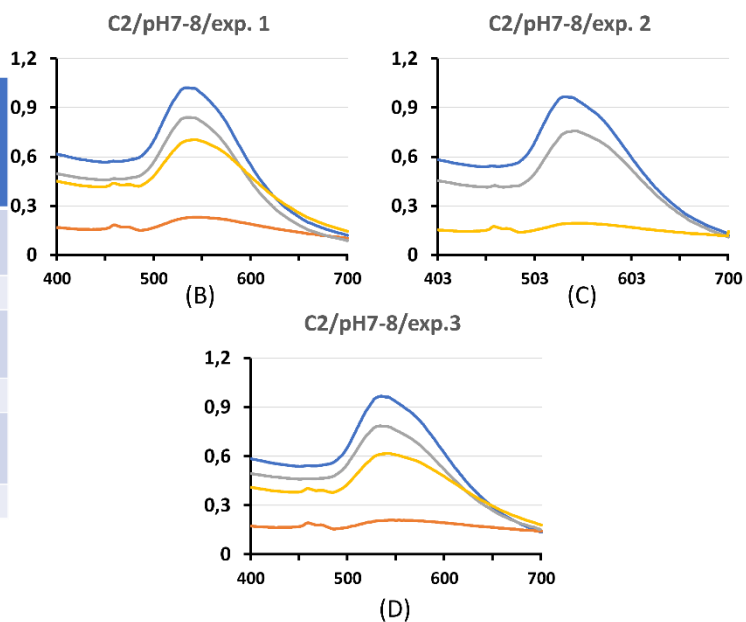


Figure 28: UV-VIS spectroscopy of 3 experiments showing SPR peaks (A) and absorption profiles (B-D) where AuNPs with a pH of 7-8 were coated with either 50 μ l (C2) of LPEI-SH-1kDa or water (ctrl). LPEI-SH coated and control AuNPs were continuously stirred and subjected to UV-Vis spectroscopy before coating, after 1h and 24h of coating. Blue curve: AuNP before coating, yellow curve: AuNP after 1h of coating, orange curve: AuNP after 24h of coating, grey curve: control AuNPs.

AuNP with a pH of 8-9

All experiments showed aggregation after 24 hours. Additionally, the control of experiment 3 showed a SPR shift (it can be assumed that the aqua regia cleaning of the mag bars was incomplete). (See figure 29)

Coating with these parameters was not successful.

C2/ LPEISH-1kDa/ pH 8-9/ 24h

pH	Exp.:	SPR before coating	SPR 1hour after coating	Final SPR 24h after coating	Shift in nm
8-9	1	536	539	Agg	/
	Ctrl	536	536	535	
	2	535	541	Agg	/
	Ctrl	535	535	535	
	3	535	542	Agg	/
	Ctrl	535	541	543	

(A)

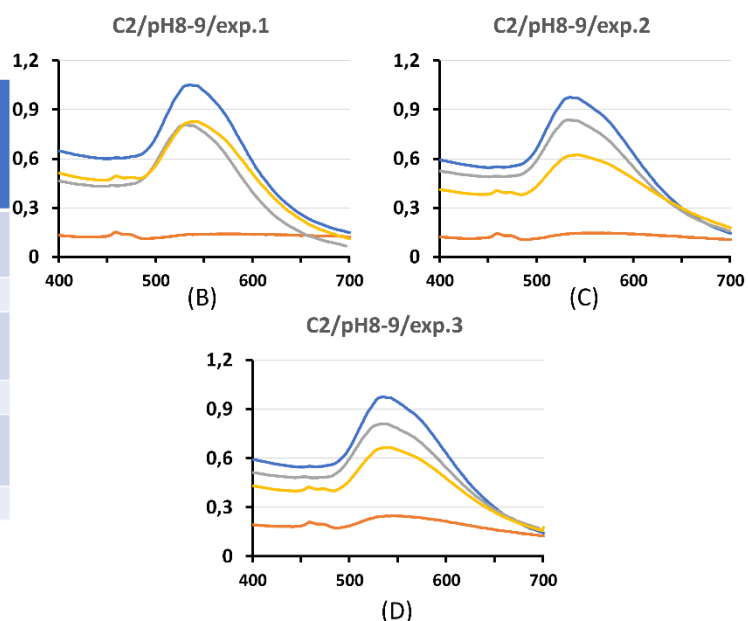


Figure 29: UV-VIS spectroscopy of 3 experiments showing SPR peaks (A) and absorption profiles (B-D) where AuNPs with a pH of 8-9 were coated with either 50 μ l (C2) of LPEI-SH-1kDa or water (ctrl). LPEI-SH coated and control AuNPs were continuously stirred and subjected to UV-Vis spectroscopy before coating, after 1h and 24h of coating. Blue curve: AuNP before coating, yellow curve: AuNP after 1h of coating, orange curve: AuNP after 24h of coating, grey curve: control AuNPs.

C3 (100 μ l of LPEISH-1kDa)

The samples were coated with 100 μ l of LPEISH-1kDa. 3 different pH were tested, and the samples were stirred for 24 hours.

AuNP with a pH of 5-6

All experiments showed aggregation after 24 hours at the latest. The sample in experiment 3 already aggregated after 1 hour and additionally the control showed a SPR shift (it can be assumed that the aqua regia cleaning of the mag bars was incomplete), which is why no additional measurement was taken after 24 hours for this experiment. Also, the control of experiment 1 showed a SPR shift. Coating with these parameters was not successful. (See figure 30)

C3/ LPEISH-1kDa/ pH 5-6/ 24h

pH	Exp.:	SPR before coating	SPR 1hour after coating	Final SPR 24h after coating	Shift in nm
5-6	1	534	543	Agg	/
	Ctrl	534	536	541	
	2	534	542	Agg	/
	Ctrl	534	535	535	
	3	535	Agg	Agg	/
	Ctrl	535	535	541	

(A)

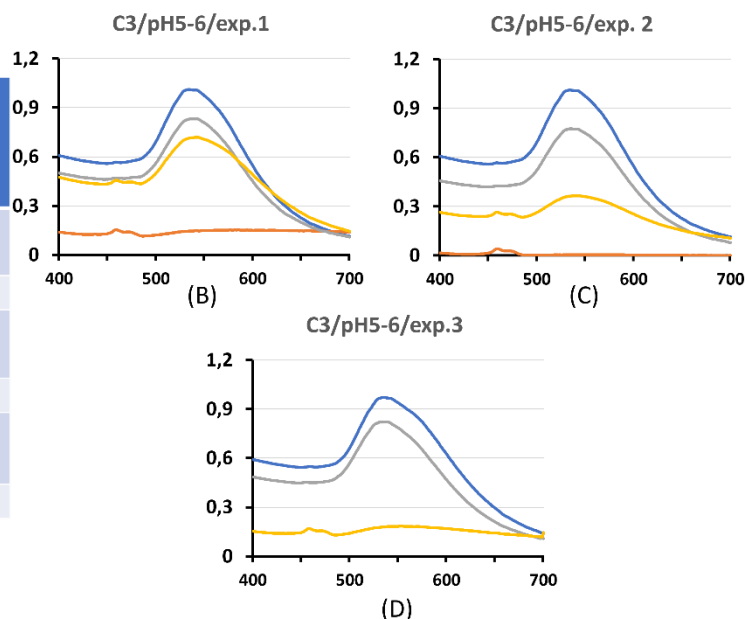


Figure 30: UV-VIS spectroscopy of 3 experiments showing SPR peaks (A) and absorption profiles (B-D) where AuNPs with a pH of 5-6 were coated with either 100 μ l (C3) of LPEI-SH-1kDa or water (ctrl). LPEI-SH coated and control AuNPs were continuously stirred and subjected to UV-Vis spectroscopy before coating, after 1h and 24h of coating. Blue curve: AuNP before coating, yellow curve: AuNP after 1h of coating, orange curve: AuNP after 24h of coating, grey curve: control AuNPs.

AuNP with a pH of 7-8

All experiments already showed aggregation 1 hour after coating. Additionally, the control of experiment 2 showed a SPR shift (it can be assumed that the aqua regia cleaning of the mag bars was incomplete), which is why no measurement was taken after 24 hours for this experiment. Coating with these parameters was not successful. (See figure 31)

C3/ LPEISH-1kDa/ pH 7-8/ 24h

pH	Exp.:	SPR before coating	SPR 1hour after coating	Final SPR 24h after coating	Shift in nm
5-6	1	535	Agg	Agg	/
	Ctrl	535	536	535	
	2	535	Agg	Agg	/
	Ctrl	535	542	541	
	3	535	Agg	Agg	/
	Ctrl	535	535	535	

(A)

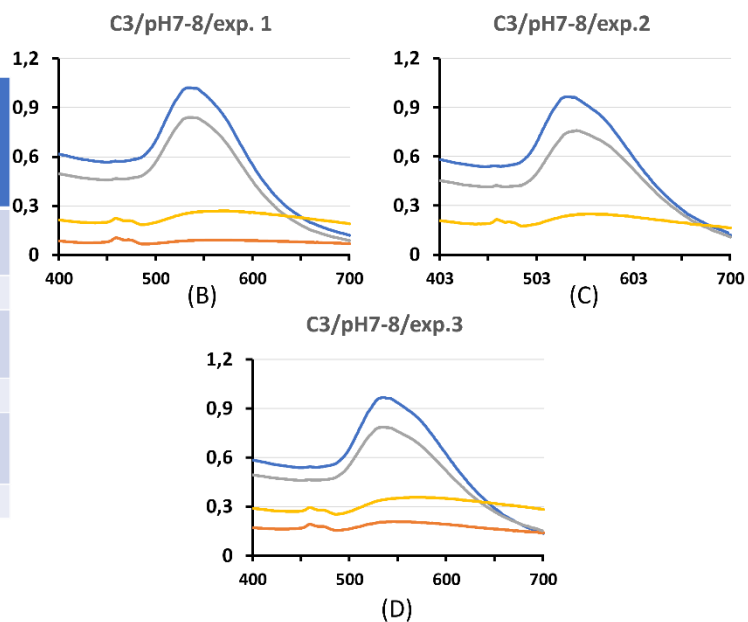


Figure 31: UV-VIS spectroscopy of 3 experiments showing SPR peaks (A) and absorption profiles (B-D) where AuNPs with a pH of 7-8 were coated with either 100 μ l (C3) of LPEI-SH-1kDa or water (ctrl). LPEI-SH coated and control AuNPs were continuously stirred and subjected to UV-Vis spectroscopy before coating, after 1h and 24h of coating. Blue curve: AuNP before coating, yellow curve: AuNP after 1h of coating, orange curve: AuNP after 24h of coating, grey curve: control AuNPs.

AuNP with a pH of 8-9

Both experiments showed aggregation after 24 hours at the latest. In experiment 2 the sample already aggregated after 1 hour and additionally the control showed a SPR shift (it can be assumed that the aqua regia cleaning of the mag bars was incomplete), which is why no measurement was taken after 24 hours for this experiment. (See figure 32)

Coating was not successful with these parameters.

C3/ LPEISH-1kDa/ pH 8-9/ 24h

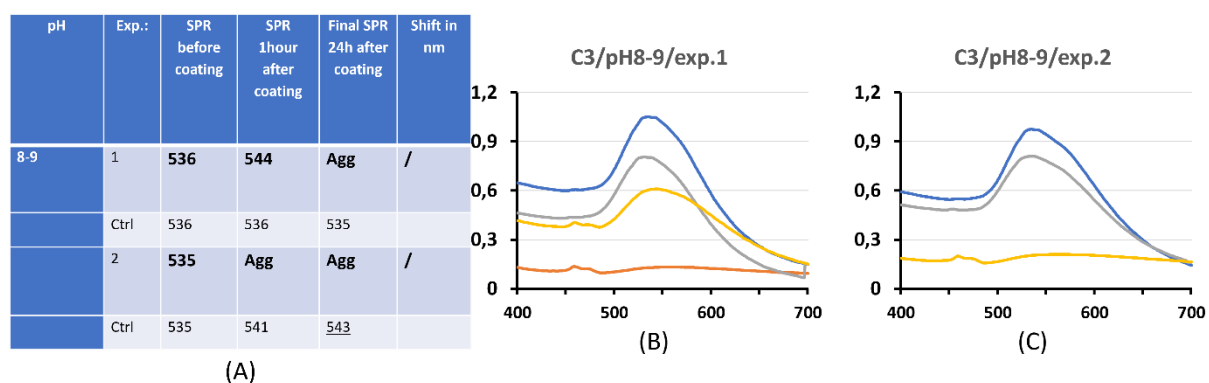


Figure 32: UV-VIS spectroscopy of 2 experiments showing SPR peaks (A) and absorption profiles (B,C) where AuNPs with a pH of 8-9 were coated with either 100 μ l (C3) of LPEI-SH-1kDa or water (ctrl). LPEI-SH coated and control AuNPs were continuously stirred and subjected to UV-Vis spectroscopy before coating, after 1h and 24h of coating. Blue curve: AuNP before coating, yellow curve: AuNP after 1h of coating, orange curve: AuNP after 24h of coating, grey curve: control AuNPs.

Although positive results occurred, especially with lower amounts of LPEISH of 1kDa (C1), overall, it can be said that the attempts of coating gold nanoparticles with LPEISH of 1 kDa have not yielded promising results.

8.3.1.2 AuNP coating with LEPI-SH of 5kDa

C1 (25µl of LPEISH-5kDa)

The samples were coated with 25µl of LPEISH-5kDa. 3 different pH were tested, and the samples were stirred for 24 hours.

AuNP with a pH of 5-6

There is an indication of coating in experiments 3 and 4, but a SPR shift of 3nm only in experiment 3 (See figure 33). The control of experiment 1 aggregated (figure 33; B; grey curve), hence it can be assumed that the aqua regia cleaning of the mag bars was incomplete and therefore this experiment cannot be counted as valid. Although the coating seemed successful in experiment 2 (SPR shift of 7nm), the curve received 24 hours after coating approaching the x-axis indicates aggregation (figure 33; C; orange curve).

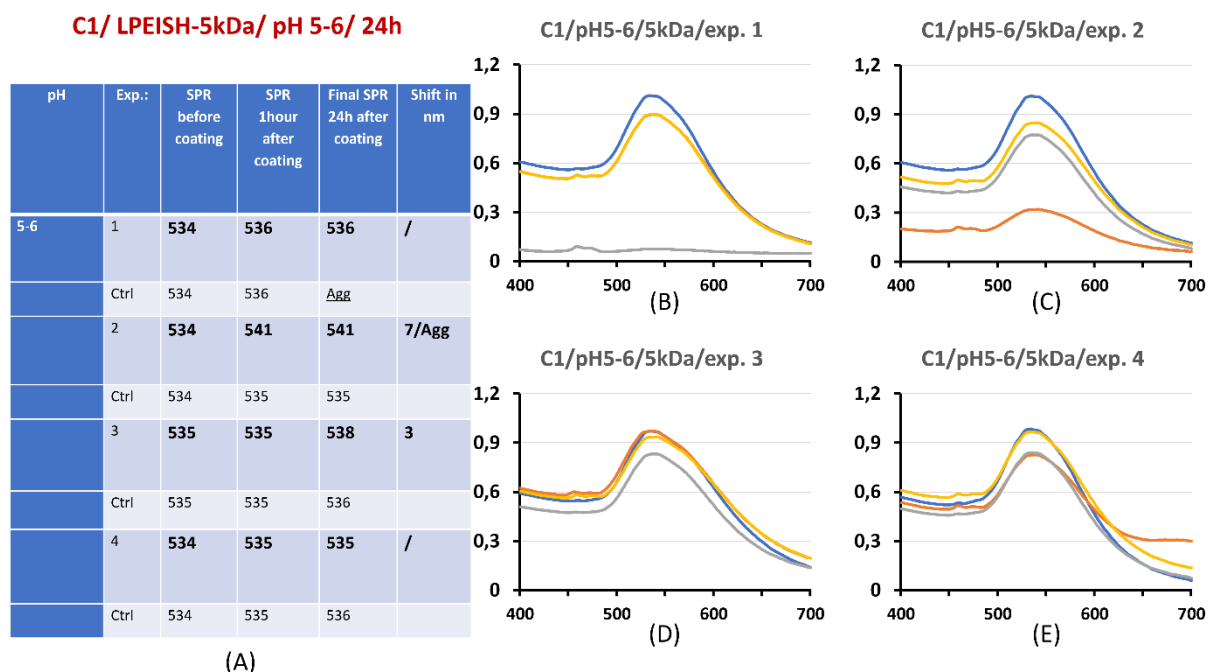


Figure 33: UV-VIS spectroscopy of 4 experiments showing SPR peaks (A) and absorption profiles (B-E) where AuNPs with a pH of 5-6 were coated with either 25µl (C1) of LPEI-SH-5kDa or water (ctrl). LPEI-SH coated and control AuNPs were continuously stirred and subjected to

UV-Vis spectroscopy before coating, after 1h and 24h of coating. Blue curve: AuNP before coating, yellow curve: AuNP after 1h of coating, orange curve: AuNP after 24h of coating, grey curve: control AuNPs.

AuNP with a pH of 7-8

In experiments 2,4 and 5 it can be assumed that coating was successful, but with a significant SPR shift of 7nm only in experiment 2 (see figure 34). While there is also an indication of coating in experiments 1 and 3 (SPR shifts of 6nm and 2nm), there is also a tendency for aggregation, because the curves received 24 hours after coating are approaching the x-axis over time in these two experiments (figure 34; B, D; orange curve).

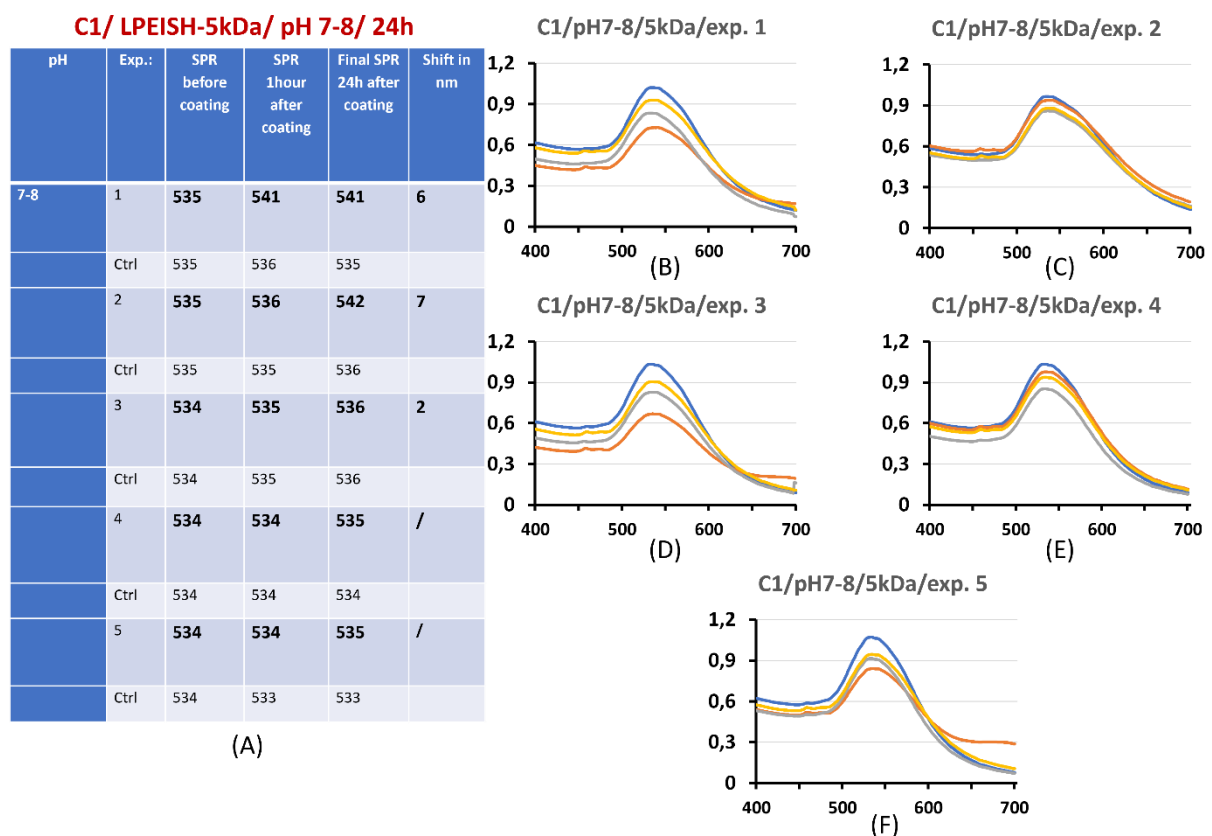


Figure 34: UV-VIS spectroscopy of 5 experiments showing SPR peaks (A) and absorption profiles (B-F) where AuNPs with a pH of 7-8 were coated with either 25µl (C1) of LPEI-SH-5kDa or water (ctrl). LPEI-SH coated and control AuNPs were continuously stirred and subjected to UV-Vis spectroscopy before coating, after 1h and 24h of coating. Blue curve: AuNP before

coating, yellow curve: AuNP after 1h of coating, orange curve: AuNP after 24h of coating, grey curve: control AuNPs.

AuNP with a pH of 8-9

An indication of coating is seen in experiments 1,3 and 4, although a significant SPR shift was only observed in experiment 3 (shift of 7nm). Experiment 2 is not valid, due to a SPR shift of the control, as it can be assumed that the aqua regia cleaning of the mag bars was incomplete. (See figure 35)

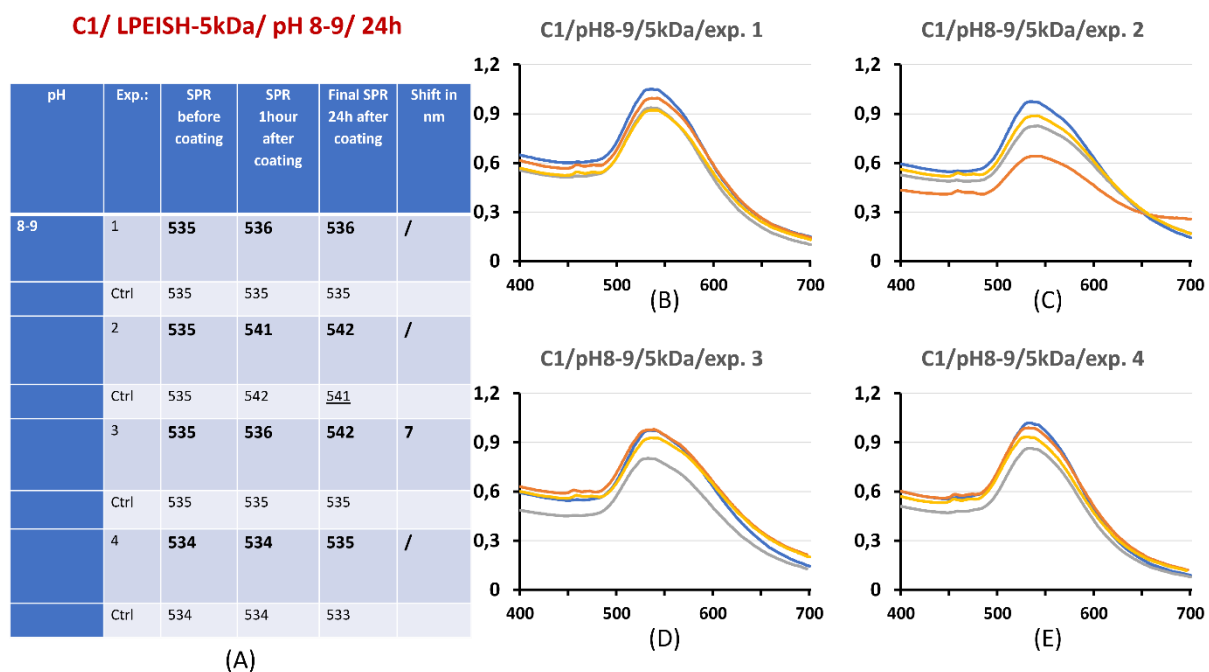


Figure 35: UV-VIS spectroscopy of 4 experiments showing SPR peaks (A) and absorption profiles (B-E) where AuNPs with a pH of 8-9 were coated with either 25µl (C1) of LPEI-SH-5kDa or water (ctrl). LPEI-SH coated and control AuNPs were continuously stirred and subjected to UV-Vis spectroscopy before coating, after 1h and 24h of coating. Blue curve: AuNP before coating, yellow curve: AuNP after 1h of coating, orange curve: AuNP after 24h of coating, grey curve: control AuNPs.

C2 (50µl of LPEISH-5kDa)

The samples were coated with 50µl of LPEISH-5kDa. 3 different pH were tested, and the samples were stirred for 24 hours.

AuNP with a pH of 5-6

Experiments 3 and 4 show an indication of coating, with SPR shifts of 7nm and 2nm (see figure 36). Although experiment 1 also seemed to be successful (shift of 3nm), due to the aggregated control it is not valid, as it can be assumed that the aqua regia cleaning of the mag bars was incomplete (figure 35; B; grey curve). The second experiment resulted in aggregation of the final sample and therefore is not valid as well (figure 35; C; orange curve).

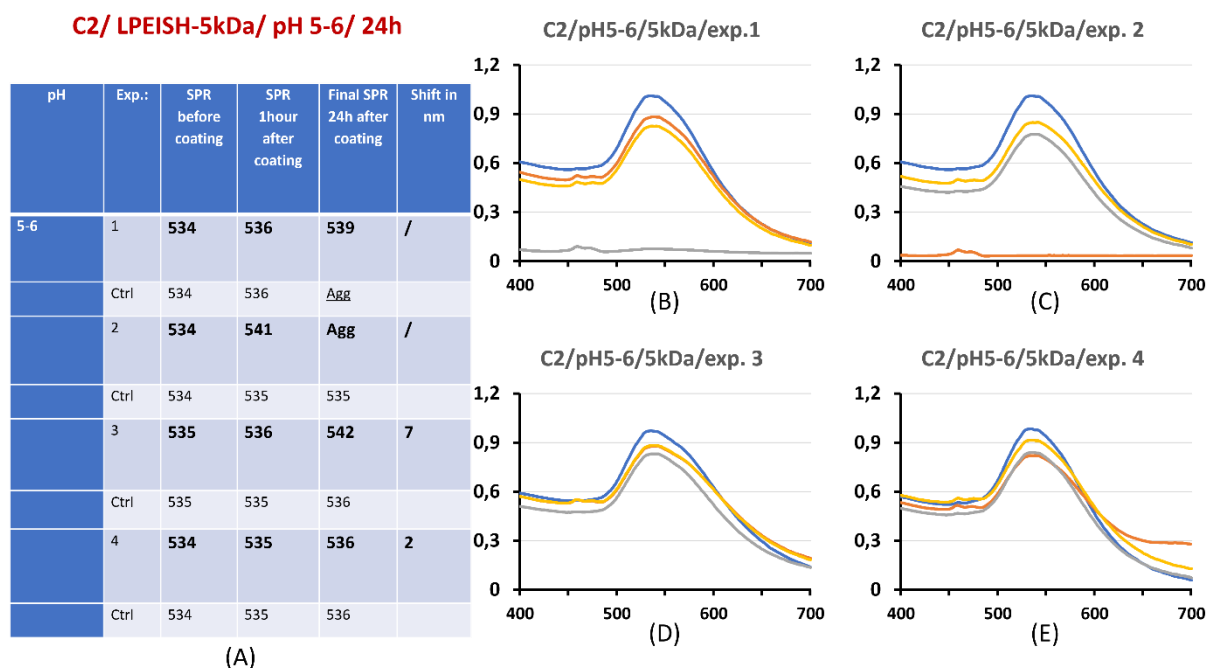


Figure 36: UV-VIS spectroscopy of 4 experiments showing SPR peaks (A) and absorption profiles (B-E) where AuNPs with a pH of 5-6 were coated with either 50µl (C2) of LPEI-SH-5kDa or water (ctrl). LPEI-SH coated and control AuNPs were continuously stirred and subjected to UV-Vis spectroscopy before coating, after 1h and 24h of coating. Blue curve: AuNP before coating, yellow curve: AuNP after 1h of coating, orange curve: AuNP after 24h of coating, grey curve: control AuNPs.

AuNP with a pH of 7-8

An indication of coating is seen in experiment 2 and 4 (see figure 37), whereby a significant SPR shift (6nm) was only observed in experiment 2. The other experiments resulted in aggregation (figure 37; B, D, F; orange curve)

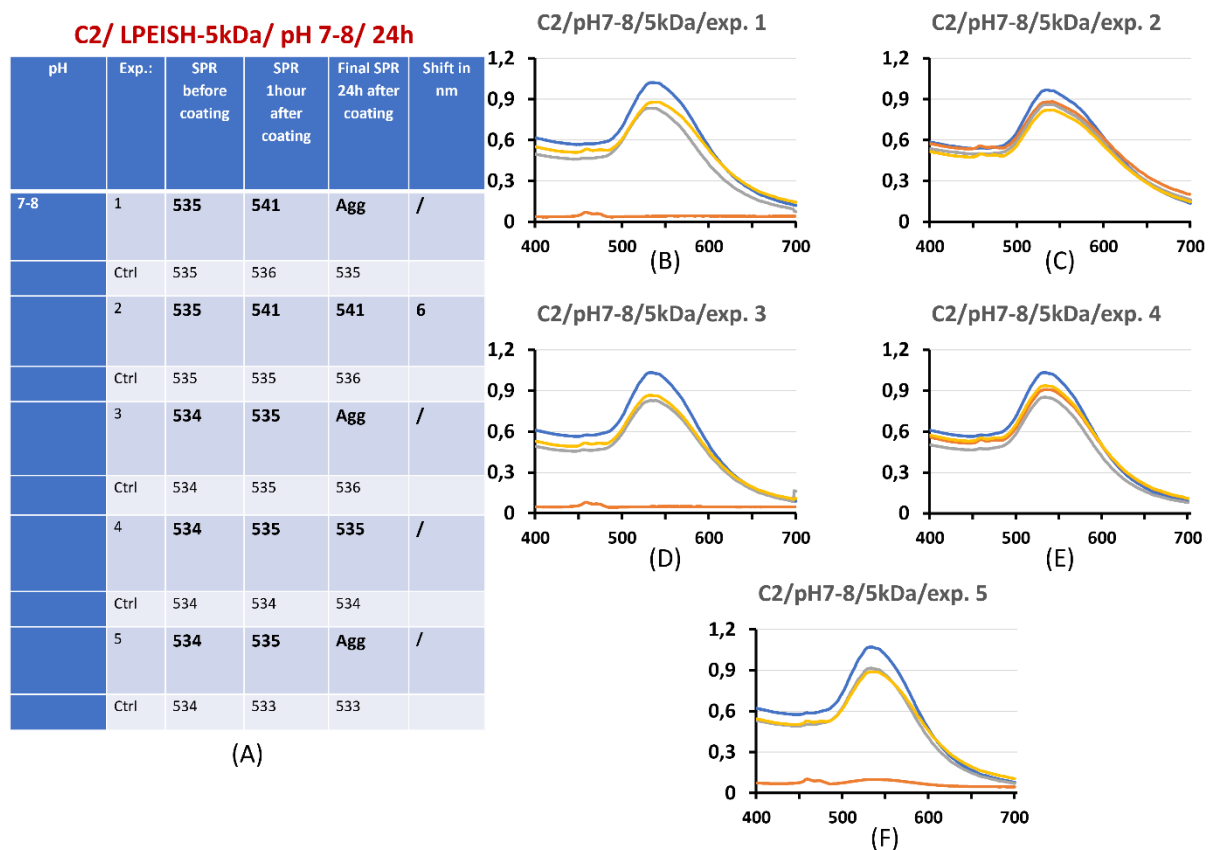


Figure 37: UV-VIS spectroscopy of 5 experiments showing SPR peaks (A) and absorption profiles (B-F) where AuNPs with a pH of 7-8 were coated with either 50 μ l (C2) of LPEI-SH-5kDa or water (ctrl). LPEI-SH coated and control AuNPs were continuously stirred and subjected to UV-Vis spectroscopy before coating, after 1h and 24h of coating. Blue curve: AuNP before coating, yellow curve: AuNP after 1h of coating, orange curve: AuNP after 24h of coating, grey curve: control AuNPs.

AuNP with a pH of 8-9

An indication of coating is seen in experiments 1, 3 and 4 (see figure 38), with significant SPR shifts in experiment 1 and 3 (6nm and 7nm). Experiment two resulted in aggregation (figure 38; C; orange curve), additionally the control sample showed a SPR shift (it can be assumed that the aqua regia cleaning of the mag bars was incomplete).

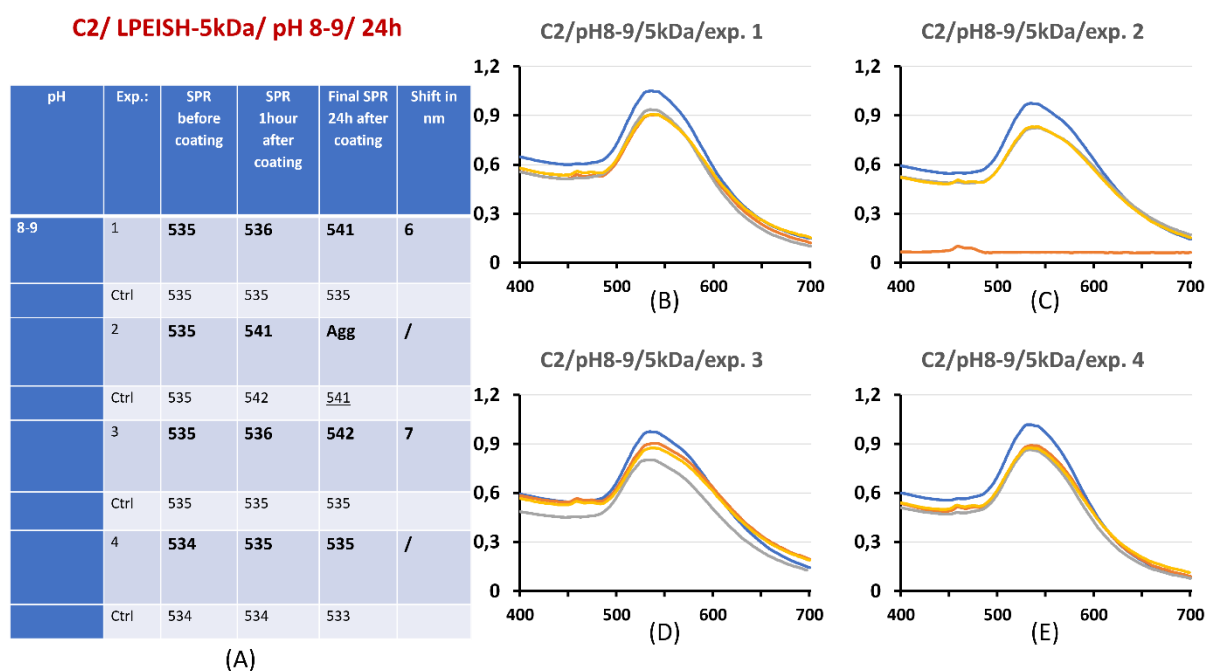


Figure 38: UV-VIS spectroscopy of 4 experiments showing SPR peaks (A) and absorption profiles (B-E) where AuNPs with a pH of 8-9 were coated with either 50 μ l (C2) of LPEI-SH-5kDa or water (ctrl). LPEI-SH coated and control AuNPs were continuously stirred and subjected to UV-Vis spectroscopy before coating, after 1h and 24h of coating. Blue curve: AuNP before coating, yellow curve: AuNP after 1h of coating, orange curve: AuNP after 24h of coating, grey curve: control AuNPs.

C3 (100 μ l of LPEISH-5kDa)

The samples were coated with 100 μ l of LPEISH-5kDa. 3 different pH were tested, and the samples were stirred for 24 hours.

AuNP with a pH of 5-6

An indication of coating is seen in experiments 2 and 4 (see figure 39), with a significant SPR shift (7nm) only in experiment 2. Experiment 1 seemed to be successful, but due to the aggregation of the control this experiment is not valid (figure 39; B; grey curve), as it can be assumed that the aqua regia cleaning of the mag bars was incomplete. Experiment 3 resulted in aggregation (figure 39; D; orange curve).

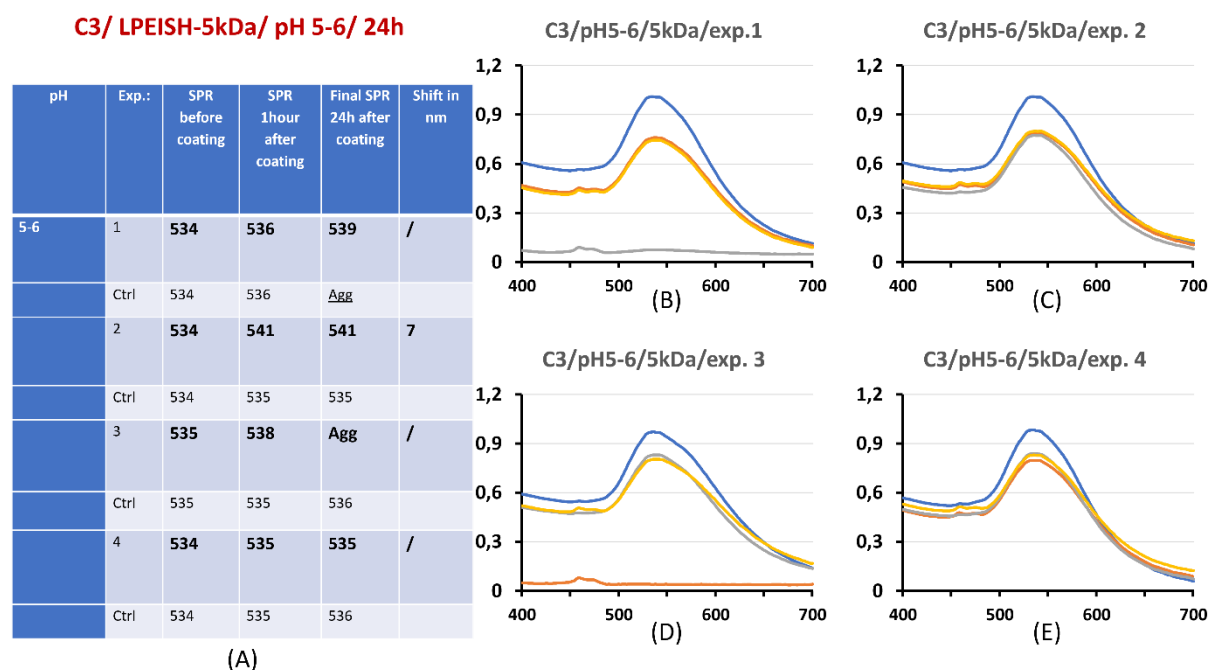


Figure 39: UV-VIS spectroscopy of 4 experiments showing SPR peaks (A) and absorption profiles (B-E) where AuNPs with a pH of 5-6 were coated with either 100 μ l (C3) of LPEI-SH-5kDa or water (ctrl). LPEI-SH coated and control AuNPs were continuously stirred and subjected to UV-Vis spectroscopy before coating, after 1h and 24h of coating. Blue curve: AuNP before coating, yellow curve: AuNP after 1h of coating, orange curve: AuNP after 24h of coating, grey curve: control AuNPs.

AuNP with a pH of 7-8

An Indication of coating is seen in experiments 1, 3, 4 and 5 (See figure 40), with significant SPR shifts in experiment 1 and 5 (6nm and 2nm). Experiment 2 also allows the conclusion that

coating was successful, but with the tendency that aggregation will take place over time as the curve approaches the x-axis. (Figure 40; C; orange curve)

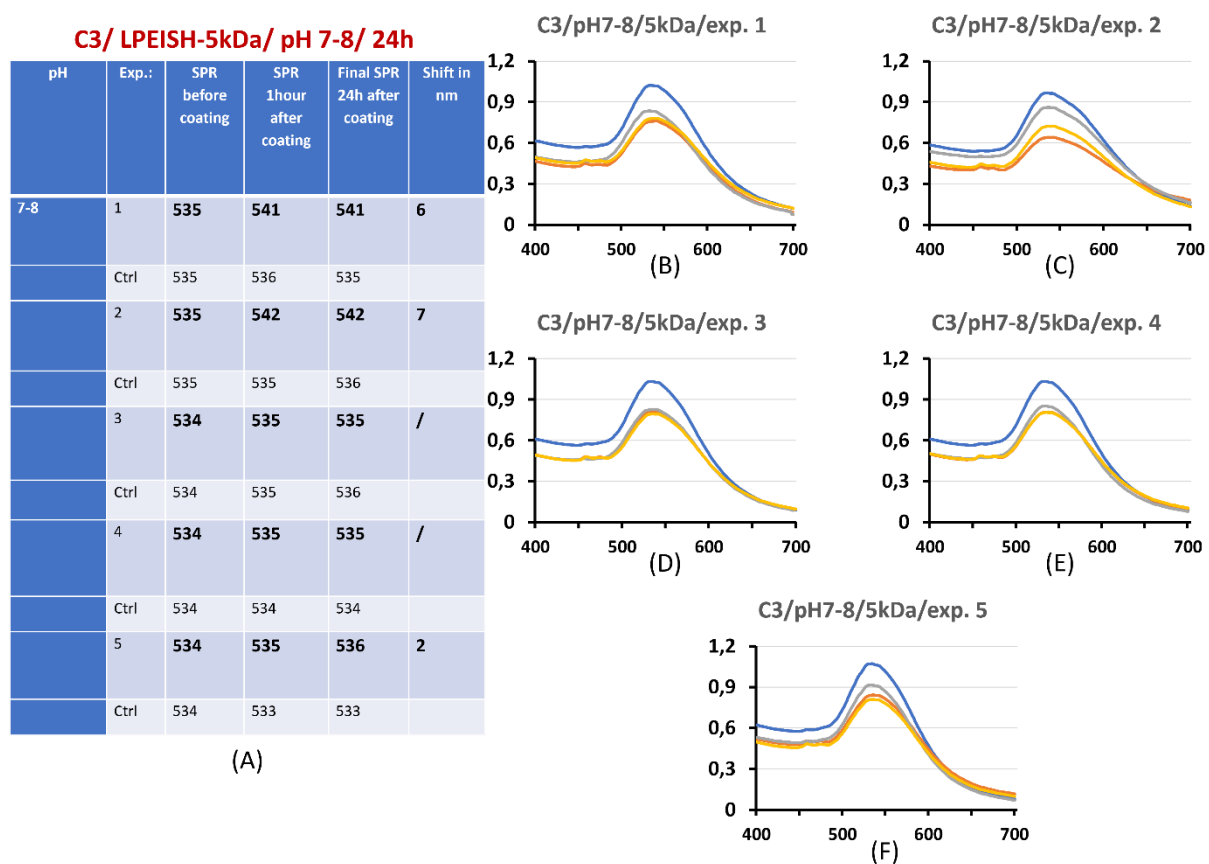


Figure 40: UV-VIS spectroscopy of 5 experiments showing SPR peaks (A) and absorption profiles (B-F) where AuNPs with a pH of 7-8 were coated with either 100 μ l (C3) of LPEI-SH-5kDa or water (ctrl). LPEI-SH coated and control AuNPs were continuously stirred and subjected to UV-Vis spectroscopy before coating, after 1h and 24h of coating. Blue curve: AuNP before coating, yellow curve: AuNP after 1h of coating, orange curve: AuNP after 24h of coating, grey curve: control AuNPs.

AuNP with a pH of 8-9

An indication of coating is seen in experiments 1, 3 and 4, with significant SPR shifts in each of these experiments (7nm, 7nm and 2nm). Although experiment 2 seemed to be successful, due to the SPR shift of the control the experiment is not valid, as it can be assumed that the aqua regia cleaning of the mag bars was incomplete. (See figure 41)

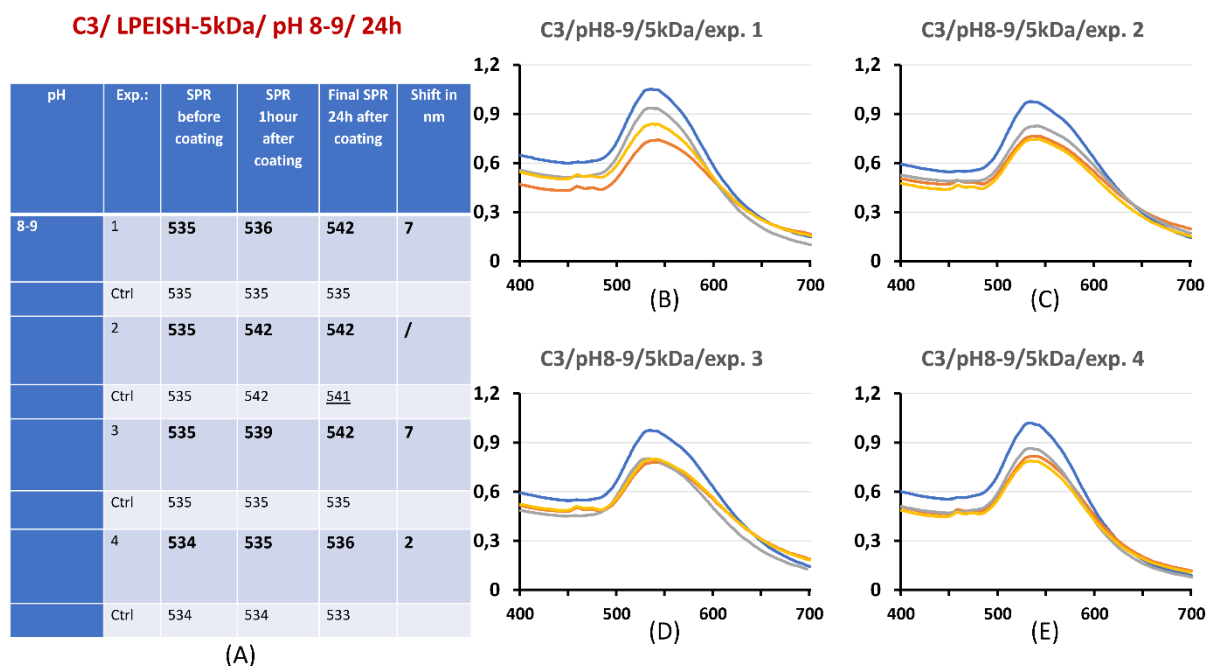


Figure 41: UV-VIS spectroscopy of 4 experiments showing SPR peaks (A) and absorption profiles (B-E) where AuNPs with a pH of 8-9 were coated with either 100 μ l (C3) of LPEI-SH-5kDa or water (ctrl). LPEI-SH coated and control AuNPs were continuously stirred and subjected to UV-Vis spectroscopy before coating, after 1h and 24h of coating. Blue curve: AuNP before coating, yellow curve: AuNP after 1h of coating, orange curve: AuNP after 24h of coating, grey curve: control AuNPs.

8.3.2 Experiments with a stir-time of 72 hours

8.3.2.1 AuNP coating with LPEI-SH of 1kDa

C1 (25 μ l of LPEISH-1kDa)

The samples were coated with 25 μ l of LPEISH-1kDa. 3 different pH were tested, and the samples were stirred for 72 hours.

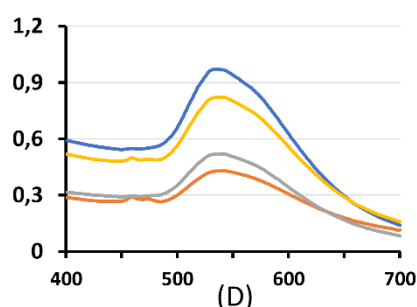
One experiment was done for each pH. Although the experiments with pH 5-6 and pH 7-8 showed a significant SPR shift (7nm and 8nm), it is more likely that aggregation already occurred in these experiments as the curve of the final SPR is already very close to the x-axis. The experiment with pH 8-9 was aggregated as well. (See figure 42)

C1/ LPEISH-1kDa/ pH 5-6/ 72h

pH	Exp.:	SPR before coating	SPR 1hour after coating	Final SPR 72h after coating	Shift in nm
5-6	1	535	535	542	7
	Ctrl	535	535	536	

(A)

C1/pH5-6/1kDa/exp.1



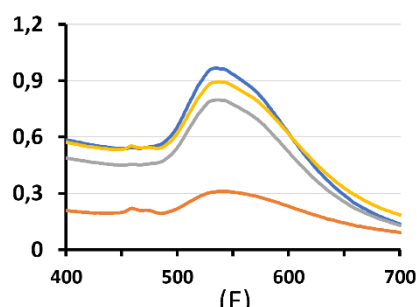
(D)

C1/ LPEISH-1kDa/ pH 7-8/ 72h

pH	Exp.:	SPR before coating	SPR 1hour after coating	Final SPR 72h after coating	Shift in nm
7-8	1	535	537	543	8
	Ctrl	535	536	535	

(B)

C1/pH7-8/1kDa/exp.1



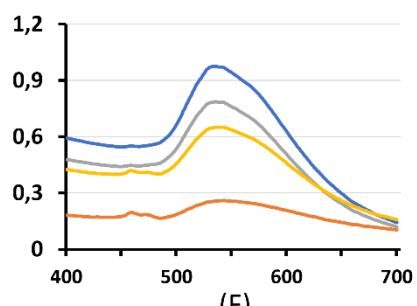
(E)

C1/ LPEISH-1kDa/ pH 8-9/ 72h

pH	Exp.:	SPR before coating	SPR 1hour after coating	Final SPR 72h after coating	Shift in nm
8-9	1	535	537	Agg	/
	Ctrl	535	542	535	

(C)

C1/pH8-9/1kDa/exp.1



(F)

Figure 42: UV-VIS spectroscopy of 3 different experiments, showing SPR peaks (A-C) and absorption profiles (D-F) where gold nanoparticles with different pH were coated with either 25 μ l (C1) of LPEISH-1kDa or water (ctrl). LPEI-SH coated and control AuNPs were continuously stirred and subjected to UV-Vis spectroscopy before coating, after 1h and 72h of coating. Blue curve: AuNP before coating, yellow curve: AuNP after 1h of coating, orange curve: AuNP after 72h of coating, grey curve: control AuNPs.

C2 (50 μ l of LPEISH-1kDa)

The samples were coated with 50 μ l of LPEISH-1kDa. 3 different pH were tested, and the samples were stirred for 72 hours.

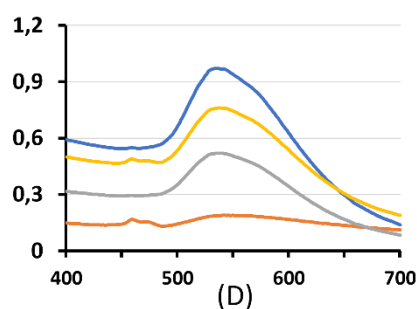
All experiments resulted in aggregation, after 72 hours at the latest. (See figure 43)

C2/ LPEISH-1kDa/ pH 5-6/ 72h

pH	Exp.:	SPR before coating	SPR 1hour after coating	Final SPR 72h after coating	Shift in nm
5-6	1	535	537	Agg	/
	Ctrl	535	535	536	

(A)

C2/pH5-6/1kDa/exp.1

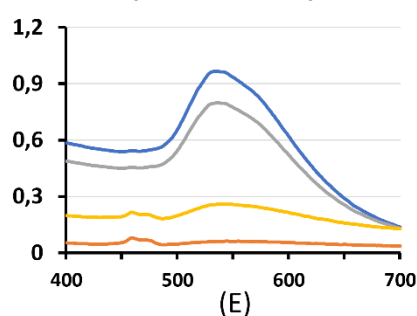


C2/ LPEISH-1kDa/ pH 7-8/ 72h

pH	Exp.:	SPR before coating	SPR 1hour after coating	Final SPR 72h after coating	Shift in nm
7-8	1	535	Agg	Agg	/
	Ctrl	535	536	535	

(B)

C2/pH7-8/1kDa/exp.1



C2/ LPEISH-1kDa/ pH 8-9/ 72h

pH	Exp.:	SPR before coating	SPR 1hour after coating	Final SPR 72h after coating	Shift in nm
8-9	1	534	536	Agg	/
	Ctrl	534	536	536	

(C)

C2/pH8-9/1kDa/exp.1

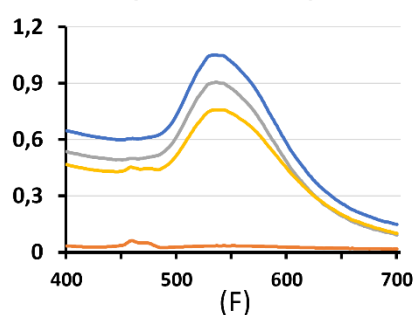


Figure 43: UV-VIS spectroscopy of 3 different experiments, showing SPR peaks (A-C) and absorption profiles (D-F) where gold nanoparticles with different pH were coated with either 50µl (C2) of LPEISH-1kDa or water (ctrl). LPEI-SH coated and control AuNPs were continuously stirred and subjected to UV-Vis spectroscopy before coating, after 1h and 72h of coating. Blue curve: AuNP before coating, yellow curve: AuNP after 1h of coating, orange curve: AuNP after 72h of coating, grey curve: control AuNPs.

C3 (100µl of LPEISH-1kDa)

The samples were coated with 100µl of LPEISH-1kDa. 3 different pH were tested, and the samples were stirred for 72 hours.

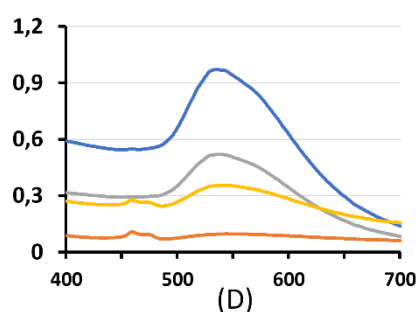
All experiments resulted in aggregation, after 72 hours at the latest. (See figure 44)

C3/ LPEISH-1kDa/ pH 5-6/ 72h

pH	Exp.:	SPR before coating	SPR 1hour after coating	Final SPR 72h after coating	Shift in nm
5-6	1	535	543	Agg	/
	Ctrl	535	535	536	

(A)

C3/pH5-6/1kDa/exp.1

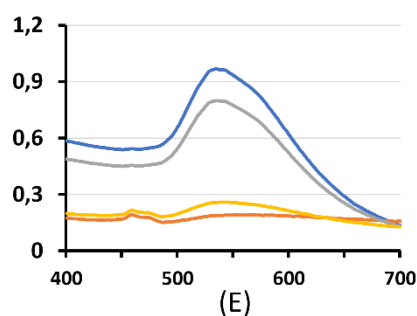


C3/ LPEISH-1kDa/ pH 7-8/ 72h

pH	Exp.:	SPR before coating	SPR 1hour after coating	Final SPR 72h after coating	Shift in nm
7-8	1	535	Agg	Agg	8
	Ctrl	535	536	535	

(B)

C3/pH7-8/1kDa/exp. 1



C3/ LPEISH-1kDa/ pH 8-9/ 72h

pH	Exp.:	SPR before coating	SPR 1hour after coating	Final SPR 72h after coating	Shift in nm
8-9	1	535	Agg	Agg	/
	Ctrl	535	542	535	

(C)

C3/pH8-9/1kDa/exp. 1

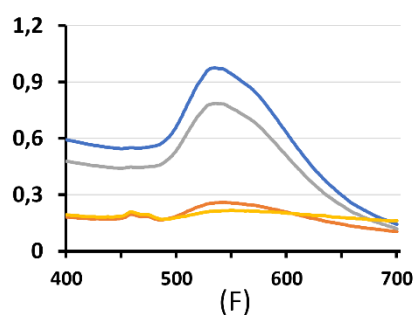


Figure 44: UV-VIS spectroscopy of 3 different experiments, showing SPR peaks (A-C) and absorption profiles (D-F) where gold nanoparticles with different pH were coated with either 100 μ l (C3) of LPEISH-1kDa or water (ctrl). LPEI-SH coated and control AuNPs were continuously stirred and subjected to UV-Vis spectroscopy before coating, after 1h and 72h of coating. Blue curve: AuNP before coating, yellow curve: AuNP after 1h of coating, orange curve: AuNP after 72h of coating, grey curve: control AuNPs.

8.3.2.2 AuNP coating with LEPI-SH of 5kDa

C1 (25µl of LPEISH-5kDa)

The samples were coated with 25µl of LPEISH-5kDa. 2 experiments were done, and the AuNP solution was adjusted to pH 7-8.

An indication of coating is seen in experiment 2, whereas experiment 1 resulted in aggregation. (See figure 45)

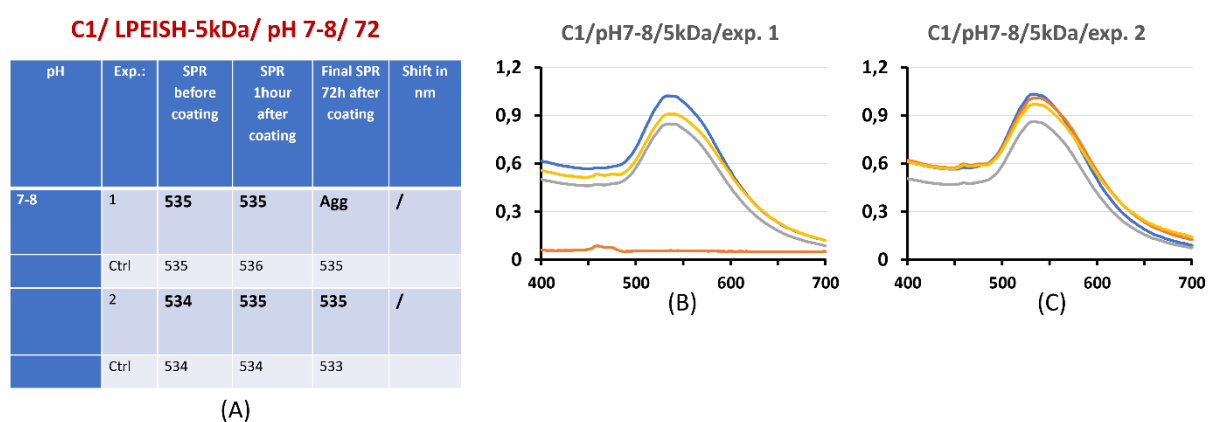


Figure 45: UV-VIS spectroscopy of 2 experiments showing SPR peaks (A) and absorption profiles (B,C) where AuNPs with a pH of 7-8 were coated with either 25µl (C1) of LPEI-SH-5kDa or water (ctrl). LPEI-SH coated and control AuNPs were continuously stirred and subjected to UV-Vis spectroscopy before coating, after 1h and 72h of coating. Blue curve: AuNP before coating, yellow curve: AuNP after 1h of coating, orange curve: AuNP after 72h of coating, grey curve: control AuNPs.

C2 (50µl of LPEISH-5kDa)

The samples were coated with 50µl of LPEISH-5kDa. 2 experiments were done, and the AuNP solution was adjusted to pH 7-8.

An indication of coating is seen in experiment 2, whereas experiment 1 resulted in aggregation. (See figure 46)

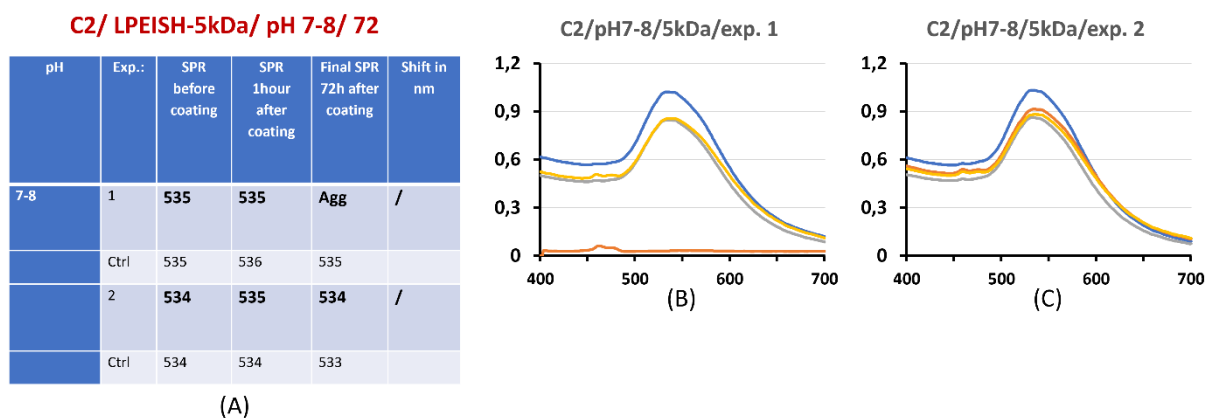


Figure 46: UV-VIS spectroscopy of 2 experiments showing SPR peaks (A) and absorption profiles (B,C) where AuNPs with a pH of 7-8 were coated with either 50 μ l (C2) of LPEI-SH-5kDa or water (ctrl). LPEI-SH coated and control AuNPs were continuously stirred and subjected to UV-Vis spectroscopy before coating, after 1h and 72h of coating. Blue curve: AuNP before coating, yellow curve: AuNP after 1h of coating, orange curve: AuNP after 72h of coating, grey curve: control AuNPs.

C3 (100 μ l of LPEISH-5kDa)

The samples were coated with 100 μ l of LPEISH-5kDa. 2 experiments were done, and the AuNP solution was adjusted to pH 7-8.

An indication of coating is seen in experiment 1, with a significant SPR shift of 6nm, whereas experiment 2 resulted in aggregation. (See figure 47)

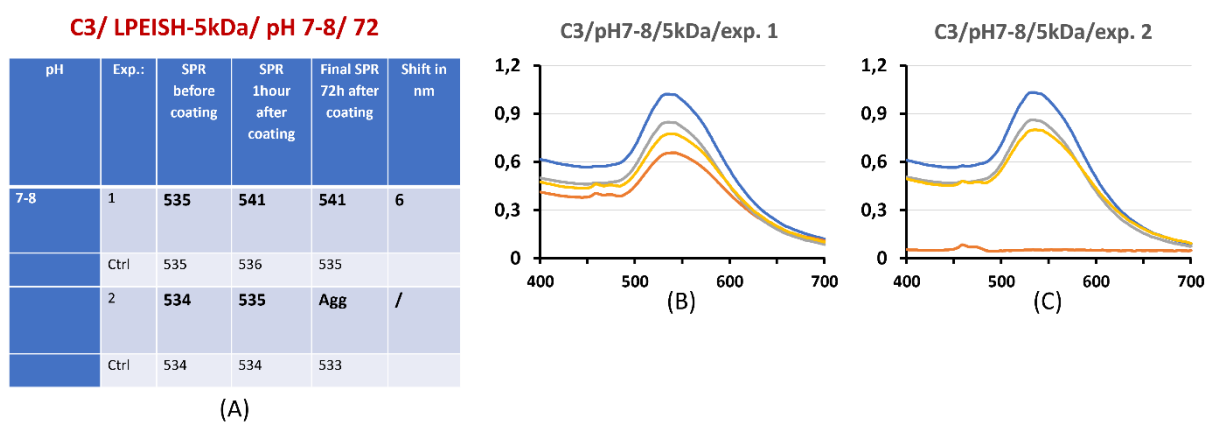


Figure 47: UV-VIS spectroscopy of 2 experiments showing SPR peaks (A) and absorption profiles (B,C) where AuNPs with a pH of 7-8 were coated with either 100 μ l (C3) of LPEI-SH-

5kDa or water (ctrl). LPEI-SH coated and control AuNPs were continuously stirred and subjected to UV-Vis spectroscopy before coating, after 1h and 72h of coating. Blue curve: AuNP before coating, yellow curve: AuNP after 1h of coating, orange curve: AuNP after 72h of coating, grey curve: control AuNPs.

9 Conclusion and Outlook

When it comes to the transport of nucleic acids, metal- and polycationic based carriers are becoming more and more important. These vehicles are relatively easy to manufacture and have already shown excellent results regarding biodistribution in many studies. In this thesis the focus was set on testing and/or optimizing polyplexes, quantoplexes and auropolyplexes. Since further information about the behavior of the SSO polyplexes in serum was of advantage, in addition to the *in vivo* experiments, almost at the same time, the behavior of the SSO polyplexes in serum was investigated *in vitro* using gel electrophoresis. This allowed a different point of view into the behavior of polyplexes in serum besides the *in vivo* experiments. The first Project of this thesis concluded that the polyplexes provided the desired protection of the SSOs, and that there was at most a slight opening of the polyplexes. In general, all *in vitro* polyplex experiments (seen in figure 14 and figure15) demonstrated that the SSOs loaded in polyplexes were protected and hence not affected by Serum or HBG. Whereas the naked SSOs either bound to components of the serum or got degraded by serum. On the other hand, naked SSOs in HBG showed no signs of degradation.

The second project of this thesis dealt with testing of quantoplexes and subsequently the improvement of quantoplexes by finding the optimal amount of LPEI to complex with the given quantum dots. Since the stability of the quantoplexes in the *in vivo* experiments was a problem, these test and optimization steps were necessary. Firstly, the quantoplexes that were also used in the *in vivo* experiments were tested in serum by using gel electrophoresis. It was seen that the pDNA and the QDs within in the quantoplexes were not affected by serum or HGB. On the other hand, the naked pDNA got degraded by serum compared to the naked pDNA in HBG, which was not affected by HBG. The quantoplexes in the *in vitro* experiments behaved as expected and did not yet provide any information as to why the stability was not given *in vivo*. Since there was a new batch of quantum dots, that was used to produce the quantoplexes, they were compared to the old batch in terms of their ability to complex with LPEI, to see if differences between the two batches existed. At this point the first irregularities occurred, and it was seen that the batches behaved differently regarding the complexation with LPEI. The new QDs showed complexation with LPEI starting at 80ng of LPEI, with a tendency that a lower amount of LPEI could also lead to complexation. Whereas the old batch of QDs showed a complexation starting at 100ng of LPEI.

Thereupon an attempt was made to optimize the complexing step between LPEI and the quantum dots, by trying to find the lowest possible amount of LPEI that fully complexes with the new batch of quantum dots. Here it was observed that the new batch of quantum dots seemed to get degraded, as suddenly more bands were visible in the gel electrophoresis. This led to the testing of the new quantum dots alone using gel electrophoresis, which finally showed that there was indeed a problem with the new batch. Again, additional bands could be observed, which indicated impurity or degradation. Finally, it was concluded that problems had arisen because the two batches had been manufactured by different users and that probably production errors in the new batch led to instabilities in the quantoplexes. If there are any further quantoplex experiments planned in the future, the testing of the quantum dots alone in advance would be a great help in the further process of quantoplex production, as shown by these results.

The initial step in the production of auropolyplexes is the coating of the AuNPs with LPEISH. Since this step is associated with many obstacles, such as instability, aggregation, and irreproducibility, the third project of this thesis focused on optimizing the coating of gold nanoparticles with LPEISH. Various parameters were tested, and any changes of the SPR were recorded with the help of UV-VIS spectrophotometry. Whereby a SPR shift of a few nanometers or no shift but without a huge absorbance drop was considered as successful coating. Due to problems with the aqua regia cleaning of the mag bars in some experiments, SPR shifts and sometimes aggregations of the control occurred. These experiments were subsequently classified as invalid. In general, the experiments in which LPEISH of 5kDa was used for coating gave much more positive results than those where LPEISH of 1kDa was used (see table 16). Also, it can be said that the experiments with a stirring time of 24 hours worked better than those that were stirred for 72 hours. Since a validation of the positive results could not be carried out, it cannot be concluded with certainty that those results were successful coatings. In conclusion the experiments done with LPEISH of 5kDa can be built upon, and a check by NTA would be a step forward in future experiments.

Table 16: The parameters which indicated successful coating in the auropolyplex project are shown below.

	pH	Concentration	Stir time
LPEISH-1kDa	pH 7-8	C1	24h
	pH 8-9	C1	24h
LPEISH-5kDa	pH 5-6	C1, C2, C3	24h
	pH 7-8	C1, C3	24h
	pH 8-9	C1, C2, C3	24h

10 References

1. Jenny Y, Chien RYH. Drug Delivery Trends in Clinical Trials and Translational Medicine. *J Pharm Sci.* 2008;99(5):2386–2398. doi:10.1002/jps
2. Rödl W, Taschauer A, Schaffert D, Wagner E, Ogris M. Synthesis of polyethylenimine-based nanocarriers for systemic tumor targeting of nucleic acids. *Methods Mol Biol.* 2019;1943:83-99. doi:10.1007/978-1-4939-9092-4_6
3. Weng Y, Huang Q, Li C, et al. Improved Nucleic Acid Therapy with Advanced Nanoscale Biotechnology. *Mol Ther - Nucleic Acids.* 2020;19(March):581-601. doi:10.1016/j.omtn.2019.12.004doi:10.1016/j.ajps.2014.10.001
4. Li J, Wang Y, Zhu Y, Oupický D. Recent advances in delivery of drug-nucleic acid combinations for cancer treatment. *J Control Release.* 2013;172(2):589-600. doi:10.1016/j.jconrel.2013.04.010
5. Sridharan K, Gogtay NJ. Therapeutic nucleic acids: current clinical status. *Br J Clin Pharmacol.* Published online 2016:659-672. doi:10.1111/bcp.12987
6. Germershaus O, Nultsch K. Localized, non-viral delivery of nucleic acids: Opportunities, challenges and current strategies. *Asian J Pharm Sci.* 2015;10(3):159-175.
7. Dias N, Stein CA. Antisense oligonucleotides: Basic concepts and mechanisms. *Mol Cancer Ther.* 2002;1(5):347-355.
8. Havens MA, Duelli DM, Hastings ML. Targeting RNA splicing for disease therapy. *Wiley Interdiscip Rev RNA.* 2013;4(3):247-266. doi:10.1002/wrna.1158
9. Bauman J, Jearawiriyapaisarn N, Kole R. Therapeutic potential of splice-switching oligonucleotides. *Oligonucleotides.* 2009;19(1):1-13. doi:10.1089/oli.2008.0161
10. Havens MA, Hastings ML. Splice-switching antisense oligonucleotides as therapeutic drugs. *Nucleic Acids Res.* 2016;44(14):6549-6563. doi:10.1093/nar/gkw533
11. Wirth T, Ylä-Herttua S. Gene therapy used in cancer treatment. *Biomedicines.* 2014;2(2):149-162. doi:10.3390/biomedicines2020149
12. Akbulut, H., Ocal, M., & Sonugur G. Cancer gene therapy. In: *Gene Therapy - Principles and Challenges.*; 2015. doi:10.5124/jkma.1998.41.8.836
13. Elsbahy M, Nazarali A, Foldvari M. Non-Viral Nucleic Acid Delivery: Key Challenges and Future Directions. *Curr Drug Deliv.* 2012;8(3):235-244. doi:10.2174/156720111795256174

14. El-Sayed A, Futaki S, Harashima H. Delivery of macromolecules using arginine-rich cell-penetrating peptides: Ways to overcome endosomal entrapment. *AAPS J.* 2009;11(1):13-22. doi:10.1208/s12248-008-9071-2
15. Neu M, Fischer D, Kissel T. Recent advances in rational gene transfer vector design based on poly(ethylene imine) and its derivatives. *J Gene Med.* 2005;7(8):992-1009. doi:10.1002/jgm.773
16. Gao X, Kim K, Liu D. Nonviral gene delivery: What we know and what is next. *AAPS J.* 2007;9(1):92-104. doi:10.1080/0305764940240113
17. Prud'homme A, Nabki F. Comparison between linear and branched polyethylenimine and reduced graphene oxide coatings as a capture layer for micro resonant CO₂ gas concentration sensors. *Sensors (Switzerland).* 2020;20(7). doi:10.3390/s20071824
18. Zintchenko A, Susha AS, Concia M, et al. Drug nanocarriers labeled with near-infrared-emitting quantum dots (quantoplexes): Imaging fast dynamics of distribution in living animals. *Mol Ther.* 2009;17(11):1849-1856. doi:10.1038/mt.2009.201
19. Mukthavaram R, Wrasidlo W, Hall D, Kesari S, Makale M. Assembly and targeting of liposomal nanoparticles encapsulating quantum dots. *Bioconjug Chem.* 2011;22(8):1638-1644. doi:10.1021/bc200201e
20. Giljohann DA, Seferos DS, Daniel WL, Massich MD, Patel PC, Mirkin CA. Gold nanoparticles for biology and medicine. *Angew Chemie - Int Ed.* 2010;49(19):3280-3294. doi:10.1002/anie.200904359
21. Singh P, Pandit S, Mokkalapati VRSS, Garg A, Ravikumar V, Mijakovic I. Gold nanoparticles in diagnostics and therapeutics for human cancer. *Int J Mol Sci.* 2018;19(7). doi:10.3390/ijms19071979
22. Ding Y, Jiang Z, Saha K, et al. Gold nanoparticles for nucleic acid delivery. *Mol Ther.* 2014;22(6):1075-1083. doi:10.1038/mt.2014.30
23. Boisselier E, Astruc D. Gold nanoparticles in nanomedicine: preparations, imaging, diagnostics, therapies and toxicity. *Chem Soc Rev.* 2009;38(6):1759-1782. doi:10.1039/b806051g
24. M.C. Daniel DA. Gold nanoparticles: assembly, supramolecular chemistry, quantum-size-related properties, and applications toward. *Chem Rev.* 2004;104:293– 346.

25. Amendola V, Pilot R, Frasconi M, Maragò OM, Iati MA. Surface plasmon resonance in gold nanoparticles: A review. *J Phys Condens Matter*. 2017;29(20). doi:10.1088/1361-648X/aa60f3
26. Yeh YC, Creran B, Rotello VM. Gold nanoparticles: Preparation, properties, and applications in bionanotechnology. *Nanoscale*. 2012;4(6):1871-1880. doi:10.1039/c1nr11188d
27. Huang X, El-Sayed MA. Gold nanoparticles: Optical properties and implementations in cancer diagnosis and photothermal therapy. *J Adv Res*. 2010;1(1):13-28. doi:10.1016/j.jare.2010.02.002
28. Eustis S, El-Sayed MA. Why gold nanoparticles are more precious than pretty gold: Noble metal surface plasmon resonance and its enhancement of the radiative and nonradiative properties of nanocrystals of different shapes. *Chem Soc Rev*. 2006;35(3):209-217. doi:10.1039/b514191e
29. Wurster EC, Elbakry A, Göpferich A, Breunig M. Layer-by-layer assembled gold nanoparticles for the delivery of nucleic acids. *Methods Mol Biol*. 2013;948:171-182. doi:10.1007/978-1-62703-140-0_12
30. Xue Y, Li X, Li H, Zhang W. Quantifying thiol-gold interactions towards the efficient strength control. *Nat Commun*. 2014;5. doi:10.1038/ncomms5348
31. Häkkinen H. The gold-sulfur interface at the nanoscale. *Nat Chem*. 2012;4(6):443-455. doi:10.1038/nchem.1352
32. Yarzhemsky VG, Battocchio C. The structure of gold nanoparticles and Au based thiol self-organized monolayers. *Russ J Inorg Chem*. 2011;56(14):2147-2159. doi:10.1134/
33. Taschauer A, Polzer W, Pöschl S, et al. Combined Chemisorption and Complexation Generate siRNA Nanocarriers with Biophysics Optimized for Efficient Gene Knockdown and Air-Blood Barrier Crossing. *ACS Appl Mater Interfaces*. 2020;12(27):30095-30111. doi:10.1021/acsami.0c06608S003602361114004X
34. Amendola V, Meneghetti M. Size evaluation of gold nanoparticles by UV-vis spectroscopy. *J Phys Chem C*. 2009;113(11):4277-4285. doi:10.1021/jp8082425
35. Inc. C. Introduction-to-gold-nanoparticle-characterization. *Cytodiagnosics*. <https://www.cytodiagnosics.com/pages/introduction-to-gold-nanoparticle-characterization#:~:text=LSPR of gold nanoparticles results,measured by UV-Vis>

spectroscopy.&text=The peak optical density (OD,concentration of nanoparticles in solution.

36. Rahman S. Size and Concentration Analysis of Gold Nanoparticles with Ultraviolet-Visible Spectroscopy. Undergrad J Math Model One + Two Size. 2016;7(1).
37. Park SH, Raines RT. Green fluorescent protein as a signal for protein-protein interactions. Protein Sci. 1997;6(11):2344-2349. doi:10.1002/pro.5560061107
38. Yilmaz M, Ozic C, Gok Ihami. Principles of Nucleic Acid Separation by Agarose Gel Electrophoresis. Gel Electrophor - Princ Basics. Published online 2012. doi:10.5772/38654
39. Lee PY, Costumbrado J, Hsu CY, Kim YH. Agarose gel electrophoresis for the separation of DNA fragments. J Vis Exp. 2012;(62):1-5. doi:10.3791/3923
40. Scientific T. Nucleic Acid Gel Electrophoresis—A Brief Overview and History. <https://www.thermofisher.com/at/en/home/life-science/cloning/cloning-learning-center/invitrogen-school-of-molecular-biology/na-electrophoresis-education/na-separation-overview.html>
41. Hellman LM, Fried MG. Electrophoretic mobility shift assay (EMSA) for detecting protein-nucleic acid interactions. Nat Protoc. 2007;2(8):1849-1861. doi:10.1038/nprot.2007.249
42. Song Y, Xu L, Wu Q, et al. A New Strategy to Reduce Toxicity of Ethidium Bromide by Alternating Anions: New Derivatives with Excellent Optical Performances, Convenient Synthesis, and Low Toxicity. Small Methods. 2020;4(3):1-6. doi:10.1002/smtd.201900779
43. Sigmon J, Larcom LL. The effect of ethidium bromide on mobility of DNA fragments in agarose gel electrophoresis. Electrophoresis. 1996;17(10):1524-1527. doi:10.1002/elps.1150171003